personal buildup for

Force Motors Ltd.

MTZ worldwide 2/2009 as epaper released on 19.01.2009
http://www.mtz-worldwide.com

Inhalt:

MTZ

WORLDWIDE

02 | February 2009 Volume 70

www.MTZ-online.com

The New BMW Six-cylinder Diesel Engine

For more information visit:
www.MTZ-online.com

COVER STORY

The New BMW Six-cylinder Diesel Engine

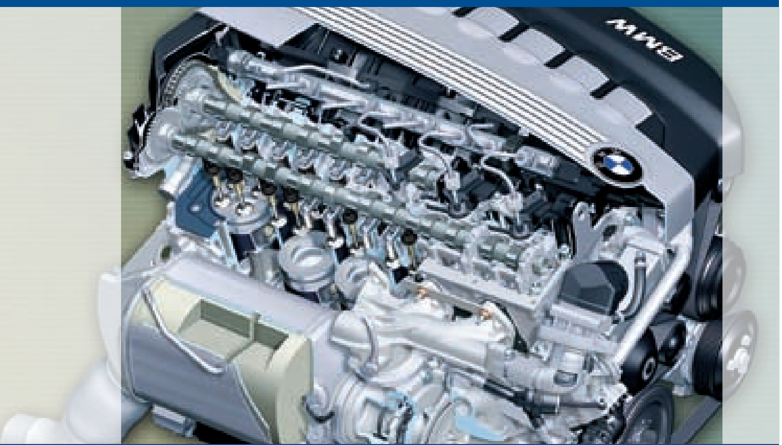

4
The **3.0 l Six-cylinder Diesel Engine**, alongside the 2.0 l four-cylinder diesel engine already launched in 2007, represents the second essential mainstay of the diesel engine program at the BMW Group. It was used for the first time in September 2008 as a 180 kW and 520 Nm version in the 330d and as the 540 Nm version in the 730d.

Wanted: Concepts for 2020

Dear Reader,

Yesterday, the European Parliament adopted the energy-climate legislation package, which had already been agreed by the EU Commission, on first reading. This establishes an almost irreversible basis for the next ten years of engine development. According to the new legislation, the emission limit of 130 grams of CO_2 for the new car fleet will not come into force until 2015. Many people in the industry were pleased with this compromise, whereas environmental organisations expressed their unanimous outrage. An average fleet limit value of 130 grams is an ambitious target, but one that is surely achievable within this time frame. What often goes unnoticed in this atmosphere of relief is the fact that Article 1 of the legislation sets a target of 95 grams for 2020. And this represents a much greater challenge for the industry. The full impact of what needs to happen over the next ten years becomes clearly apparent when we consider that the best car on the Environmental List compiled by the Verkehrsclub Deutschland (VCD), the Toyota Prius, currently has a CO_2 emission of 104 grams. The best premium mid-sized vehicle is a BMW 318d with 122 grams. These are the best – and even in the case of the 3-Series BMW, they are relatively small cars. An average value of 95 grams is unlikely to be achievable purely by better internal combustion engines: it would represent a reduction in fuel consumption by 40 % in just eleven years. This would bring modern diesel engines close to the optimum Carnot process. Partial electrification is a possible solution, but with the given energy mix it is not carbon-neutral, and legislation will no doubt take this fact into account at some point.

What possibilities remain then, if improvements to the powertrain are finite and the laws of physics are ultimately invincible? Even if, as a lover of fast and beautiful cars, I find it difficult to accept: there is no alternative to miniaturisation, lightweight design and downsizing of our vehicles. In Germany, we will have to completely redefine the term "premium" within the next two vehicle generations. Perhaps one day, luxury will no longer have anything to do with size.

Johannes Winterhagen,
Wiesbaden, 19 December 2008

Johannes Winterhagen
Editor-in-Chief

MTZ WORLDWIDE
02I2009

Founded 1939 by
Prof. Dr.-Ing. E. h. Heinrich Buschmann and
Dr.-Ing. E. h. Prosper L'Orange

Organ of the Fachverband Motoren und Systeme im VDMA, Verband Deutscher Maschinen- und Anlagenbau e. V., Frankfurt/Main, for the areas combustion engines and gas turbines

Organ of the Forschungsvereinigung Verbrennungskraftmaschinen e. V. (FVV)

Organ of the Wissenschaftliche Gesellschaft für Kraftfahrzeug- und Motorentechnik e. V. (WKM)

Organ of the Österreichischer Verein für Kraftfahrzeugtechnik (ÖVK)

Cooperation with the STG, Schiffbautechnische Gesellschaft e. V., Hamburg, in the area of ship drives by combustion engines

The New BMW Six-cylinder Diesel Engine

The 3.0 l six-cylinder diesel engine, alongside the new 2.0 l four-cylinder diesel engine already launched in 2007, represents the second essential mainstay of the diesel engine program at the BMW Group. It is used in different power levels in the majority of BMW series of cars and thus makes a significant contribution toward meeting the future global demands regarding fuel consumption and emission figures. In order to take into account the series thinking with regard to uniformity of concept and components, the six-cylinder engine has been derived consistently from the four-cylinder version. This new engine was used for the first time in September 2008 as a 180 kW and 520 Nm version in the 330d and as the 540 Nm version in the 730d. Both models meet the EU5 emission limits, while the 330d is additionally offered as a EU6 model.

1 Objective

The aim was to create a new, future-proof series of engines based on the new four-cylinder diesel engine [1] launched in 2007 with the following attributes: more efficient, lighter, more powerful, cleaner and more compact. In detail this means:

- increase in power and torque to maintain BMW's leading position in global competition
- basis for different power versions
- reduction of CO_2 emissions
- technical prerequisite for compliance with future emission regulations (EU5, EU6, USA)
- reduction of weight and engine dimensions as package contribution toward compliance with future requirements regarding exhaust gas treatment and protection of pedestrians
- flexibility with regard to use in existing and future vehicle concepts
- maintenance of the modularity of the four- and six-cylinder diesel engine for use of the flexible BMW production network and of cost-per-unit effects due to a high proportion of carry-over parts.

2 Design

The new six-cylinder diesel engine, **Figure 1**, is derived from the four-cylinder with a new design basic engine, a chain drive moved to the rear for package reasons (to meet future pedestrian protection requirements), a vacuum pump moved into the oil sump and the arrangement of all auxiliary components on the left side of the engine. This creates space on the right side of the engine for the exhaust gas treatment components and the turbocharger unit. The very compact air intake with integrated swirl flaps is flanged onto the side of the cylinder head which is 29 mm lower than the previous engine and has parallel inlet channels. The engine-mounted intake silencer is positioned at the back under the acoustic cover. In addition to the installation space measures, appropriate selection of components has reduced total engine weight by a further 5 kg compared to the previous version. The third-generation common-rail injection system with a maximum injection pressure of 1800 bar includes a new twin-ram high pressure pump and advanced piezo injectors. The exhaust system with the hot-attached electrical exhaust-gas recirculation (AGR) valve, the external AGR-cooler bypass for maximizing the AGR temperature spread, in combination with the internal engine measures and the new injection system ensure compliance with the EU5 emission limits. To comply with the EU6 emission limits which will apply after 2014, a regulated NO_X storage catalytic converter is used additionally in the 330d.

3 Engine Description

3.1 Building Block

The design of the new six-cylinder engine is based on the consistent implementation of the building block principle. This results in a high number of carry-over parts or components of the same design shared between the four- and six-cylinder engines. This significantly reduces the development costs, enabling the production and assembly of the new engines to be performed in combination. Different components are only used where there is a necessity of differentiation for functional or package reasons. **Figure 2** represents the division of the individual components into the respective groups: carry-over part/same design/different part.

3.2 Basic Design

The basic dimensioning corresponds to the four-cylinder engine, the components are designed for a permanent ignition pressure of 180 bar. The main dimensions are shown in the **Table**.

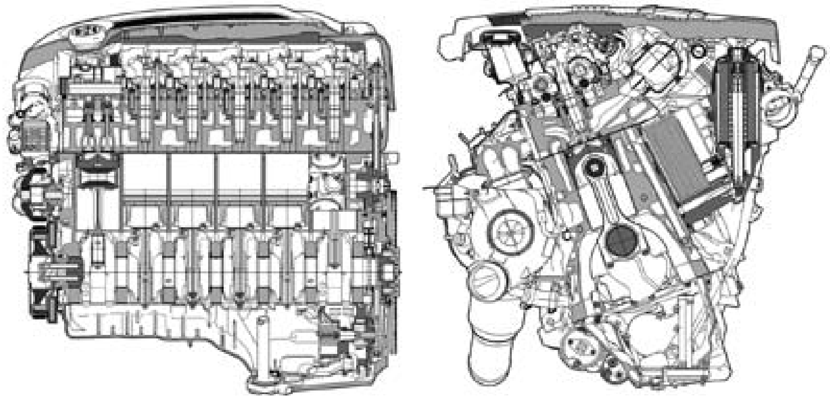

Figure 1: Longitudinal and cross section of the new BMW six-cylinder engine

The Authors

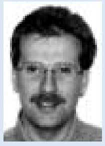

Dipl.-Ing. Johannes Dworschak
is head of the test department for mechanics and cooling of diesel engines at the BMW Group in Steyr (Austria).

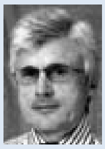

Dipl.-Ing. Werner Neuhauser
is head of the test department for fuel-mixture generation and combustion of six-cylinder diesel engines at the BMW Group in Steyr (Austria).

Dipl.-Ing. Erwin Rechberger
is project manager for six-cylinder diesel engines in the diesel engine development department of the BMW Group in Steyr (Austria).

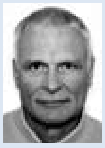

Johann Stastny
is head of department for basic engine design in the diesel engine development department at the BMW Group in Steyr (Austria).

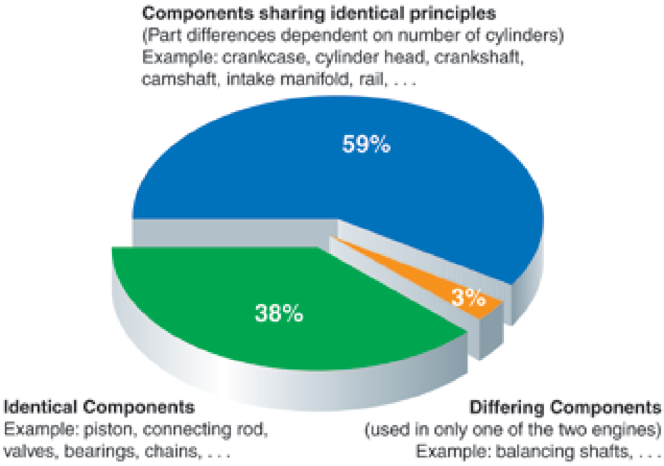

Figure 2: BMW engine family four-/six-cylinder

Table: Main dimensions

Parameter	Unit		Parameter	Unit	
Basic engine dimensions			**Conrod bearing**		
Displacement	cm^3	2993	Diameter	mm	50
Bore	mm	84	Width (pin)	mm	24
Stroke	mm	90	**Piston**		
Stroke-to-bore ratio	—	1,07	Compression height	mm	47
Cylinder volume	cm^3	499	Head land height	mm	9,12
Conrod length	mm	138	**Piston pin**		
Stroke-to-conrod ratio	—	0,326	Diameter	mm	32
Block height	mm	289	Length	mm	64
Cylinder distance	mm	91	**Valves**		
Main bearing			Diameter, Intake/Exhaust	mm	27,2 / 24,6
Diameter	mm	55	Valve lift, Intake/Exhaust	mm	7,5 / 8
Width	mm	25	Valve-shaft diameter	mm	5
			Compression ratio	—	16,5:1

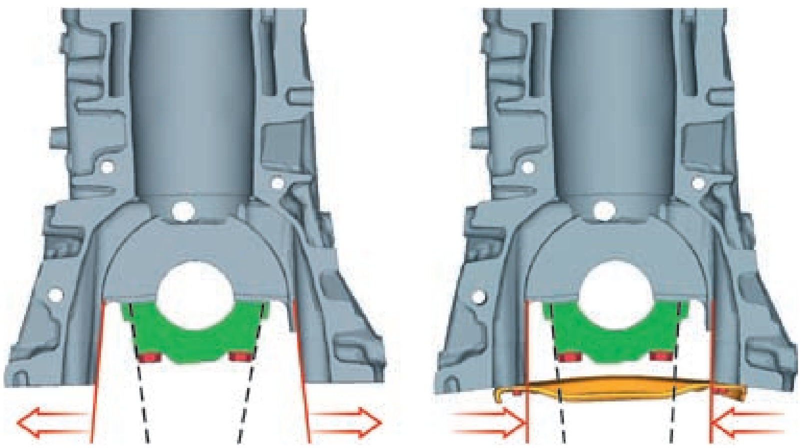

Figure 3: Pre-tensioning of crankcase

3.3 Description of Components

3.3.1 Engine Block

As in the previous model [2], a high-strength Al-Si-Mg alloy is used, cast in a gravity die. The bearing surfaces are steel sleeves that are thermally inserted into the block. To reduce the thermal loading, the block around the cylinders is drilled with cooling bores of 1.5 mm diameter. The skirts of the deep-skirt crank case are stiffened with steel cross brackets. Due to the lower thermal expansion coefficient of steel as opposed to aluminium, a compressive pre-stressing is generated in the high-load zones in the thrust bearings that reduces the component loading caused by the ignition pressure, **Figure 3**.

3.3.2 Crankshaft Drive

In the design of the crankshaft particular attention was paid to the lowest possible weight while ensuring high rigidity and economical manufacturing costs. The dimensioning of the main and piston bearings already selected for the four-cylinder model was carried over. While retaining the 20 % compensation of the rotating inertial forces, detailed optimization enabled the weight of the crankshaft to be reduced by 1 kg compared to the previous version, which benefits the dynamics of the engine. A new feature is the rotation of the counterweights by 30 °, enabling the unfinished part to be forged in one plane, eliminating the “twist” process. **Figure 4** shows the crankshaft with the twisting of the counterweights relative to the crank and casting.

3.3.3 Control Mode and Drive of the High Pressure Pump

As with all BMW engines, the chain drive is designed for zero maintenance over the life of the engine. The two-part drive is derived from the four-cylinder engine and positioned at the back of the engine. In order to synchronize the feeding of fuel by the high-pressure pump with the injection, the transmission ratio differs in comparison with the four-cylinder engine. The design of the lightweight camshafts is copied from the previous engine.

3.3.4 Air Ducting

The redesigned intake air ducting for the 730d includes an intake silencer mounted perpendicular to the engine which can deform in its vertical dimension, **Figure 5**. The cover, which simultaneously acts as an acoustic cover, is connected to the air filter housing and can slide on specially designed pillars. The filter element made of fully synthetic flow material is also designed to be deformable. The vertically deformable parts and the free space above the engine created the deformable zone necessary for pedestrian protection. This avoids the need for expensive bodywork modifications for pedestrian protection.

Figure 4: Crankshaft – design counterweights

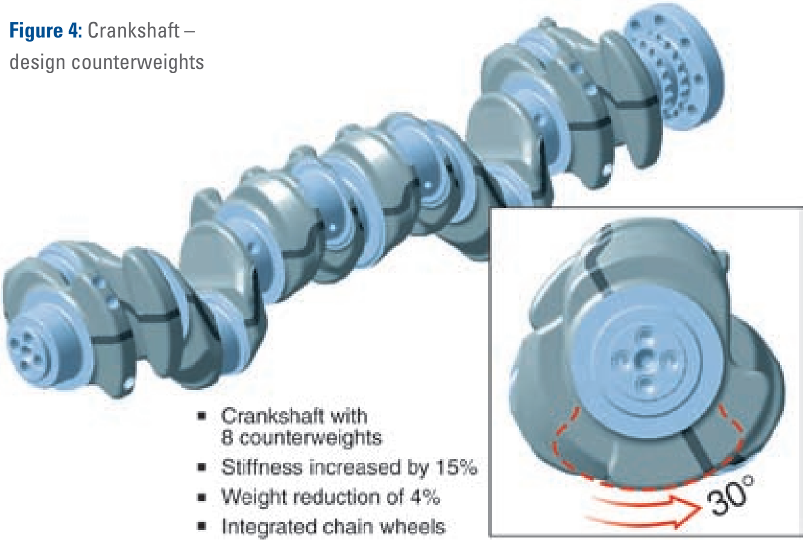

3.4 Mounting Parts

In the plastic cylinder head cover a spring plate separator is used instead of the previously used cyclone separator. Prestressed metal spring plates ensure constant flow characteristics regardless of the blow-by mass flow and ensure a high degree of separation over the entire operating range.

Analogous to the four-cylinder engine, the auxiliary units – generator, power steering pump and air-conditioning compressor – are arranged on the left of the engine attached to the unit carrier which is designed as a carry-over part. In contrast to the previous engine, the drive is now provided by means of only one belt, enabling the drag torque of the auxiliary unit drive to be significantly reduced. The oil filter module is now designed as a weight-optimized plastic component with an engine oil cooler integrated into its base.

4 Fuel Mixture Generation

4.1 Combustion Chamber Configuration

When redesigning the combustion chamber it was important to meet the demands not only for maximum power density, but also for the lowest emissions. The two inlet ducts divided into swirl and fill channel are positioned on the side of the cylinder head to reduce the height of the engine. In the transition area to the air intake, the filling channel has a round cross-section that permits the use of an effective channel shut-off to increase the charge motion in the combustion chamber at low engine speeds. In this way, a very high, continuously adjustable swirl-spread of 0.38 to 1.1 is achieved (according to Tippelmann).

The four valves actuated with roller cam followers are arranged parallel to the cylinder axis around the central injector in order to avoid valve seat pocket perturbance in the piston. Based on the four-cylinder engine, the piston bowl has been developed further to meet the EU5 requirements. In combination with the relatively low compression ration of 16.5:1, the NO_x emissions and the fuel consumption could both be reduced and the power density increased while retaining the maximum injection pressure. In addition, the new combustion procedure is characterized by an increased combustion rate with high thermodynamic efficiency.

To improve cold-starting and warm-up behavior of the new engine, a fast glow system using ceramic glow plugs has been used for the first time in a six-cylinder diesel engine. These glow plugs with a maximum glow temperature of 1300 °C conduct high energy to the combustion chamber and, despite the low compression ratio, guarantee very good combustion stability even after a cold start. The high number of permissible cycles of the ceramic plug also permits glowing dependent on operating point in partial load operation to reduce the HC and CO emissions. In addition, this system offers further noise reduction during the warm-up phase.

4.2 Turbocharging

For the new six-cylinder engine, the exhaust gas turbocharger with turbine-side variable guide vanes of the previous engine was optimized in many details and adapted to the new package of requirements. The thermodynamic properties are significantly improved in particular by the new compression wheel and the redesign of the turbine guide vanes. This results in an extended pump-

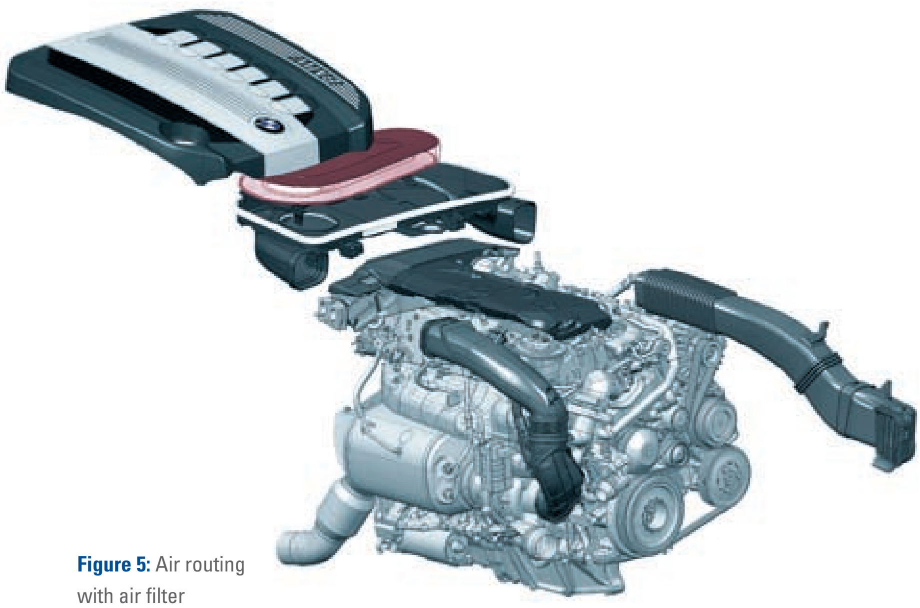

Figure 5: Air routing with air filter

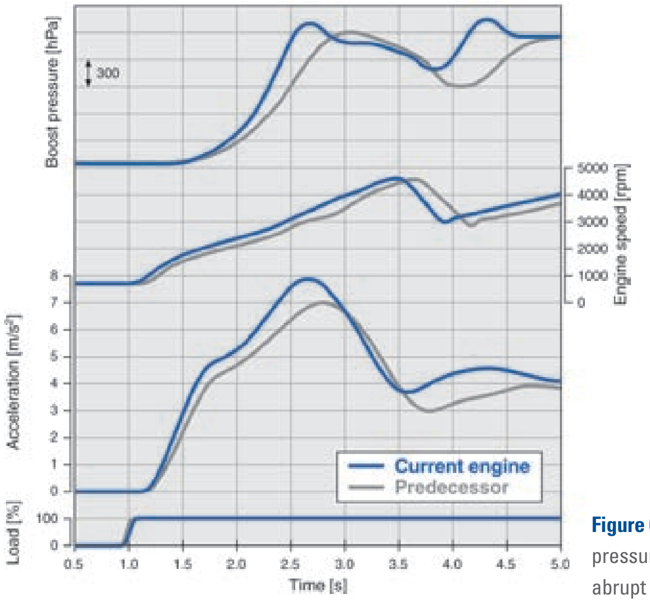

Figure 6: Improved boost pressure rise during abrupt Load increase

ing limit and an improved turbine efficiency with closed guide vanes which has a significantly positive effect on the vehicle dynamics and turbocharger acoustic properties.

The bearing case of the turbocharger is thermally isolated in order to reduce the load on the bearing. An electrical actuator with self-diagnostic capability ensures precise and fast charge pressure regulation with a low hysteresis.

Figure 6 shows the improvement achieved in comparison with the predecessor model during a typical customer startup procedure. The faster build-up of charge pressure in the new engine results in more spontaneous delivery of power and faster acceleration of the vehicle.

4.3 Exhaust-gas Recirculation

Apart from the combustion chamber optimization, an efficient, temperature-regulated and precisely dosable exhaust-gas recirculation is the key element for reducing nitrogen oxide and thus complying with the EU5 emission limits. The performance-optimized stainless steel exhaust gas cooler is positioned at the front of the engine, while the electrically operated recirculation valve is located in the inlet housing of the radiator. Further cooling is effected by the subsequent routing of the exhaust recirculation duct in the cylinder head.

To avoid the formation of condensate and to reduce the HC and CO emissions, the recirculation gas is fed in the warm-up phase or in light-load operation via an uncooled line that bypasses the fresh-air charging, **Figure 7**. The switching between these two routes is performed by a bypass valve controlled by the digital diesel electronics.

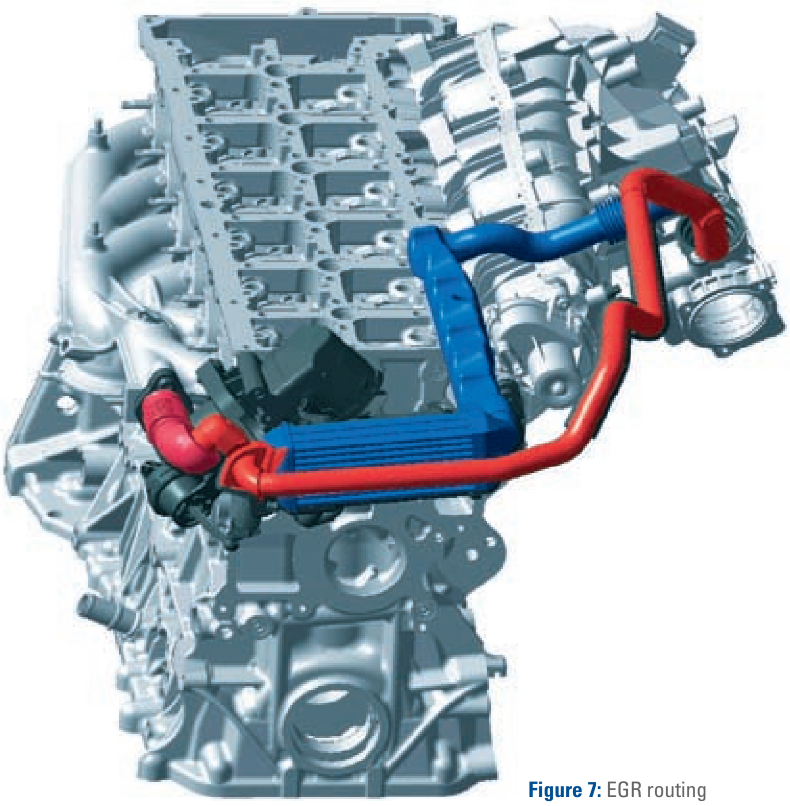

Figure 7: EGR routing

4.4 Injection System

A Bosch piezo-common-rail injection system with a maximum 1800 bar injection pressure is used for the new six-cylinder engine. The twin-ram pump with suction control required for this engine is derived from the single-piston pump used in the four-cylinder engine. Here too, great emphasis was placed on the building block principle that includes carry-over parts among the high-pressure components and actuators as well as an identical concept for the housing.

Due to the piston drive by means of roller plungers and optimized hydraulics it was possible to reduce the driving power by 20 % compared to the type of pump used previously. The transmission ratio of 1:0.75 between high-pressure pump and crankshaft guarantees a supply of fuel synchronized to the injection.

The piezo injector that has been further developed for the EU5 engine is now equipped with a seven-hole jet that has proven to be the best compromise with regard to partial load and full load characteristics. The shortening of the injection hole for better breakup of the jet and reduction of the dead space in order to reduce HC/CO were the main focus of these optimizations. The whole package is completed with detailed measures at the throttle plate and a new, non-deforming nozzle material.

The fuel is fed from the tank by means of a pressure-regulated in-tank pump that is controlled by the engine electronics.

4.5 Engine Control

The demands for engine control have risen sharply in the face of future emission legislation and the associated increases in software functions, sensors and actuators, as well as through the use of the higher-performance „FlexRay“ data transmission systems in the new 730d. For this reason, as new generation of control devices is used with the significantly more powerful processor „TC 1796“ and larger memory capacity.

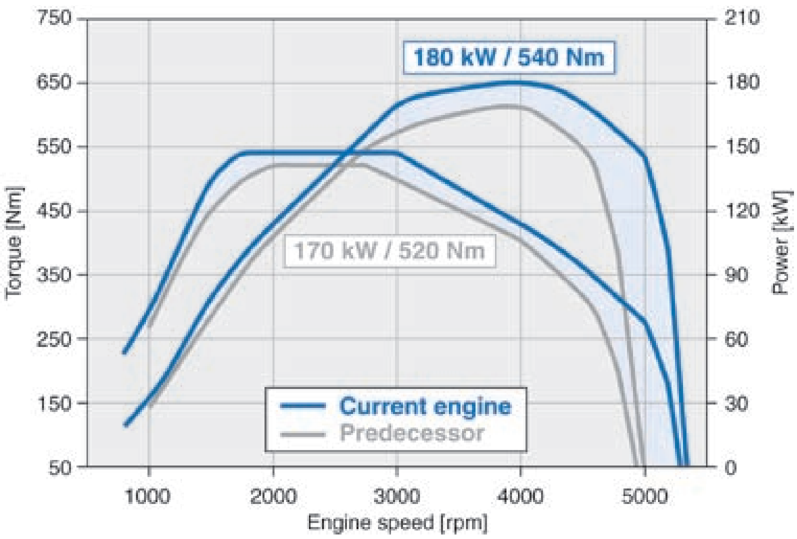

Figure 8: Power output and torque curve

5 Implementation of “BMW Efficient Dynamics”

5.1 Power and Torque

The new six-cylinder engine achieves a rated output of 180 kW and with a specific output of 60 kW/l displacement marks an optimum value for single-stage turbocharged six-cylinder diesel engines. The maximum torque is 540 Nm and is available at speeds as low as 1750/min. **Figure 8** illustrates the full-load characteristics in comparison with the previous engine. Apart from raising the maximum torque and the rated output, the usable range of speed has also been significantly extended. The cutback speed is now 5400/min, which considerably improves driving pleasure and underscores the sporting nature of the unit.

5.2 Fuel Consumption and Driving Performance

Apart from increasing the performance yield, one of the main objectives of the development was to reduce fuel consumption. By means of the consistent implementation of a host of measures on the basic engine aimed at reducing friction and the thermodynamically optimized combustion an average reduction of 4 % was achieved in the engine characteristic map.

Extended with hybrid functions, such as the intelligent generator regulation (iGR) with braking energy recovery [3], the use of the advanced six-speed automatic gearbox with reduced torque converter slip and other in-car CO_2 reducing measures, it was possible to reduce the fuel consumption of the 730d in the European test cycle from 7.8 l/100 km to just 7.2 l/100 km (192 g CO_2/km). The new 730d thus represents an unprecedented peak value in its class, **Figure 9**. In combination with the significantly improved performance (0-100 km/h in 7.2 s) this car is a convincing example of the BMW philosophy of “Efficient Dynamics”.

With a consumption of just 5.7 l/100 km or 152 g CO_2/km, and acceleration figures of 6.1 s in the 0 to 100 km/h sprint, the 330d occupies a leading position in the range of compact high-performance diesel cars.

5.3 Emissions

With the aid of the new exhaust-gas recirculation (AGR) cooling concept, it has been possible to reduce the temperature in the air intake by about 20 K compared to the previous model which, in connection with the new combustion proce-

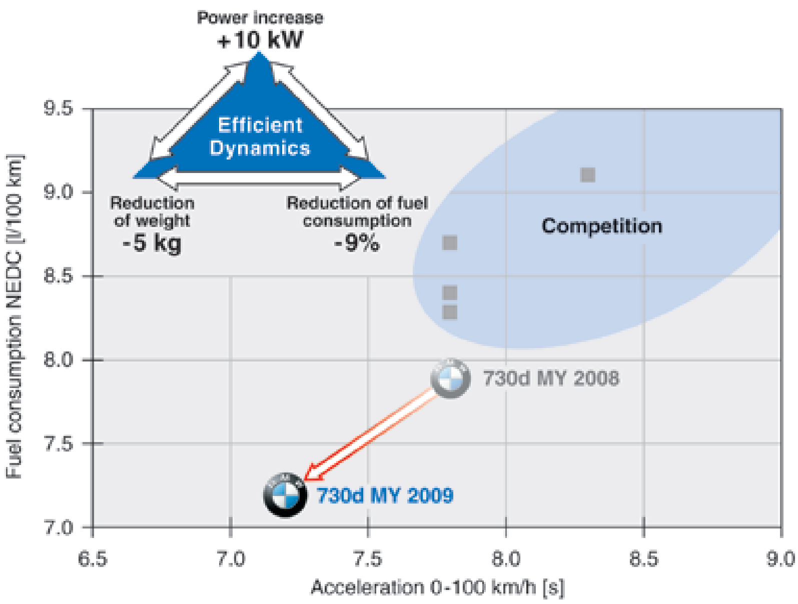

Figure 9: Fuel consumption and driving performance in comparison with competitors

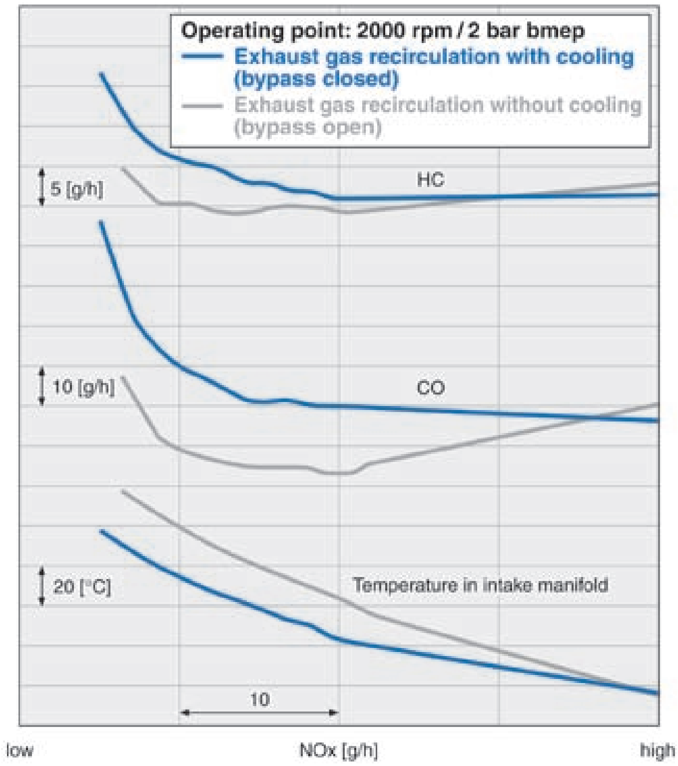

Figure 10: Influence of EGR bypass on emissions

dure, results in a significant improvement in the NO_x-particle trade off. In the engine warm-up phase the pronounced cooling of the AGR gas with regard to rising HC and CO emissions as well as condensate formation is critical, for which reason the exhaust gas is routed through a switchable, uncooled bypass channel during this phase. **Figure 10** shows the positive effect on emissions during the warm-up phase.

The standard use of a maintenance-free particle filter guarantees that the level of particle emissions remains below the traceability level.

By means of this host of optimizations, it will be possible to comply reliably with the forthcoming EU5 limit values even for heavy vehicles without additional NO_x-reducing exhaust gas treatment. The new engine thus represents an excellent basis for further developments to meet future emission limits.

6 "BMW BluePerfomance" for Complying with the EU6 Standard

For further reduction of NO_x in the 330d a storage catalytic converter has been integrated into exhaust gas treatment system in place of the oxidation catalytic converter. Equipped in this way, it already complies with the EU6 exhaust gas limits which do not come into force until 2014.

The rich operation (Lambda<1) for regular removal of noxious substances represents the challenge of the functional principle already familiar from the petrol engine. To achieve this, the fresh air mass is severely throttled and the exhaust gas enriched by further injection of fuel. As a result of the significant development of the coatings of storage catalytic converters, very high conversion rates are achieved today even after the effects of ageing and sulphurization.

To avoid the formation of hydrogen-sulphide during the necessary desulphurization, a toggle-operation is applied with cyclic lean phases to fill up the oxygen store.

In order to ensure that the necessary changes of operating mode run unnoticed by the driver and with the quality required for removal of noxious substances, extensive optimizations are required.

7 Summary

With its new generation of engines, BMW is setting the course for greater driving enjoyment and improved efficiency while significantly reducing emissions. With an output of 180 kW at an engine speed of 4000/min and a maximum torque of 540 Nm that is available at just 1750/min, this unit sets new standards for sporting characteristics in the field of six-cylinder diesel engines. With significantly reduced fuel consumption and CO_2 values, the second objective of the „BMW EfficientDynamics“ development strategy has been met in an impressive manner.

Even in its basic configuration, the engine is below the limits specified by the further EU5 standard for exhaust gases. Extended to include the „BMW BluePerformance“ technology, the 330d already complies with the EU6 emission limits that will not apply until 2014, without any loss of enjoyment in the driving experience. This means that in the competitive world of six-cylinder diesel engined cars, BMW not only occupies the No. 1 position in terms of performance, but also for fuel consumption and emissions.

References

[1] Steinparzer, F.; Mattes, W.; Nefischer, P.; Wichtl, R.: Der neue Vierzylinder-Dieselmotor von BMW (The new 2.0l 4-cylinder engine from BMW). In: MTZ 2007, No. 11 and 12

[2] Steinparzer, F.; Mattes, W.; Nefischer, P.; Wichtl, R.: BMW-Sechszylinder-Dieselmotor mit Euro-4-Technik (The new 3.0l 6-cylinder engine from BMW). In: MTZ 2004 No. 7

[3] Liebl, J.: BMW Efficient Dynamics – Emissionsminderung kann auch faszinieren (Reducing emission can also be fascinating). Emission Control 2008, Dresden

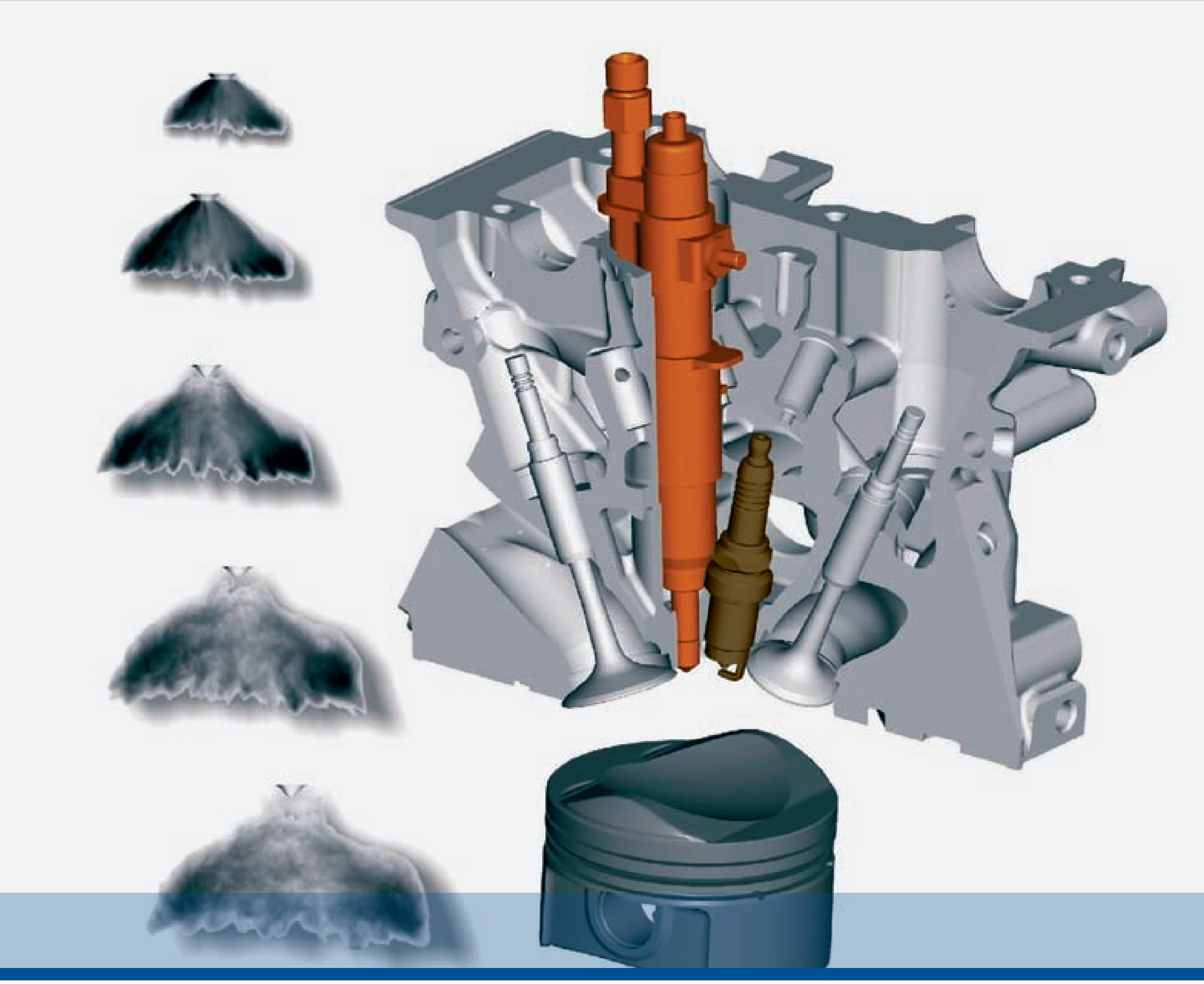

The Potential of Turbo-charged Gasoline Engines with Spray Guided Direct Injection

In this article a 2.0 l turbocharged FSI engine forms the basis for analysis of spray guided combustion with central location of injector and spark plug. The long duration experience in the field of the Volkswagen brands since introducing the first generation of gasoline direct injection into market in 1999 stands for extraordinary competence in the domain of gasoline direct injection.

1 Introduction

Since the 1970s, stratified charge in DI gasoline engines has been the focus of a wide range of investigations. Currently, the largest potential in terms of a customerrelevant reduction in fuel consumption can be seen in the spray guided combustion process with centrally located injectors and outward opening nozzles [1, 2].

The combination of stratified charge and turbo charging represents a promising variant [3] and a major challenge in this combustion process. The aim is to find a compromise from the reduced compression compared to naturally aspirated engines, a high charge air movement – essential for turbocharged engines –, the design of exhaust gas recirculation systems and the way pistons and the combustion chamber roof are engineered, whilst making allowance for the different modes of operation.

2 Motivation

A glance at the current global energy reserves and resources clearly shows that it is of no consequence which type of energy is considered. The reserves are finite and the costs of making resources accessible will rise. Current scenarios anticipate that the maximum flow of oil production will be reached by about 2010 [4]. Within the next 10 to 20 years a rise in the difference between reserves/resources and demand will lead to a dramatic rise in fuel prices. Against this background, the development of low consumption drive technologies to achieve a short to mid-term reduction in the energy requirement is of utmost importance in addition to alternative drive concepts.

The application of demonstrable operating zones in different modes of operation of the turbocharged, spray guided combustion process in the characteristic map and a subsequent projection of experienced consumption potentials over comparable engines are the subject of examinations. The determined best-case fuel consumption engine maps are critically evaluated under consideration of the maximal acceptable nitric oxide emissions, the needed charge motion for full load operation and the light-off limit of the exhaust gas aftertreatment system. Subsequent fuel projections give information about the fuel consumption reduction potential in several driving cycles. Finally, the achieved fuel consumption when running the engine in stratified mode is compared to conventional homogenous mode.

3 Spray Guided Gasoline Direct Injection

A survey from Shell [5] and also a current survey and prognosis from Esso [6] show that on modern combustion engines a

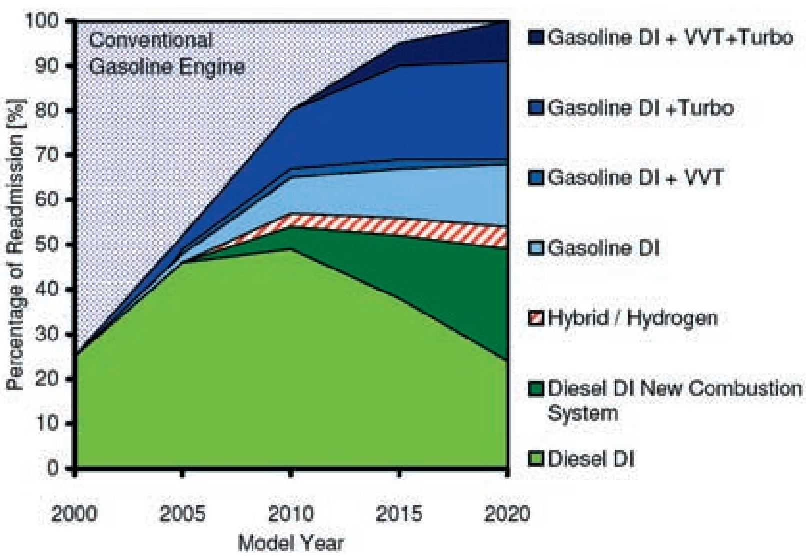

Figure 1: Prognosis of mix of different combustion processes for 2000 to 2020 (Source: Group Research of Volkswagen AG)

The Authors

Dipl.-Ing.
Jürgen Willand
is head of research gasoline engines within the research department of Volkswagen AG in Wolfsburg (Germany).

Dr.-Ing.
Kay Schintzel
was project manager drivetrain gasoline engines within the research department of Volkswagen AG in Wolfsburg (Germany).

Dipl.-Ing.
Henrik Hoffmeyer
is doctoral candidate in the field drivetrain gasoline engines within the research department of Volkswagen AG in Wolfsburg (Germany).

declining average consumption is evident. Despite major advancements in the development of alternative vehicle drive systems and energy sources, the combustion engine in all its derivatives is still the dominating drive system in motor vehicles. **Figure 1** shows a prognosis of percentages of new registrations with new and future combustion processes in the European sector.

As a result of the continually rising individual requirement for mobility from modern societies and the mid-term use of combustion engines, without alternative, the development of new gasoline engine combustion processes to reduce fuel consumption and harmful emissions is of considerable importance.

One approach is represented by spray guided gasoline direct injection with turbo charging and stratified charge (TSGI – Turbocharged Spray Guided Injection). **Figure 2** shows the concept of the turbocharged spray-guided gasoline direct injection.

The aim was to broaden the onroad fuel consumption relevant map range by means of stratified charge. The piezo injector used in these investigations is located centrally in the combustion chamber roof and the spark plug is located laterally on the exhaust side [7, 8].

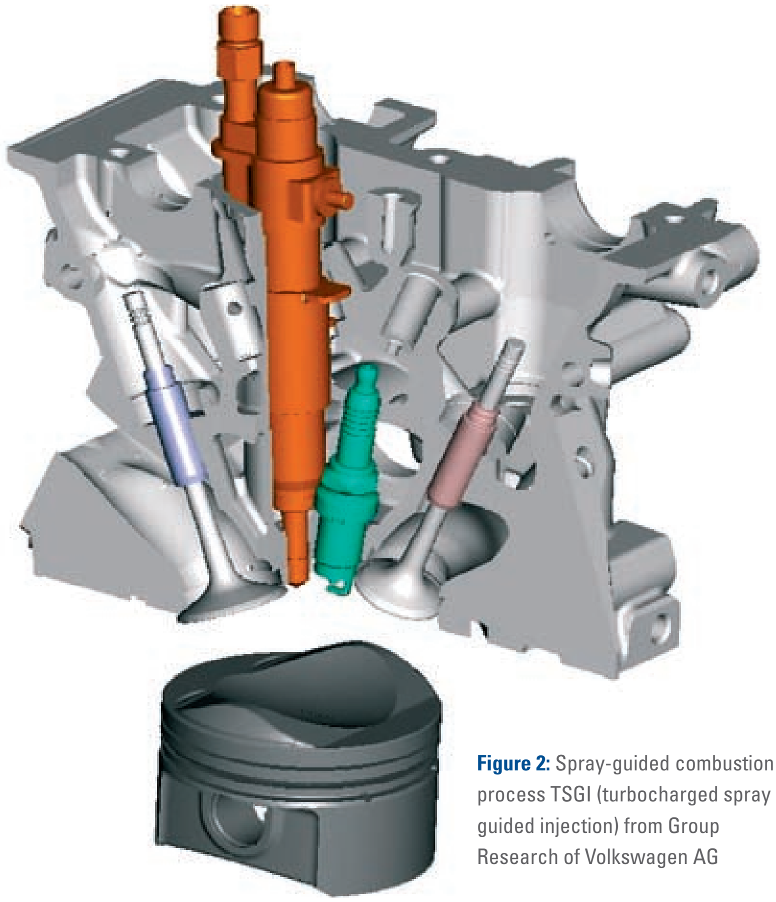

Figure 2: Spray-guided combustion process TSGI (turbocharged spray guided injection) from Group Research of Volkswagen AG

4 Results

Stationary test bench investigations are the fundament of evaluation of the turbocharged spray guided combustion process. Besides the detailed analysis of the stratified mode other possible injection modes have to be compared and evaluated. Thus operation strategies can be developed and their influence of the entire potential can be determined.

4.1 Operating Modes of Spray Guided Combustion Process

Next to injection timing and fuel pressure, further technical parameters such as charge air movement flap, externally cooled exhaust gas recirculation and nitrogen oxide emissions after treatment are required for optimal application of stratified mode.

As super ordinate operating modes of the spray guided combustion process, the following should be subject to closer investigation and evaluation, **Table**.

On the engine test bench, the test engine was run in the different injection modes. In doing so load variations at different engine speeds were carried out. **Figure 3** shows exemplarily the indicated specific fuel consumption ISFC and the NO_x mass flow rate NO_x at a load variation at rev = 1500 rpm.

Starting at an indicated mean pressure of IMEP = 2 bar, the engine is run in stratified mode with activated EGR (SCH+EGR). Where the consumption curves in lean stoichiometrical compression stroke injection (SCH + EGR) operation cross with lean stoichiometrical suction stroke injection (HMM) operation at a load of IMEP = 6 bar, this marks the determined reasonable upper load threshold of the advantage in efficiency of stratified operation (1).

Running the engine in lean homogeneous suction stroke injection (HMM), the nitric oxide emissions reach with further increasing engine load up to seven bar (2) a limit of 70 g/h. Based on extensive experience in the field, this limit is chosen for the maximal acceptable raw emission impact on a nitric oxide storage catalyst.

Consequently, the engine injection mode is switched to stoichiometrical homogenous suction stroke injection with EGR (HOM+EGR). This can be used as con-

Table: Operating modes of the spray guided combustion process for turbo-charged engines

Injection mode	Mixture formation	λ	AGR	Naming
Suction stroke injection	homogeneous	$\lambda = 1$	–	HOM
Suction stroke injection	homogeneous	$\lambda = 1$	External EGR	HOM + EGR
Suction stroke injection	homogeneous	$\lambda > 1$	–	HMM
Compression stroke injection	stratified	$\lambda > 1$	External EGR	SCH + EGR

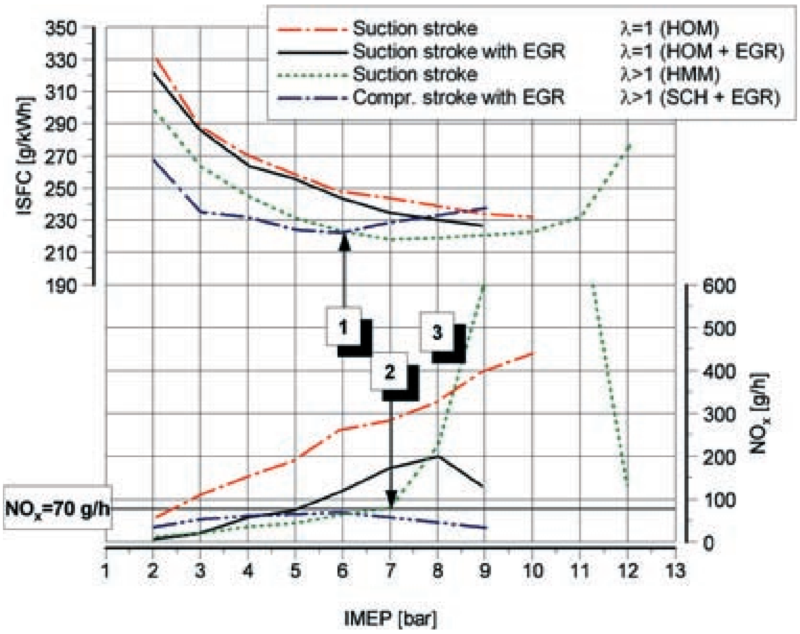

Figure 3: Indicated specific fuel consumption and nitrogen oxide mass flow of TSGI operating modes for a load variation; n_{mot}=1500 rpm, gas exchange, injection and ignition point optimal for fuel consumption, EGR rate maximum

sumption favorable injection strategy from 8 bar on up to full load condition (3).

The strong increase of nitric oxide emissions in lean homogeneous mode (HMM) can be reasoned by a continuous decrease of excess air with increasing engine load. Thus, the nitric oxide emissions show the characteristic progress when decreasing air-/fuel ratio with a peak at about λ=1.15.

For thermodynamical analysis of the pressure curves recorded during test bench investigations a split of losses according to Weberbauer et al [9] is helpful. **Figure 4** shows the distribution of loss of a detailed pressure curve analysis of the operating modes at a constant driving point of the NEDC. Starting from the theoretical degree of efficiency, calculated from the geometric compression ratio and a constant isentropic exponent, the losses are calculated from

- the thermodynamic compression ratio ($\Delta\eta_\varepsilon$)
- the actual charge as a function of the air/fuel ratio and the overall residual gas rate, expressed via the isentropic exponent ($\Delta\eta_\kappa$)
- energy release at the calculated fifty percent energy conversion point ($\Delta\eta_{MFB50\%}$)
- incomplete combustion ($\Delta\eta_{HC+CO}$)
- in consideration of the real combustion curve ($\Delta\eta_{Comb}$)
- in consideration of the real gas properties ($\Delta\eta_{Calorics}$)
- by the wall heat transfer ($\Delta\eta_{Wall\ heat}$)
- in consideration of real expansion ($\Delta\eta_{Exp}$)
- the gas exchange ($\Delta\eta_{Gas\ ex}$).

It is possible to see an advantage in the efficiency factor here through dethrottling ($\Delta\eta_{Gas\ ex}$) with the use of external, cooled EGR in homogenous mode. This advantage increase when diluting the charge with air in the lean stoichiometrical suction stroke injection (HMM) mode. By diluting with air, the polytrope exponent rises ($\Delta\eta_\kappa$). The caloric losses are lower ($\Delta\eta_{Calorics}$). Moreover, the wall heat losses ($\Delta\eta_{Wall\ heat}$) decline from the greater degree of diluting. The higher achievable diluting rate leads to a higher air requirement. Further dethrottling is possible. The degree of indicated efficiency (η_i) rises.

In stratified charge mode, the losses from the actual charge are not as high due to greater diluting, though this advantage is balanced out in part by a greater internal residual gas quantity compared with suction stroke injection modes. Due to the lower enthalpy at the turbine there is an unfavorable decline in scavenging at low load in stratified charge mode. With regards to the constant volume cycle process, the near optimum 50 % conversion point shortly after ignition TDC, **Figure 5**, leads to an almost maximum degree of efficiency in the constant volume cycle process ($\Delta\eta_{MFB50\%}$).

However, at a rate of 20 % EGR results at this point in less stable combustion ($\Delta\eta_{HC+CO}$ increases) and also a longer combustion period with longer burnout ($\Delta\eta_{Comb}$) compared to stoichiometrical suction stroke injection (HOM) mode and also just marginally lower wall heat losses ($\Delta\eta_{Wall\ heat}$). The longer burnout partly balances out the advantage of lower gas temperatures close to the combustion chamber wall. Despite the poor degree of turbine efficiency, the gas exchange losses are marginal. The advantage of dethrottling far outweighs this.

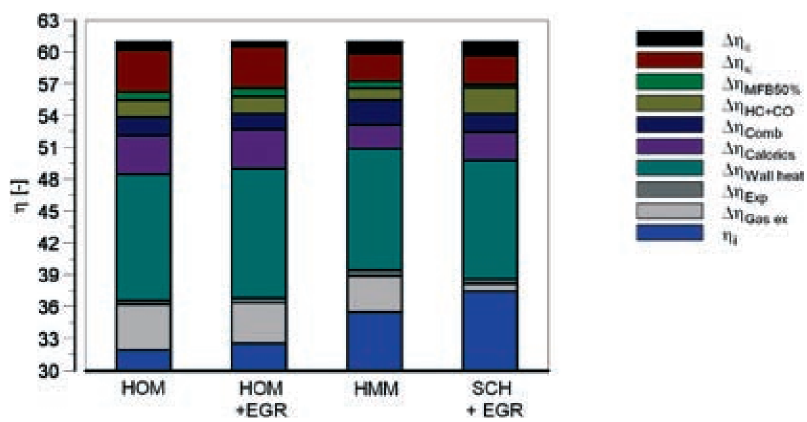

Figure 4: Split of losses of TSGI operating modes at characteristic constant driving point in NEDC; rev = 1500 rpm, IMEP = 4 bar; gas exchange, injection and ignition point at optimum for fuel consumption, EGR rate maximum

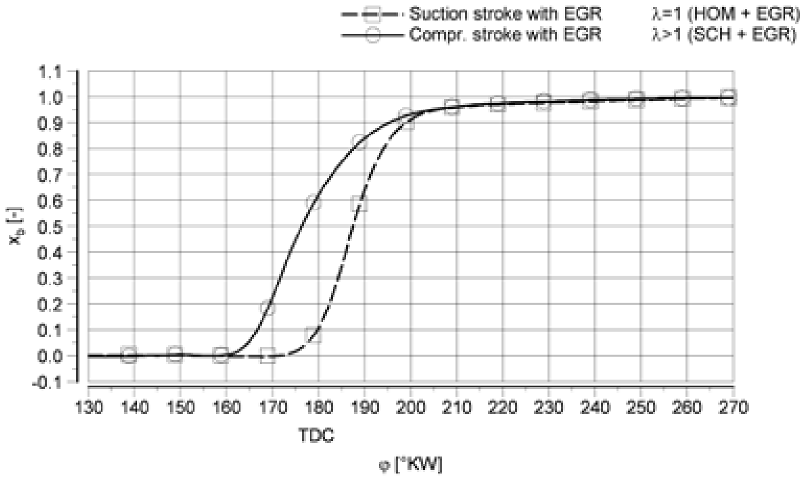

Figure 5: Normalized mass fraction burned x_b for stoichiometric suction stroke injection with EGR (HOM+EGR) and lean compression stroke injection with EGR (SCH+EGR) at characteristic constant driving point in NEDC; TDC: φ = 180° CA; rev = 1500 rpm, IMEP = 4 bar; gas exchange, injection and ignition point at optimum for fuel consumption, EGR rate maximum

In summary, the advantage in consumption in stratified charge mode arises mainly from the reduction in gas exchange losses. The theoretical advantage from the greater degree of diluting is countermanded in the turbocharged engine on one hand by the unfavorable degree of turbine efficiency as a result of low exhaust gas temperature. On the other hand, the required high EGR rates lead to a less stable combustion with respective losses.

Moreover, when running a turbo charged engine, a reduced spark position is necessary for avoiding a thermal overloading. This leads to disadvantages in stratified charge mode.

4.2 Engine Map During Operation with Stratified Charge

The effective engine map range in stratified charge mode is restricted by the available exhaust gas after treatment of nitrogen oxide mass flow rates. **Figure 6** shows in green the effective engine map ranges for a applicable stratified charge mode. The engine map range with low tumble is illustrated in grey in consideration of the exhaust gas after treatment systems available on the market today (max. nitrogen oxide mass flow rate $NO_{x,DS}$ = 70 g/h). The blue area describes the achievable engine map range with high tumble in consideration of the exhaust gas after treatment systems available on the market today (max. nitrogen oxide mass flow rate $NO_{x,DS}$ = 70 g/h). Finally, the red area marks the engine map range when the light-off temperature of the catalyst is fallen below its limit.

With a charge optimized intake port advantageous for stratified charge operation in consideration of nitric oxide emissions with a low tumble, a large share of the load collective in the NEDC can be covered with an effective engine map range up to a load of IMEP = 6 to 7 bar and up to an engine speed of rev = 3500 to 4000 rpm (grey illustrated). For a turbocharged engine with stratified charge operation, a turbo intake port with high tumble in the flow rate is indispensable for satisfactory high and full load combustion.

To generate increased turbulent kinetic energy, targeted discharges are engineered in the intake port. This leads to a reduction in the effective flow rate cross sectional area in the region of the intake valves and thereby to locally higher flow velocities during intake as well as a higher turbulent fluctuation intensity [11]. The due to the higher flow velocity induced flow impulse leads to increased cyclic fluctuations and destabilizes the stratified charge at the withdrawn ignition site and therefore an unstable ignition. To achieve satisfactory stability in the mixture formation and combustion, considerably "earlier" injection and ignition points are necessary compared to stratified operation with a charge optimized intake port. The subsequent "premature" point of combustion leads to increased NO_x emissions, lower exhaust gas temperatures and also indicated efficiency factor losses. In this way, the useable engine map range is markedly reduced at higher and also lower loads (blue and red area).

Figure 7 shows the full load development of the three investigated engine configurations characterized by the point minimal engine speed at maximum brake torque. In the context of full-load investigations it could be observed that within a reasonable combination of turbo charging and stratified operation there is a specific load threshold of 150 Nm/l or 75 kW/l [10], (Mark 1). Limiting values are the increasing knock tendency and unacceptable smoke emissions caused by insufficient carburetion. An increase of maximum torque up to the aspired 175 Nm/l

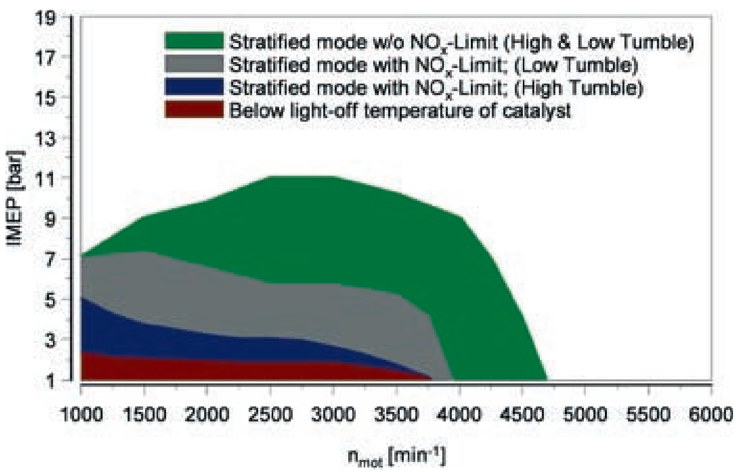

Figure 6: Engine map ranges in stratified charge operation for a turbocharged, spray guided combustion process; Nitric oxide emission limit (stratified mode) 70 g/h

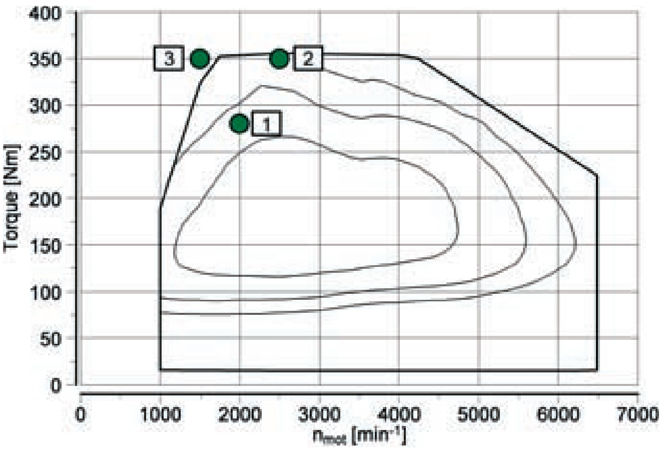

Figure 7: Characteristic full load operation points for three engine configurations

can only be reached by using a turbo intake port with high tumble (Mark 2).

Caused by the increased charge motion when using a high tumble inlet port, the carburetion is sustainable improved and the limit of engine knock is moved to advantageous timing point. But in stratified mode, the increased charge motion leads to a smaller usable engine map like shown in Figure 6.

Due to an optimization of the exhaust valve timings, which can be produced using a variable valve train, the maximum brake torque at lower engine speeds can be increased considerably (Mark 3). The valve lift timing optimization leads additionally to a reduction of gas exchange losses during part load condition.

4.3 Fuel Consumption Projections

In order to also take the overall potential into consideration at the end of the detailed analysis of combustion properties and subsequent changes in the degree of efficiency, fuel consumption projections were carried out for different engine versions. **Figure 8** shows calculated fuel consumptions differences in the NEDC for three engine configurations with or without stratified mode.

When combining turbo charging with stratified operation using a low tumble intake port (1) an advantage in fuel consumption of a about 10 % is achievable compared to the homogenous suction stroke injection mode. Concerning the full load performance, this engine configuration is limited up to a maximal specific brake torque of 150 Nm/l. Using a high tumble intake port for achieving a maximal specific brake torque of 175 Nm/l (2), the advantage in fuel consumption because of stratified operation is reduced to 6 % due to the reduced applicable range of stratified mode in the engine map, Figure 6. There is no change of fuel consumption in homogenous mode to be expected.

Engineering variable valve train technology (3), the NEDC fuel consumption can be lowered up to 10 % in homogenous mode compared to engine configuration (2) with a conventional exhaust cam shaft. Due to the considerably reduced gas exchange losses using optimized gas exchange timings, most of the possible fuel consumption potential of stratified operation can be achieved. An additional operation using charge stratification will achieve a residual advantage in fuel consumption of only 2.5 %.

Furthermore, it becomes perspicuous that, with an optimization of a conventional combustion processes, outstanding results in fuel consumption can be achieved. Depending on the “downsizing factor”, robust stoichiometrical homogenous combustion processes are able to achieve lower driving cycle consumptions than the more sensible stratified combustion processes [12]. In consideration of a cost-benefit ratio an optimized conventional combustion process seems to be the preferential solution.

5 Summary and Outlook

The theoretical advantage of enhancing the useable characteristic map range with stratified charge is not accessible due to the nitrogen oxide exhaust after treatment systems available today as a series production solution. The generation of high charge air movement, necessary to achieve a satisfactory low-end torque response, further restricts the effective characteristic map range. Together with the shift in operating point towards higher loads and contemporaneously reduced engine speeds, which is targeted for turbocharged engines, a noticeable advantage

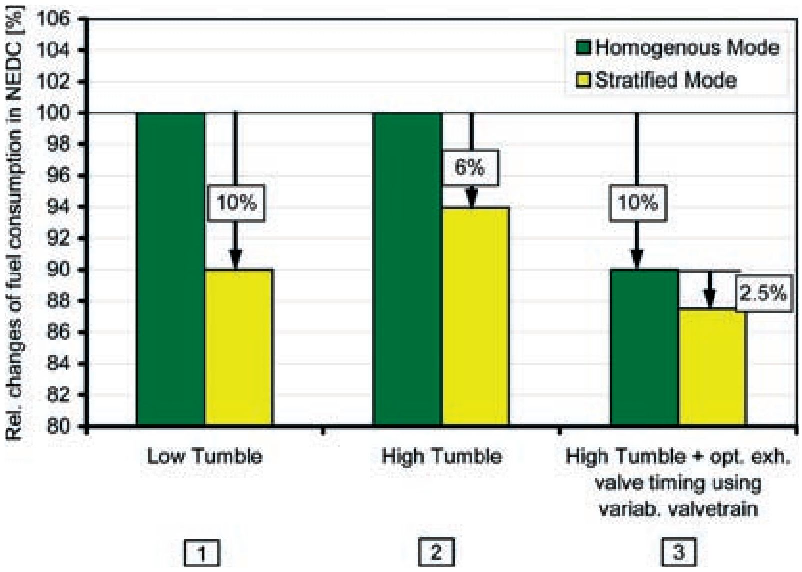

Figure 8: Fuel consumption projections for three engine configurations with and without stratified mode in the NEDC; VW Golf V, vehicle weight and gear transmission ratio from serial production, Nitric oxide emission limit (stratified mode) 70 g/h

in consumption is currently no longer evident for the customer. Today competing downsizing technologies show a higher potential for reducing fuel consumption in the NEDC as well as for the customer.

The future of the turbocharged, spray guided combustion process is linked with the conversion potential and fuel consumption related conversion efficiency of available exhaust gas after treatment systems in the future. As a further challenge a combustion process with a stable and efficient combustion at part load as well as a satisfying full load performance needs to be proposed.

References

[1] Waltner, A.; Lückert, P.; Schaupp, U.; Rau, E.; Kemmler, R.; Weller, R.: Die Zukunftstechnologie des Ottomotors: Strahlgeführte Direkteinspritzung mit Piezo-Injektor. 27. Internationales Wiener Motorensymposium; Wien (2006)

[2] Willand, J.; Suck, G.; Schintzel, K.: Anforderungen an die Einspritzsysteme strahlgeführter Brennverfahren. 4. Tagung Diesel- und Benzindirekteinspritzung; Haus der Technik Berlin (2004)

[3] Klüting, M.; Missy, S.; Schwarz, C.: Potentiale des strahlgeführten Benzin-DI-Brennverfahrens in Verbindung mit Aufladung. 26. Internationales Wiener Motorensymposium, S. 103-122; Wien (2005)

[4] Campbell: Uppsala Hydrocarbon Depletion Study Group, Scenario Update by http://www.peakoil.net/uhdsg/Default.htm; (2004)

[5] N.N.: Shell PKW Szenarien bis 2030, Flexibilität bestimmt Motorisierung, (2004)

[6] N.N.: ESSO Energieprognose 2003, (2003)

[7] Schintzel, K.; Willand, J.; Hoffmeyer, H.; Die Entwicklung strahlgeführter Brennverfahren im Spannungsfeld zwischen Potenzial und Kosten. 5. Tagung Diesel- und Benzindirekteinspritzung; Haus der Technik Berlin (2006)

[8] Schintzel, K.; Willand, J.: Klopfphänomene am Beispiel ausgewählter Motoren der Volkswagen AG. 2. IAV-Symposium „2. Tagung Klopfregelung für Ottomotoren – Trends für Serienentwickler"; Berlin (2006)

[9] Weberbauer, F.; Rauscher, M.; Kulzer, A.; Knopf, M.; Bargende, M.: Allgemein gültige Verlustteilung für neue Brennverfahren. In: MTZ 2005 Nr. 2, S. 120-124

[10] Schintzel, K.; Willand, J., Hoffmeyer, H., Schulz, R.: Neue ottomotorische Brennverfahren – Alternativen zum Dieselmotor. 7. Tagung Direkteinspritzung im Ottomotor; Haus der Technik Essen (2007)

[11] Wurms, R.; Kuhn, M.; Zeilbeck, A.; Adam, S.; Krebs, R.; Hatz, W.: Die Audi Turbo FSI Technologie. 13. Aachener Kolloquium Fahrzeug- und Motorentechnik; Aachen (2003)

[12] Willand, J.: Motortrends zur CO_2-Reduzierung: Downsizing oder Teillastbrennverfahren? MTZ-Konferenz „Der Antrieb von morgen"; München (2008)

IMPRINT

MTZ WORLDWIDE

www.MTZ-online.com

02|2009 · February 2009 · Volume 70

Springer Automotive Media | GWV Fachverlage GmbH
P.O. Box 15 46 · 65173 Wiesbaden · Germany
Abraham-Lincoln-Straße 46 · 65189 Wiesbaden · Germany

Managing Directors Dr. Ralf Birkelbach, Albrecht Schirmacher
Advertising Director Thomas Werner
Production Director Ingo Eichel
Sales Director Gabriel Göttlinger

EDITORS-IN-CHARGE

Dr.-Ing. E. h. Richard van Basshuysen
Wolfgang Siebenpfeiffer

EDITORIAL STAFF

Editor-in-Chief
Johannes Winterhagen (win)
Phone +49 611 7878-342 · Fax +49 611 7878-462
E-Mail: johannes.winterhagen@springer.com

Vice-Editor-in-Chief
Dipl.-Ing. Michael Reichenbach (rei)
Phone +49 611 7878-341 · Fax +49 611 7878-462
E-Mail: michael.reichenbach@springer.com

Chief-on-Duty
Kirsten Beckmann M. A. (kb)
Phone +49 611 7878-343 · Fax +49 611 7878-462
E-Mail: kirsten.beckmann@springer.com

Sections

Electrics, Electronics
Markus Schöttle (scho)
Phone +49 611 7878-257 · Fax +49 611 7878-462
E-Mail: markus.schoettle@springer.com

Engine
Dipl.-Ing. (FH) Richard Backhaus (rb)
Phone +49 611 5045-982 · Fax +49 611 5045-983
E-Mail: richard.backhaus@rb-communications.de

Heavy Duty Techniques
Ruben Danisch (rd)
Phone +49 611 7878-393 · Fax +49 611 7878-462
E-Mail: ruben.danisch@springer.com

Online
Dipl.-Ing. (FH) Caterina Schröder (cs)
Phone +49 611 78 78-190 · Fax +49 611 7878-462
E-Mail: caterina.schroeder@springer.com

Production, Materials
Stefan Schlott (hlo)
Phone +49 8191 70845 · Fax +49 8191 66002
E-Mail: Redaktion_Schlott@gmx.net

Service, Event Calendar
Martina Schraad
Phone +49 212 64 235 16
E-Mail: martina.schraad@springer.com

Transmission, Research
Dipl.-Ing. Michael Reichenbach (rei)
Phone +49 611 7878-341 · Fax +49 611 7878-462
E-Mail: michael.reichenbach@springer.com

English Language Consultant
Paul Willin (pw)

Permanent Contributors
Christian Bartsch (cb), Prof. Dr.-Ing. Peter Boy (bo), Prof. Dr.-Ing. Stefan Breuer (sb), Jens Büchling (jb), Jörg Christoffel (jc), Jürgen Grandel (gl), Erich Hoepke (ho), Ulrich Knorra (kno), Prof. Dr.-Ing. Fred Schäfer (fs), Roland Schedel (rs), Bettina Seehawer (bs)

Address
P.O. Box 1546, 65173 Wiesbaden, Germany
E-Mail: redaktion@ATZonline.de

MARKETING | OFFPRINTS

Product Management Automedia
Sabrina Brokopp
Phone +49 611 7878-192 · Fax +49 611 7878-407
E-Mail: sabrina.brokopp@springer.com

Offprints
Martin Leopold
Phone +49 2642 9075-96 · Fax +49 2642 9075-97
E-Mail: leopold@medien-kontor.de

ADVERTISING | GWV MEDIA

Key Account Manager
Elisabeth Maßfeller
Phone +49 611 7878-399 · Fax +49 611 7878-140
E-Mail: elisabeth.massfeller@gwv-media.de

Ad Sales
Frank Nagel
Phone +49 611 7878-395 · Fax +49 611 7878-140
E-Mail: frank.nagel@gwv-media.de

Display Ad Manager
Susanne Bretschneider
Phone +49 611 7878-153 · Fax +49 611 7878-443
E-Mail: susanne.bretschneider@gwv-media.de

Ad Prices
Price List No. 52

SUBSCRIPTIONS

VVA-Zeitschriftenservice, Abt. D6 F6, MTZ
P. O. Box 77 77, 33310 Gütersloh, Germany
Renate Vies
Phone +49 5241 80-1692 · Fax +49 5241 80-9620
E-Mail: SpringerAutomotive@abo-service.info

SUBSCRIPTION CONDITIONS

The emagazine appears 11 times a year at an annual subscription rate of 269 €. Special rate for students on proof of status in the form of current registration certificate 124 €. Special rate for VDI/ÖVK/VKS members on proof of status in the form of current member certificate 208 €. Special rate for studying VDI members on proof of status in the form of current registration and member certificate 89 €. The subscribtion can be cancelled in written form at any time with effect from the next available issue.

PRODUCTION | LAYOUT

Heiko Köllner
Phone +49 611 7878-177 · Fax +49 611 7878-464
E-Mail: heiko.koellner@gwv-fachverlage.de

HINTS FOR AUTHORS

All manuscripts should be sent directly to the editors. By submitting photographs and drawings the sender releases the publishers from claims by third parties. Only works not yet published in Germany or abroad can generally be accepted for publication. The manuscripts must not be offered for publication to other journals simultaneously. In accepting the manuscript the publisher acquires the right to produce royalty-free offprints. The journal and all articles and figures are protected by copyright. Any utilisation beyond the strict limits of the copyright law without permission of the publisher is illegal. This applies particularly to duplications, translations, microfilming and storage and processing in electronic systems.

Springer Automotive Media is part of the specialist publishing group Springer Science+Business Media.

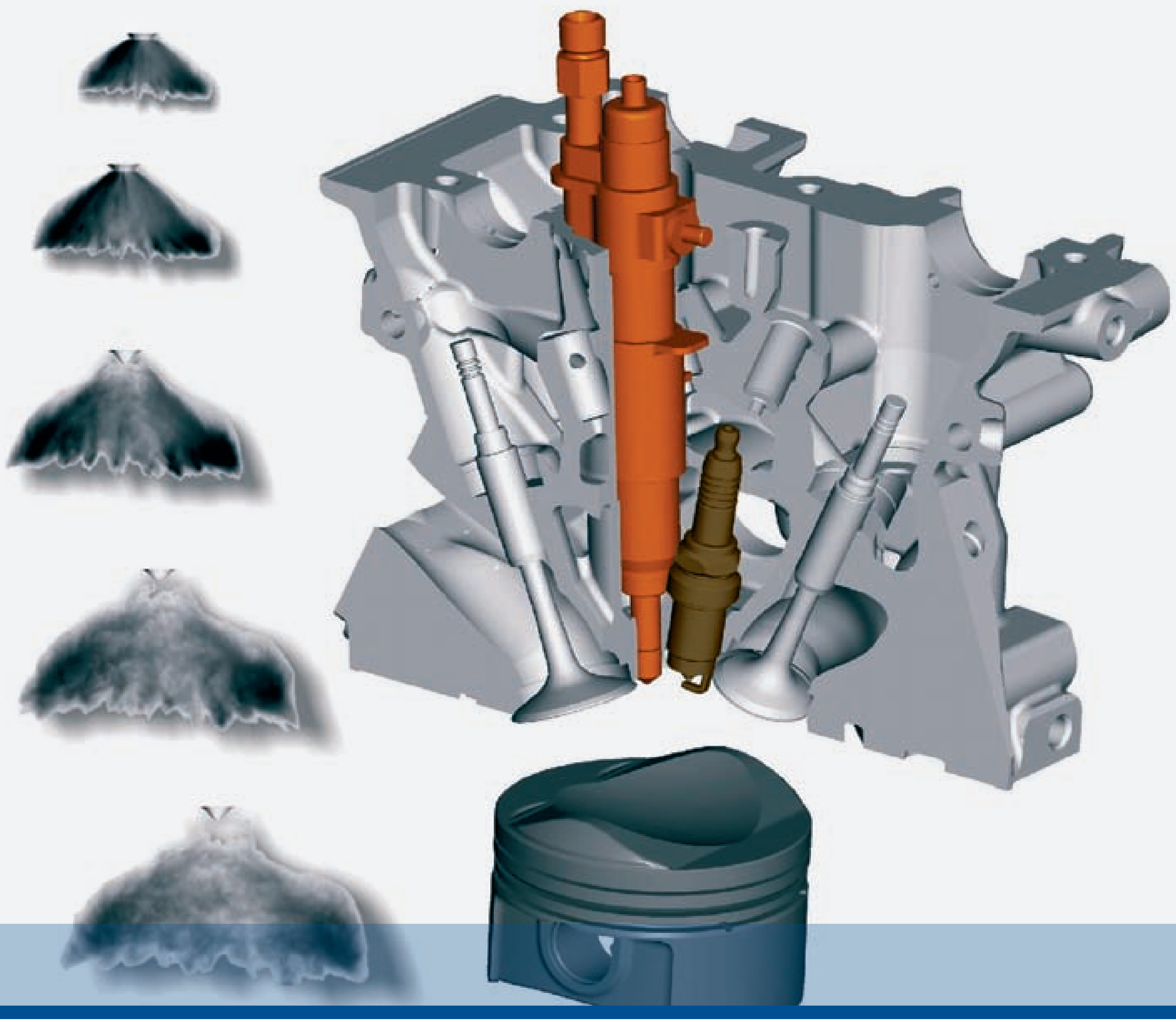

The Potential of Turbo-charged Gasoline Engines with Spray Guided Direct Injection

In this article a 2.0 l turbocharged FSI engine forms the basis for analysis of spray guided combustion with central location of injector and spark plug. The long duration experience in the field of the Volkswagen brands since introducing the first generation of gasoline direct injection into market in 1999 stands for extraordinary competence in the domain of gasoline direct injection.

1 Introduction

Since the 1970s, stratified charge in DI gasoline engines has been the focus of a wide range of investigations. Currently, the largest potential in terms of a customerrelevant reduction in fuel consumption can be seen in the spray guided combustion process with centrally located injectors and outward opening nozzles [1, 2].

The combination of stratified charge and turbo charging represents a promising variant [3] and a major challenge in this combustion process. The aim is to find a compromise from the reduced compression compared to naturally aspirated engines, a high charge air movement – essential for turbocharged engines –, the design of exhaust gas recirculation systems and the way pistons and the combustion chamber roof are engineered, whilst making allowance for the different modes of operation.

2 Motivation

A glance at the current global energy reserves and resources clearly shows that it is of no consequence which type of energy is considered. The reserves are finite and the costs of making resources accessible will rise. Current scenarios anticipate that the maximum flow of oil production will be reached by about 2010 [4]. Within the next 10 to 20 years a rise in the difference between reserves/resources and demand will lead to a dramatic rise in fuel prices. Against this background, the development of low consumption drive technologies to achieve a short to mid-term reduction in the energy requirement is of utmost importance in addition to alternative drive concepts.

The application of demonstrable operating zones in different modes of operation of the turbocharged, spray guided combustion process in the characteristic map and a subsequent projection of experienced consumption potentials over comparable engines are the subject of examinations. The determined best-case fuel consumption engine maps are critically evaluated under consideration of the maximal acceptable nitric oxide emissions, the needed charge motion for full load operation and the light-off limit of the exhaust gas aftertreatment system. Subsequent fuel projections give information about the fuel consumption reduction potential in several driving cycles. Finally, the achieved fuel consumption when running the engine in stratified mode is compared to conventional homogenous mode.

3 Spray Guided Gasoline Direct Injection

A survey from Shell [5] and also a current survey and prognosis from Esso [6] show that on modern combustion engines a

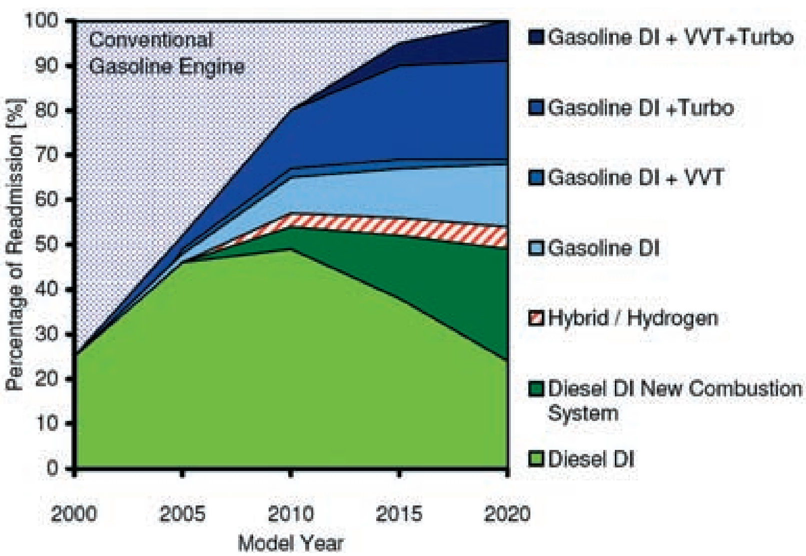

Figure 1: Prognosis of mix of different combustion processes for 2000 to 2020 (Source: Group Research of Volkswagen AG)

The Authors

Dipl.-Ing.
Jürgen Willand
is head of research gasoline engines within the research department of Volkswagen AG in Wolfsburg (Germany).

Dr.-Ing.
Kay Schintzel
was project manager drivetrain gasoline engines within the research department of Volkswagen AG in Wolfsburg (Germany).

Dipl.-Ing.
Henrik Hoffmeyer
is doctoral candidate in the field drivetrain gasoline engines within the research department of Volkswagen AG in Wolfsburg (Germany).

declining average consumption is evident. Despite major advancements in the development of alternative vehicle drive systems and energy sources, the combustion engine in all its derivatives is still the dominating drive system in motor vehicles. **Figure 1** shows a prognosis of percentages of new registrations with new and future combustion processes in the European sector.

As a result of the continually rising individual requirement for mobility from modern societies and the mid-term use of combustion engines, without alternative, the development of new gasoline engine combustion processes to reduce fuel consumption and harmful emissions is of considerable importance.

One approach is represented by spray guided gasoline direct injection with turbo charging and stratified charge (TSGI – Turbocharged Spray Guided Injection). **Figure 2** shows the concept of the turbocharged spray-guided gasoline direct injection.

The aim was to broaden the onroad fuel consumption relevant map range by means of stratified charge. The piezo injector used in these investigations is located centrally in the combustion chamber roof and the spark plug is located laterally on the exhaust side [7, 8].

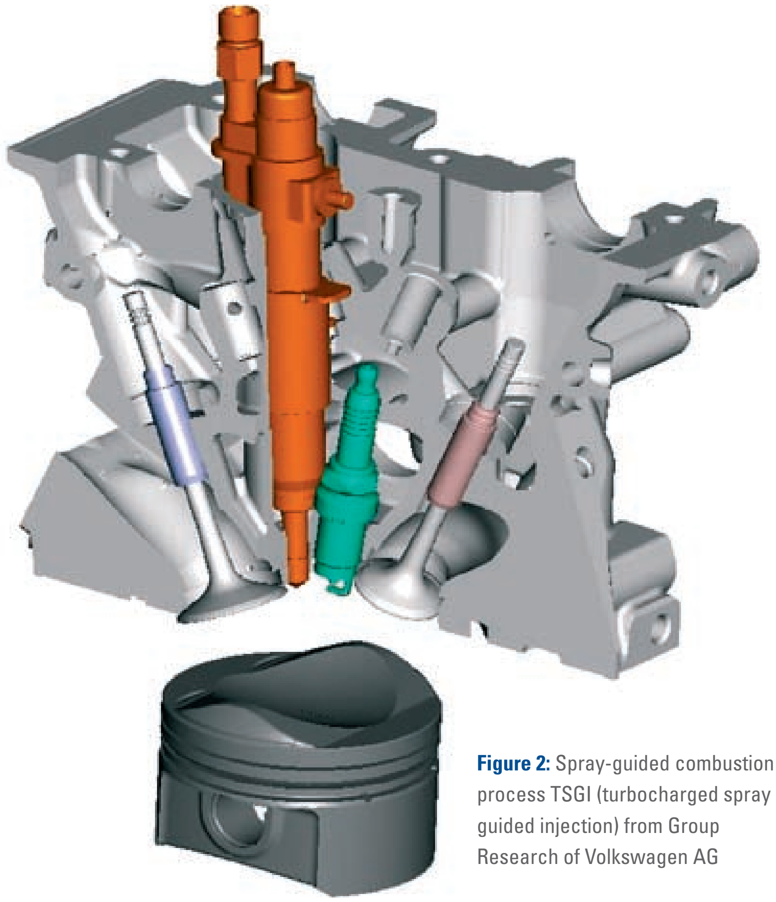

Figure 2: Spray-guided combustion process TSGI (turbocharged spray guided injection) from Group Research of Volkswagen AG

4 Results

Stationary test bench investigations are the fundament of evaluation of the turbocharged spray guided combustion process. Besides the detailed analysis of the stratified mode other possible injection modes have to be compared and evaluated. Thus operation strategies can be developed and their influence of the entire potential can be determined.

4.1 Operating Modes of Spray Guided Combustion Process

Next to injection timing and fuel pressure, further technical parameters such as charge air movement flap, externally cooled exhaust gas recirculation and nitrogen oxide emissions after treatment are required for optimal application of stratified mode.

As super ordinate operating modes of the spray guided combustion process, the following should be subject to closer investigation and evaluation, **Table**.

On the engine test bench, the test engine was run in the different injection modes. In doing so load variations at different engine speeds were carried out. **Figure 3** shows exemplarily the indicated specific fuel consumption ISFC and the NO_x mass flow rate NO_x at a load variation at rev = 1500 rpm.

Starting at an indicated mean pressure of IMEP = 2 bar, the engine is run in stratified mode with activated EGR (SCH+EGR). Where the consumption curves in lean stoichiometrical compression stroke injection (SCH + EGR) operation cross with lean stoichiometrical suction stroke injection (HMM) operation at a load of IMEP = 6 bar, this marks the determined reasonable upper load threshold of the advantage in efficiency of stratified operation (1).

Running the engine in lean homogeneous suction stroke injection (HMM), the nitric oxide emissions reach with further increasing engine load up to seven bar (2) a limit of 70 g/h. Based on extensive experience in the field, this limit is chosen for the maximal acceptable raw emission impact on a nitric oxide storage catalyst.

Consequently, the engine injection mode is switched to stoichiometrical homogenous suction stroke injection with EGR (HOM+EGR). This can be used as con-

Table: Operating modes of the spray guided combustion process for turbo-charged engines

Injection mode	Mixture formation	λ	AGR	Naming
Suction stroke injection	homogeneous	λ = 1	–	HOM
Suction stroke injection	homogeneous	λ = 1	External EGR	HOM + EGR
Suction stroke injection	homogeneous	λ > 1	–	HMM
Compression stroke injection	stratified	λ > 1	External EGR	SCH + EGR

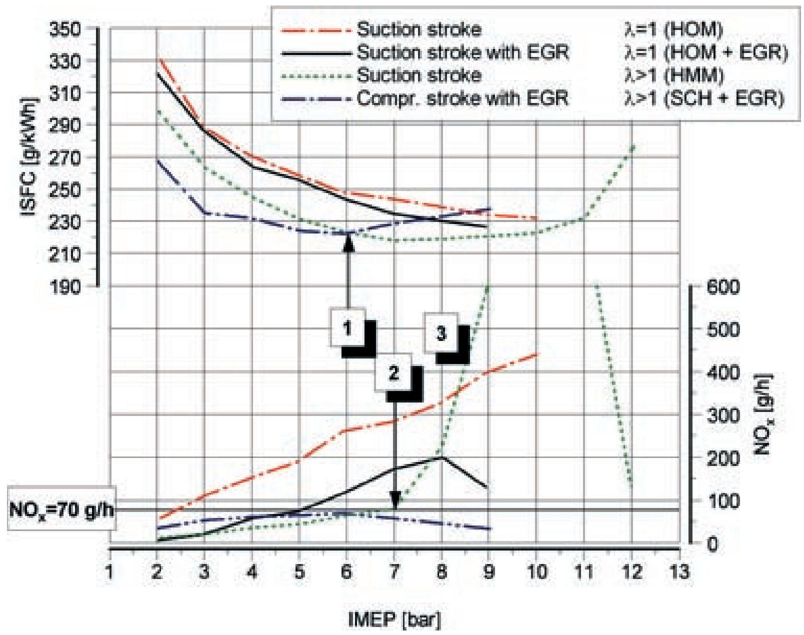

Figure 3: Indicated specific fuel consumption and nitrogen oxide mass flow of TSGI operating modes for a load variation; n_{mot}=1500 rpm, gas exchange, injection and ignition point optimal for fuel consumption, EGR rate maximum

sumption favorable injection strategy from 8 bar on up to full load condition (3).

The strong increase of nitric oxide emissions in lean homogeneous mode (HMM) can be reasoned by a continuous decrease of excess air with increasing engine load. Thus, the nitric oxide emissions show the characteristic progress when decreasing air-/fuel ratio with a peak at about λ=1.15.

For thermodynamical analysis of the pressure curves recorded during test bench investigations a split of losses according to Weberbauer et al [9] is helpful. **Figure 4** shows the distribution of loss of a detailed pressure curve analysis of the operating modes at a constant driving point of the NEDC. Starting from the theoretical degree of efficiency, calculated from the geometric compression ratio and a constant isentropic exponent, the losses are calculated from

– the thermodynamic compression ratio ($\Delta\eta_\varepsilon$)
– the actual charge as a function of the air/fuel ratio and the overall residual gas rate, expressed via the isentropic exponent ($\Delta\eta_\kappa$)
– energy release at the calculated fifty percent energy conversion point ($\Delta\eta_{MFB50\%}$)
– incomplete combustion ($\Delta\eta_{HC+CO}$)
– in consideration of the real combustion curve ($\Delta\eta_{Comb}$)
– in consideration of the real gas properties ($\Delta\eta_{Calorics}$)
– by the wall heat transfer ($\Delta\eta_{Wall\ heat}$)
– in consideration of real expansion ($\Delta\eta_{Exp}$)
– the gas exchange ($\Delta\eta_{Gas\ ex}$).

It is possible to see an advantage in the efficiency factor here through dethrottling ($\Delta\eta_{Gas\ ex}$) with the use of external, cooled EGR in homogenous mode. This advantage increase when diluting the charge with air in the lean stoichiometrical suction stroke injection (HMM) mode. By diluting with air, the polytrope exponent rises ($\Delta\eta_\kappa$). The caloric losses are lower ($\Delta\eta_{Calorics}$). Moreover, the wall heat losses ($\Delta\eta_{Wall\ heat}$) decline from the greater degree of diluting. The higher achievable diluting rate leads to a higher air requirement. Further dethrottling is possible. The degree of indicated efficiency (η_i) rises.

In stratified charge mode, the losses from the actual charge are not as high due to greater diluting, though this advantage is balanced out in part by a greater internal residual gas quantity compared with suction stroke injection modes. Due to the lower enthalpy at the turbine there is an unfavorable decline in scavenging at low load in stratified charge mode. With regards to the constant volume cycle process, the near optimum 50 % conversion point shortly after ignition TDC, **Figure 5**, leads to an almost maximum degree of efficiency in the constant volume cycle process ($\Delta\eta_{MFB50\%}$).

However, at a rate of 20 % EGR results at this point in less stable combustion ($\Delta\eta_{HC+CO}$ increases) and also a longer combustion period with longer burnout ($\Delta\eta_{Comb}$) compared to stoichiometrical suction stroke injection (HOM) mode and also just marginally lower wall heat losses ($\Delta\eta_{Wall\ heat}$). The longer burnout partly balances out the advantage of lower gas temperatures close to the combustion chamber wall. Despite the poor degree of turbine efficiency, the gas exchange losses are marginal. The advantage of dethrottling far outweighs this.

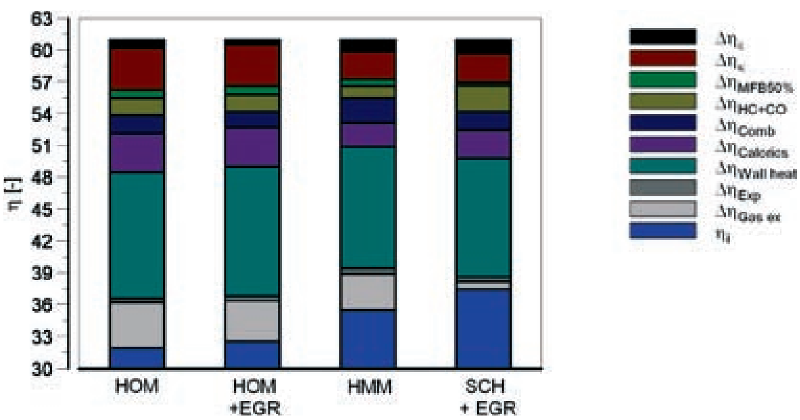

Figure 4: Split of losses of TSGI operating modes at characteristic constant driving point in NEDC; rev = 1500 rpm, IMEP = 4 bar; gas exchange, injection and ignition point at optimum for fuel consumption, EGR rate maximum

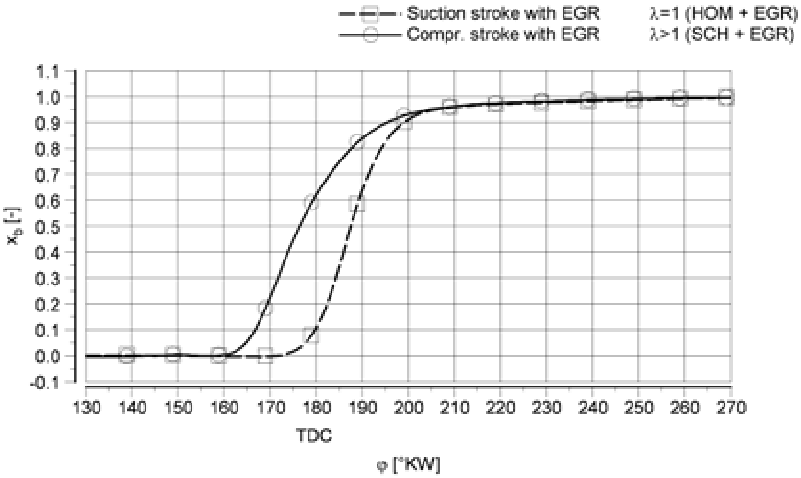

Figure 5: Normalized mass fraction burned x_b for stoichiometric suction stroke injection with EGR (HOM+EGR) and lean compression stroke injection with EGR (SCH+EGR) at characteristic constant driving point in NEDC; TDC: φ = 180° CA; rev = 1500 rpm, IMEP = 4 bar; gas exchange, injection and ignition point at optimum for fuel consumption, EGR rate maximum

In summary, the advantage in consumption in stratified charge mode arises mainly from the reduction in gas exchange losses. The theoretical advantage from the greater degree of diluting is countermanded in the turbocharged engine on one hand by the unfavorable degree of turbine efficiency as a result of low exhaust gas temperature. On the other hand, the required high EGR rates lead to a less stable combustion with respective losses.

Moreover, when running a turbo charged engine, a reduced spark position is necessary for avoiding a thermal overloading. This leads to disadvantages in stratified charge mode.

4.2 Engine Map During Operation with Stratified Charge

The effective engine map range in stratified charge mode is restricted by the available exhaust gas after treatment of nitrogen oxide mass flow rates. **Figure 6** shows in green the effective engine map ranges for a applicable stratified charge mode. The engine map range with low tumble is illustrated in grey in consideration of the exhaust gas after treatment systems available on the market today (max. nitrogen oxide mass flow rate $NO_{x,DS}$ = 70 g/h). The blue area describes the achievable engine map range with high tumble in consideration of the exhaust gas after treatment systems available on the market today (max. nitrogen oxide mass flow rate $NO_{x,DS}$ = 70 g/h). Finally, the red area marks the engine map range when the light-off temperature of the catalyst is fallen below its limit.

With a charge optimized intake port advantageous for stratified charge operation in consideration of nitric oxide emissions with a low tumble, a large share of the load collective in the NEDC can be covered with an effective engine map range up to a load of IMEP = 6 to 7 bar and up to an engine speed of rev = 3500 to 4000 rpm (grey illustrated). For a turbocharged engine with stratified charge operation, a turbo intake port with high tumble in the flow rate is indispensable for satisfactory high and full load combustion.

To generate increased turbulent kinetic energy, targeted discharges are engineered in the intake port. This leads to a reduction in the effective flow rate cross sectional area in the region of the intake valves and thereby to locally higher flow velocities during intake as well as a higher turbulent fluctuation intensity [11]. The due to the higher flow velocity induced flow impulse leads to increased cyclic fluctuations and destabilizes the stratified charge at the withdrawn ignition site and therefore an unstable ignition. To achieve satisfactory stability in the mixture formation and combustion, considerably "earlier" injection and ignition points are necessary compared to stratified operation with a charge optimized intake port. The subsequent "premature" point of combustion leads to increased NO_x emissions, lower exhaust gas temperatures and also indicated efficiency factor losses. In this way, the useable engine map range is markedly reduced at higher and also lower loads (blue and red area).

Figure 7 shows the full load development of the three investigated engine configurations characterized by the point minimal engine speed at maximum brake torque. In the context of full-load investigations it could be observed that within a reasonable combination of turbo charging and stratified operation there is a specific load threshold of 150 Nm/l or 75 kW/l [10], (Mark 1). Limiting values are the increasing knock tendency and unacceptable smoke emissions caused by insufficient carburetion. An increase of maximum torque up to the aspired 175 Nm/l

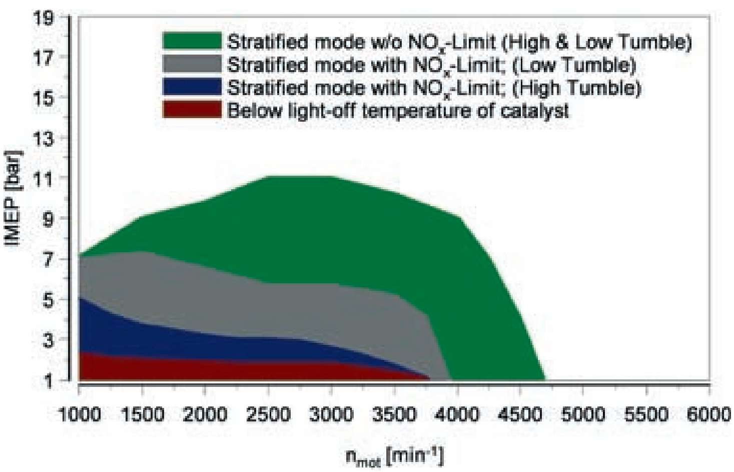

Figure 6: Engine map ranges in stratified charge operation for a turbocharged, spray guided combustion process; Nitric oxide emission limit (stratified mode) 70 g/h

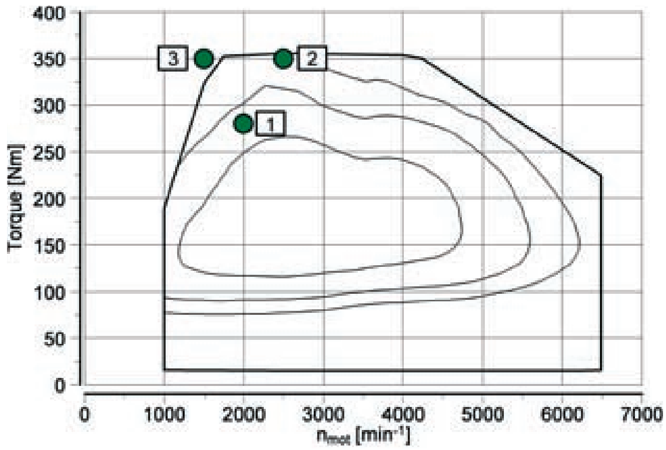

Figure 7: Characteristic full load operation points for three engine configurations

additional operation using charge stratification will achieve a residual advantage in fuel consumption of only 2.5 %.

Furthermore, it becomes perspicuous that, with an optimization of a conventional combustion processes, outstanding results in fuel consumption can be achieved. Depending on the "downsizing factor", robust stoichiometrical homogenous combustion processes are able to achieve lower driving cycle consumptions than the more sensible stratified combustion processes [12]. In consideration of a cost-benefit ratio an optimized conventional combustion process seems to be the preferential solution.

can only be reached by using a turbo intake port with high tumble (Mark 2).

Caused by the increased charge motion when using a high tumble inlet port, the carburetion is sustainable improved and the limit of engine knock is moved to advantageous timing point. But in stratified mode, the increased charge motion leads to a smaller usable engine map like shown in Figure 6.

Due to an optimization of the exhaust valve timings, which can be produced using a variable valve train, the maximum brake torque at lower engine speeds can be increased considerably (Mark 3). The valve lift timing optimization leads additionally to a reduction of gas exchange losses during part load condition.

4.3 Fuel Consumption Projections

In order to also take the overall potential into consideration at the end of the detailed analysis of combustion properties and subsequent changes in the degree of efficiency, fuel consumption projections were carried out for different engine versions. **Figure 8** shows calculated fuel consumptions differences in the NEDC for three engine configurations with or without stratified mode.

When combining turbo charging with stratified operation using a low tumble intake port (1) an advantage in fuel consumption of a about 10 % is achievable compared to the homogenous suction stroke injection mode. Concerning the full load performance, this engine configuration is limited up to a maximal specific brake torque of 150 Nm/l. Using a high tumble intake port for achieving a maximal specific brake torque of 175 Nm/l (2), the advantage in fuel consumption because of stratified operation is reduced to 6 % due to the reduced applicable range of stratified mode in the engine map, Figure 6. There is no change of fuel consumption in homogenous mode to be expected.

Engineering variable valve train technology (3), the NEDC fuel consumption can be lowered up to 10 % in homogenous mode compared to engine configuration (2) with a conventional exhaust cam shaft. Due to the considerably reduced gas exchange losses using optimized gas exchange timings, most of the possible fuel consumption potential of stratified operation can be achieved. An

5 Summary and Outlook

The theoretical advantage of enhancing the useable characteristic map range with stratified charge is not accessible due to the nitrogen oxide exhaust after treatment systems available today as a series production solution. The generation of high charge air movement, necessary to achieve a satisfactory low-end torque response, further restricts the effective characteristic map range. Together with the shift in operating point towards higher loads and contemporaneously reduced engine speeds, which is targeted for turbocharged engines, a noticeable advantage

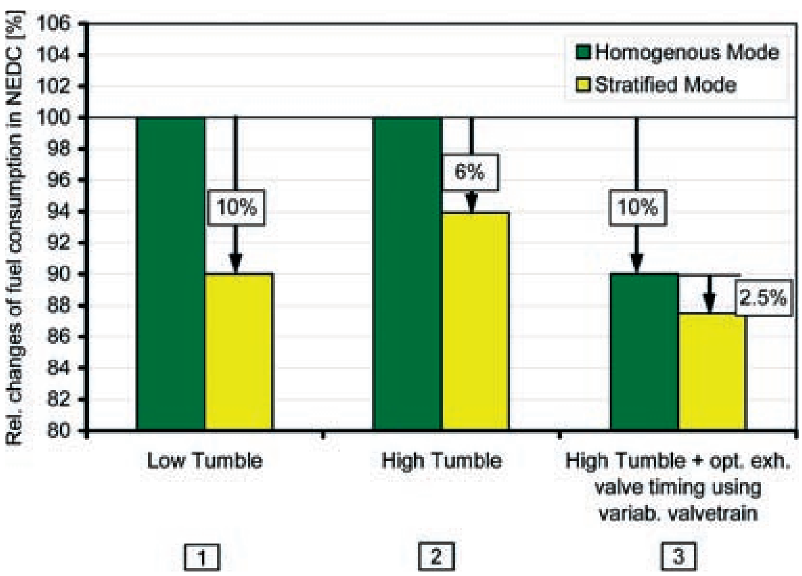

Figure 8: Fuel consumption projections for three engine configurations with and without stratified mode in the NEDC; VW Golf V, vehicle weight and gear transmission ratio from serial production, Nitric oxide emission limit (stratified mode) 70 g/h

in consumption is currently no longer evident for the customer. Today competing downsizing technologies show a higher potential for reducing fuel consumption in the NEDC as well as for the customer.

The future of the turbocharged, spray guided combustion process is linked with the conversion potential and fuel consumption related conversion efficiency of available exhaust gas after treatment systems in the future. As a further challenge a combustion process with a stable and efficient combustion at part load as well as a satisfying full load performance needs to be proposed.

References

[1] Waltner, A.; Lückert, P.; Schaupp, U.; Rau, E.; Kemmler, R.; Weller, R.: Die Zukunftstechnologie des Ottomotors: Strahlgeführte Direkteinspritzung mit Piezo-Injektor. 27. Internationales Wiener Motorensymposium; Wien (2006)

[2] Willand, J.; Suck, G.; Schintzel, K.: Anforderungen an die Einspritzsysteme strahlgeführter Brennverfahren. 4. Tagung Diesel- und Benzindirekteinspritzung; Haus der Technik Berlin (2004)

[3] Klüting, M.; Missy, S.; Schwarz, C.: Potentiale des strahlgeführten Benzin-DI-Brennverfahrens in Verbindung mit Aufladung. 26. Internationales Wiener Motorensymposium, S. 103-122; Wien (2005)

[4] Campbell: Uppsala Hydrocarbon Depletion Study Group, Scenario Update by http://www.peakoil.net/uhdsg/Default.htm; (2004)

[5] N.N.: Shell PKW Szenarien bis 2030, Flexibilität bestimmt Motorisierung, (2004)

[6] N.N.: ESSO Energieprognose 2003, (2003)

[7] Schintzel, K.; Willand, J.; Hoffmeyer, H.; Die Entwicklung strahlgeführter Brennverfahren im Spannungsfeld zwischen Potenzial und Kosten. 5. Tagung Diesel- und Benzindirekteinspritzung; Haus der Technik Berlin (2006)

[8] Schintzel, K.; Willand, J.: Klopfphänomene am Beispiel ausgewählter Motoren der Volkswagen AG. 2. IAV-Symposium „2. Tagung Klopfregelung für Ottomotoren – Trends für Serienentwickler“; Berlin (2006)

[9] Weberbauer, F.; Rauscher, M.; Kulzer, A.; Knopf, M.; Bargende, M.: Allgemein gültige Verlustteilung für neue Brennverfahren. In: MTZ 2005 Nr. 2, S. 120-124

[10] Schintzel, K.; Willand, J., Hoffmeyer, H., Schulz, R.: Neue ottomotorische Brennverfahren – Alternativen zum Dieselmotor. 7. Tagung Direkteinspritzung im Ottomotor; Haus der Technik Essen (2007)

[11] Wurms, R.; Kuhn, M.; Zeilbeck, A.; Adam, S.; Krebs, R.; Hatz, W.: Die Audi Turbo FSI Technologie. 13. Aachener Kolloquium Fahrzeug- und Motorentechnik; Aachen (2003)

[12] Willand, J.: Motortrends zur CO_2-Reduzierung: Downsizing oder Teillastbrennverfahren? MTZ-Konferenz „Der Antrieb von morgen“; München (2008)

IMPRINT

MTZ WORLDWIDE

www.MTZ-online.com

02|2009 · February 2009 · Volume 70

Springer Automotive Media | GWV Fachverlage GmbH
P.O. Box 15 46 · 65173 Wiesbaden · Germany
Abraham-Lincoln-Straße 46 · 65189 Wiesbaden · Germany

Managing Directors Dr. Ralf Birkelbach, Albrecht Schirmacher
Advertising Director Thomas Werner
Production Director Ingo Eichel
Sales Director Gabriel Göttlinger

EDITORS-IN-CHARGE

Dr.-Ing. E. h. Richard van Basshuysen
Wolfgang Siebenpfeiffer

EDITORIAL STAFF

Editor-in-Chief
Johannes Winterhagen (win)
Phone +49 611 7878-342 · Fax +49 611 7878-462
E-Mail: johannes.winterhagen@springer.com

Vice-Editor-in-Chief
Dipl.-Ing. Michael Reichenbach (rei)
Phone +49 611 7878-341 · Fax +49 611 7878-462
E-Mail: michael.reichenbach@springer.com

Chief-on-Duty
Kirsten Beckmann M. A. (kb)
Phone +49 611 7878-343 · Fax +49 611 7878-462
E-Mail: kirsten.beckmann@springer.com

Sections

Electrics, Electronics
Markus Schöttle (scho)
Phone +49 611 7878-257 · Fax +49 611 7878-462
E-Mail: markus.schoettle@springer.com

Engine
Dipl.-Ing. (FH) Richard Backhaus (rb)
Phone +49 611 5045-982 · Fax +49 611 5045-983
E-Mail: richard.backhaus@rb-communications.de

Heavy Duty Techniques
Ruben Danisch (rd)
Phone +49 611 7878-393 · Fax +49 611 7878-462
E-Mail: ruben.danisch@springer.com

Online
Dipl.-Ing. (FH) Caterina Schröder (cs)
Phone +49 611 78 78-190 · Fax +49 611 7878-462
E-Mail: caterina.schroeder@springer.com

Production, Materials
Stefan Schlott (hlo)
Phone +49 8191 70845 · Fax +49 8191 66002
E-Mail: Redaktion_Schlott@gmx.net

Service, Event Calendar
Martina Schraad
Phone +49 212 64 235 16
E-Mail: martina.schraad@springer.com

Transmission, Research
Dipl.-Ing. Michael Reichenbach (rei)
Phone +49 611 7878-341 · Fax +49 611 7878-462
E-Mail: michael.reichenbach@springer.com

English Language Consultant
Paul Willin (pw)

Permanent Contributors
Christian Bartsch (cb), Prof. Dr.-Ing. Peter Boy (bo), Prof. Dr.-Ing. Stefan Breuer (sb), Jens Büchling (jb), Jörg Christoffel (jc), Jürgen Grandel (gl), Erich Hoepke (ho), Ulrich Knorra (kno), Prof. Dr.-Ing. Fred Schäfer (fs), Roland Schedel (rs), Bettina Seehawer (bs)

Address
P.O. Box 1546, 65173 Wiesbaden, Germany
E-Mail: redaktion@ATZonline.de

MARKETING | OFFPRINTS

Product Management Automedia
Sabrina Brokopp
Phone +49 611 7878-192 · Fax +49 611 7878-407
E-Mail: sabrina.brokopp@springer.com

Offprints
Martin Leopold
Phone +49 2642 9075-96 · Fax +49 2642 9075-97
E-Mail: leopold@medien-kontor.de

ADVERTISING | GWV MEDIA

Key Account Manager
Elisabeth Maßfeller
Phone +49 611 7878-399 · Fax +49 611 7878-140
E-Mail: elisabeth.massfeller@gwv-media.de

Ad Sales
Frank Nagel
Phone +49 611 7878-395 · Fax +49 611 7878-140
E-Mail: frank.nagel@gwv-media.de

Display Ad Manager
Susanne Bretschneider
Phone +49 611 7878-153 · Fax +49 611 7878-443
E-Mail: susanne.bretschneider@gwv-media.de

Ad Prices
Price List No. 52

SUBSCRIPTIONS

VVA-Zeitschriftenservice, Abt. D6 F6, MTZ
P. O. Box 77 77, 33310 Gütersloh, Germany
Renate Vies
Phone +49 5241 80-1692 · Fax +49 5241 80-9620
E-Mail: SpringerAutomotive@abo-service.info

SUBSCRIPTION CONDITIONS

The emagazine appears 11 times a year at an annual subscription rate of 269 €. Special rate for students on proof of status in the form of current registration certificate 124 €. Special rate for VDI/ÖVK/VKS members on proof of status in the form of current member certificate 208 €. Special rate for studying VDI members on proof of status in the form of current registration and member certificate 89 €. The subscribtion can be cancelled in written form at any time with effect from the next available issue.

PRODUCTION | LAYOUT

Heiko Köllner
Phone +49 611 7878-177 · Fax +49 611 7878-464
E-Mail: heiko.koellner@gwv-fachverlage.de

HINTS FOR AUTHORS

All manuscripts should be sent directly to the editors. By submitting photographs and drawings the sender releases the publishers from claims by third parties. Only works not yet published in Germany or abroad can generally be accepted for publication. The manuscripts must not be offered for publication to other journals simultaneously. In accepting the manuscript the publisher acquires the right to produce royalty-free offprints. The journal and all articles and figures are protected by copyright. Any utilisation beyond the strict limits of the copyright law without permission of the publisher is illegal. This applies particularly to duplications, translations, microfilming and storage and processing in electronic systems.

Springer Automotive Media is part of the specialist publishing group Springer Science+Business Media.

Realized design of a VCR conrod for a truck application and prototype

Two-stage Variable Compression Ratio with Eccentric Piston Pin

By variation of the compression ratio the fuel consumption of high boosted gasoline engines can be reduced. The two-stage VCR system (variable compression ratio) enables a high share of fuel saving potential relative to full variable systems. FEV has evaluated different known and new two-stage VCR systems. Considering a low cost manufacturability and a beneficial integratability into common engine architectures the length-adjustable conrod using an eccentric piston pin in the small eye has proved as a favorable concept. The adjustment is performed by a combination of gas and mass forces.

1 Motivation and Potentials

1.1 Potential for SI Combustion Processes

The benefits of variable compression have already been widely acknowledged and documented [1, 2, 3, 8, 9, 11]. Its major benefits can be summarized as follows: Under full load conditions, a compression ratio adapted to load demand is capable of reducing knock susceptibility, thus improving full load performance and efficiency.

Further, the risk of pre-ignition, the potential for mega-knocking effects as well as a disposition to engine jerking due to retarded combustion phases can be reduced. In addition, as a contribution to component temperature protection, a variable CR offers further potential to control the exhaust gas temperature. Under part load conditions, a fuel saving potential as shown in **Figure 1** can be achieved.

For the naturally aspirated engine, the increased compression facilitated by gasoline direct injection diminishes the potential of CR variability. Through downsizing in tandem with charging, however, the benefits of VCR can be enhanced: due to the required compression ratio reduction necessitated by high boost ratios, the fuel saving potential is increased by up to 5 to 10 %. **Figure 2** shows the fuel saving potential of charged engines for various driving cycles in dependence on (mean) driving speed as well as at constant-speed driving. At low driving speeds, benefits of well over 10 % can be achieved, whereas at higher vehicle speeds a benefit of approximately 6 % is still possible. The consumption reduction does not only depend on the VCR system, but also, of course, on the characteristics of both engine and vehicle. For a two-stage VCR system, due to the fact that the compression ratio cannot be operating point-optimized as well as due to hysteresis effects, the fuel economy potential is slightly reduced.

For auto-ignition combustion processes based on the gasoline engine, the auto-ignition operating range can be extended at both higher and lower engine loads. Thus, not only can variable compression be applied in combination with modern SI combustion processes, but it also facilitates the development of new combustion technologies.

1.2 Potential for Heavy Duty Diesel Engines

The compliance of today's emission legislations for heavy duty diesel engines in commercial vehicles demand a reduction of NO_x emissions in the entire engine operating area, also including high load points. A very effective way to reduce the raw NO_x emissions at high loads is to operate the engine with high EGR rates. At the same time the air fuel ratio must be kept constant which is needed to hold the particle emissions under the allowed level. Under the boundary condition that the torque output of the engine

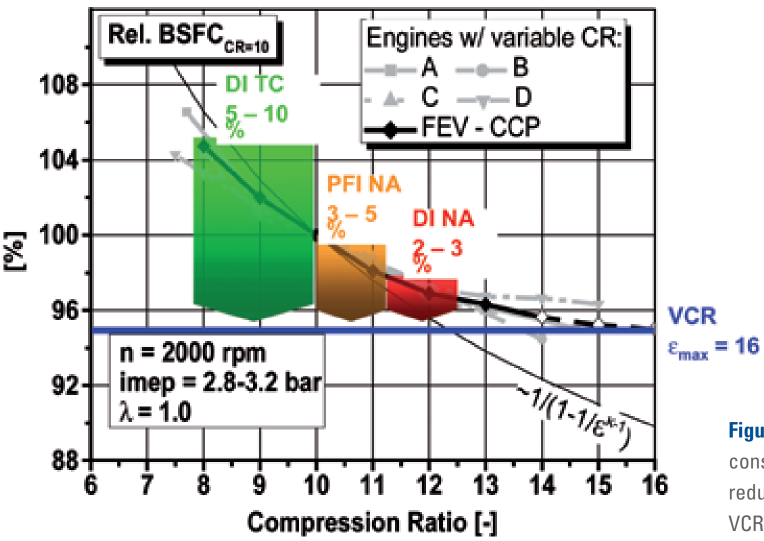

Figure 1: Fuel consumption reduction through VCR (part load)

The Authors

Prof. Dr.-Ing. Stefan Pischinger is head of the Institute for Internal Combustion Engines at RWTH Aachen (Germany).

Dr.-Ing. Karsten Wittek is head of the design department at FEV Motorentechnik GmbH in Aachen (Germany).

Dipl.-Ing. Christof Tiemann is senior project manager in the design department at FEV Motorentechnik GmbH in Aachen (Germany).

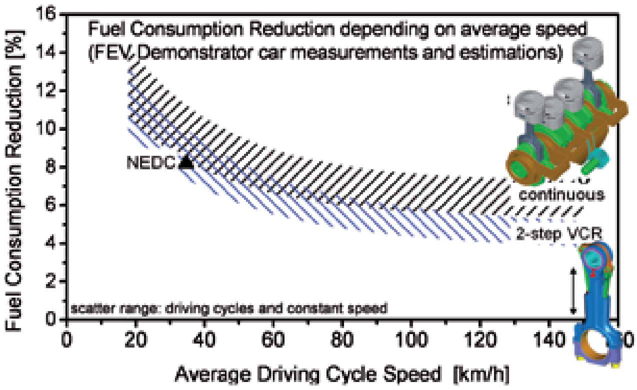

Figure 2: Fuel consumption reduction through VCR (on-road)

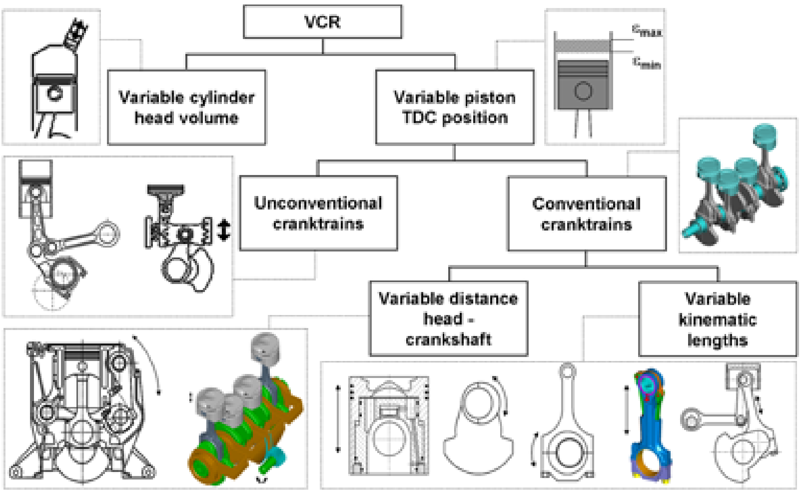

Figure 3: Classification of the VCR systems

should be kept unchanged or even increased, a higher boost pressure must be provided. As a result the PFP (peak firing pressure) requirement of the engine will rise, which requires a reinforcement of the engine structure or even a complete new engine design. The VCR technology can be seen here as an alternative solution by decreasing the CR at high loads, so that the PFP does not exceed the allowed level of an existing engine structure.

2 Overview and Assessment of VCR Systems

In order to realize a variable compression ratio the combustion chamber volume has to be varied. **Figure 3** shows various design options for VCR systems and offers a classification of approaches. The compression volume variation can be realized by implementing a switchable additional volume within the cylinder head or, alternatively, by varying the TDC (top dead center) position of the pistons. The TDC piston position can be modulated, for example, by utilizing an unconventional crank train in combination with a two-piece conrod, which is controlled by an additional shaft, or by using a rack-and-pinion gear for the transmission of power from the piston to the crankshaft [8]. Alternatively, retaining a conventional crankshaft drive, the TDC piston position can be varied by modifying the distance between the crankshaft and the cylinder head or by varying the cinematically effective lengths of the crankshaft drive. The distance between the crankshaft and the cylinder head can be modulated by tilting the cylinder head together with the cylinder barrel relative to the bearing pedestals, as in the VCR system developed by Saab [9], or by means of a translatory mechanism acting on the cylinder head and barrel unit. Utilizing an eccentrically supported crankshaft, the required distance modifications can be realized as well [2, 12]. The variation of cinematically effective lengths opens up the widest range of constructive possibilities: compression height, conrod length, and crank radius can be modified by means of eccentric bearings or by using a linear guidance device.

Apart from having the desired VCR capabilities, each of these systems comes with its respective benefits and disadvantages. As the VCR systems can be realized by the most various mechanical devices, it is safe to conclude that their adequacy with regard to requirements such as suitability for engine operation, mass producibility, etc. varies considerably. **Figure 4** shows an evaluation matrix for the various VCR systems. At low-CR engine operation, an increased combustion chamber volume within the cylinder head results in an unfavorable combustion chamber shape, which is due to the large surface-to-volume ratio. Moreover, the additional switchable volume cannot be implemented in today‘s four valve cylinder heads.

Systems which are based on unconventional cranktrains make possible a continuous adjustment and with it a precise CR control, but due to installation space requirements, especially in the engine transverse direction, significant changes to the base engine architecture are required, which have a major impact on the manufacturing process. Higher friction losses through additional bearings and an increased reciprocating mass, however, are compensated to some extent by a lower lateral piston force.

Systems which vary the distance between the crankshaft and the cylinder head are also well suited to implement a continuously variable CR; in addition, they offer the advantage that an existing cranktrain can be retained „as is“ and fully carried over.

With tilting or translatory moving of the cylinder head and barrel compound, the base engine design has to be extensively modified. The installation expenditure for the actuation mechanism, the sealing of the crankcase as well as the coupling for the moved intake and exhaust systems is considerable and adversely affects production costs and vehicle packaging.

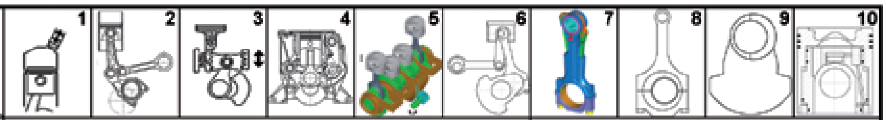

System / Criterion	1	2	3	4	5	6	7	8	9	10
Suitability for cont. VCR	Continuous VCR						2-stage VCR			
Determin. of actual CR	+	+	+	+	+	+	-	-	-	-
Combustion chamber shape	--	++	++	++	++	++	++	++	++	++
Impact on package	-	--	--	--	-	-	++	+	+	+
Modification of production	o	--	--	--	-	-	+	+	+	+
Oscillating mass	++	--	--	++	++	--	--	+	+	--
Friction	++	-	-	++	-	-	o	+	--	o
Costs	o	-	--	--	-	-	o	-	-	--

++ very good / very low neg. impact + good / low neg. impact o neutral / moderate neg. impact
- inappropriate / high neg. impact -- very inappropriate / very high neg. impact

Figure 4: Comparison of the VCR systems

An eccentric bearing crankshaft, by contrast, requires far less modification to the engine design, which is hardly affected at all; the offset between the crankshaft and the gearbox input shaft, however, has to be bridged by a compensation gear, a device which introduces additional frictional losses and also increases the overall engine length.

Most systems which modulate the cinematically effective lengths are not suitable for the realization of a continuously variable CR. These systems, however, have the advantage that they require only minor modifications to the base engine design and that the impact on the production process is comparatively low. As an exception, the system which features a permanently controlled, eccentrically positioned piston pin can be named [11], as it enables a continuous CR variation but again, as a drawback, has a major impact on the engine design as well as on the production process. Comparing the other systems shown here – preferably realized as two-step designs – the system with variable conrod length by an eccentrically mounted piston pin can be considered superior with regard to integrability and production costs. As a disadvantage, however, this approach results in an increase in reciprocating mass. The variable-length conrod with an eccentric bearing in the conrod big end can as well be easily integrated into existing engine designs, with only a minor increase in reciprocating mass. Due to the usual one-piece crankshafts, however, the system requires a two-piece eccentric, which increases the constructional expenditure and thus the manufacturing costs. The realization of a variable crank radius using an eccentric on the crankpin results in a significant increase of the conrod diameter and an attendant increase in cranktrain friction. Utilizing a piston with variable compression height, sealings and the actuating mechanism have to be integrated in the mechanically and thermally highly loaded piston, a solution which poses a major technological challenge.

For a concluding assessment of the various VCR mechanisms, a weighting of the various evaluation criteria would be necessary. The weighting of the criteria, however, would depend on the respective demands of the manufacturers; therefore, a universally valid weighting system cannot be devised.

In FEV's view, systems are to be preferred which can be easily integrated into a conventional engine architecture and which do not significantly increase production costs. Thus a VCR variant of a conventional engine can be produced without requiring special manufacturing facilities. As a prerequisite for such a variant, however, the VCR-specific components should be packaged in modules which substitute for conventional components in the assembly process [4]. In order to be competitive with other fuel saving technologies, the benefits of the VCR system for the customer should outweight the additional production costs. Thus, taking into account the tension between technological possibilities and economic demands, FEV has been focusing its development activities on two VCR systems:

1. For the realization of a continuously variable compression, FEV is investigating a system fitted with an eccentrically supported crankshaft, the so-called „crankshaft shift" system [1, 2, 4, 12, 13].
2. As a two-stage solution, FEV is working on a system fitted with a variable-length conrod, realized by an eccentric piston pin suspension, which utilizes cranktrain forces to adjust the compression ratio. This system is called the „variable-length conrod" system or "VCR conrod".

FEV has developed this two-stage VCR system for a passenger car gasoline engine application as well as for a heavy duty diesel engine application, which is described in more detail in the following sections of the present paper.

3 Two-stage VCR System „Variable-length Conrod"

3.1 Working Principle

The conrod length variation is realized by means of a rotation of an eccentric

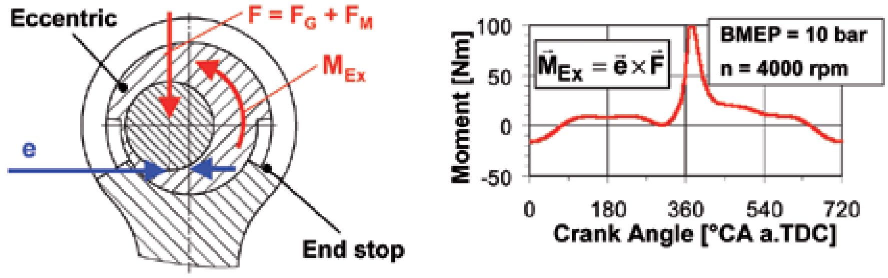

Figure 5: Formation of the eccentric moment

bearing in the conrod small end. The moment acting on the eccentric, resulting from superimposed gas and inertia forces, is used to adjust the conrod length.

This is the key feature to meet a cost effective VCR solution, because no expensive and power consuming actuators are needed and all functional elements are concentrated into only one component, the conrod [10]. As shown in **Figure 5**, the eccentric moment takes on positive as well as negative values during a combustion cycle, making possible an adjustment in both directions.

3.1.1 Support Mechanism

Figure 6 shows cross sections for a VCR conrod design for use in a passenger car SI engine. The moment acting on the eccentric is supported via linkages by hydraulic pistons. The two support chambers are connected to the oil circuit via one check valve each, and by means of a 3/2 check valve, a passage from the chamber to the crankcase can be opened. Thus it is possible for one hydraulic piston to enter more deeply into its support chamber, displacing oil from it in the process, while the other support chamber is being filled with oil. Consequently, the eccentric is able to rotate in one direction only. The adjustment process takes several working cycles to conclude; the number of cycles required for the adjustment depends on the operating point as well as the hydraulic resistance. The hydraulic resistance, which can be controlled by means of orifices, is to be adjusted in such a way that the adjustment process is finished as quick as possible, so as to avoid engine knocking during step load changes from part load to full load and, in addition, to be able to make immediate use of the improved efficiency of the higher compression at load changes to part load. The adjustment time towards high CR must not be too short, however, so as to avoid the following undesired side effects:

- Cavitation at the check valve of the enlarging support chamber
- inordinately high impact loads on the support mechanism when the end stops are reached
- calculations have demonstrated that it is possible to achieve switch-over times of under one second.

3.1.2 Initiation of Compression-ratio Transition

The reversal of the eccentric‘s direction of rotation can be triggered by actuating the 3/2 way valve, which is designed as a mechanical switch. The needed axial travel of the valve body is realized through two cam discs, as shown in **Figure 7**. In the figure the cam disc to initiate a transition towards low CR stands in working position. The functional surface of the individual cam disc consists on a tilted plane which transforms the horizontal component of the valve body path into the desired axial travel. As the valve body is arrested in the respective end position by means of a combination of spring-and-ball catches, any further impacts through subsequent engine revolutions are prevented. The change of the switching sta-

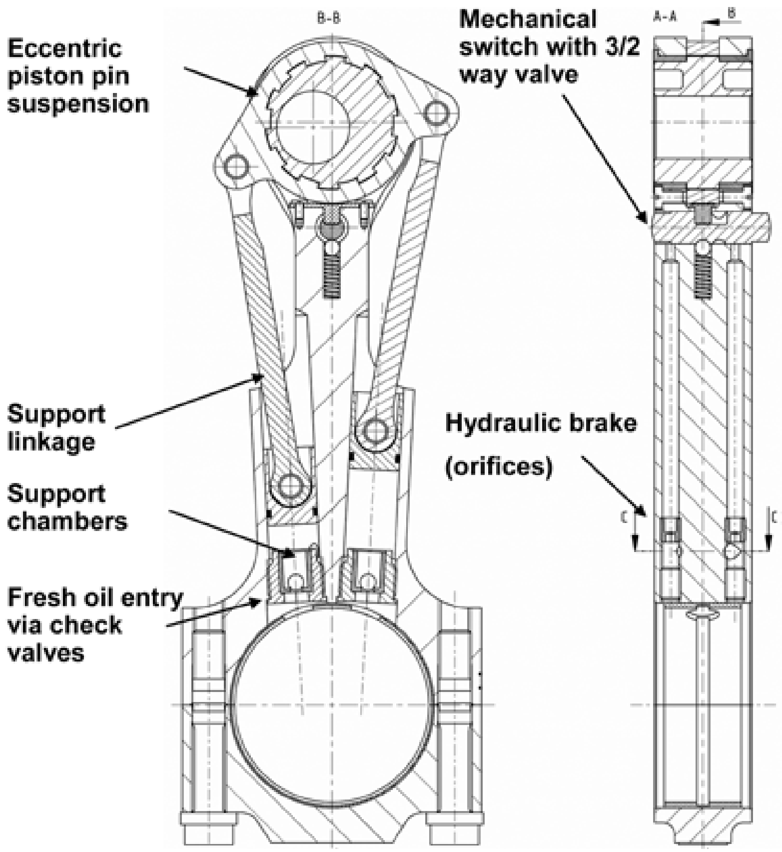

Figure 6: Layout of the VCR conrod

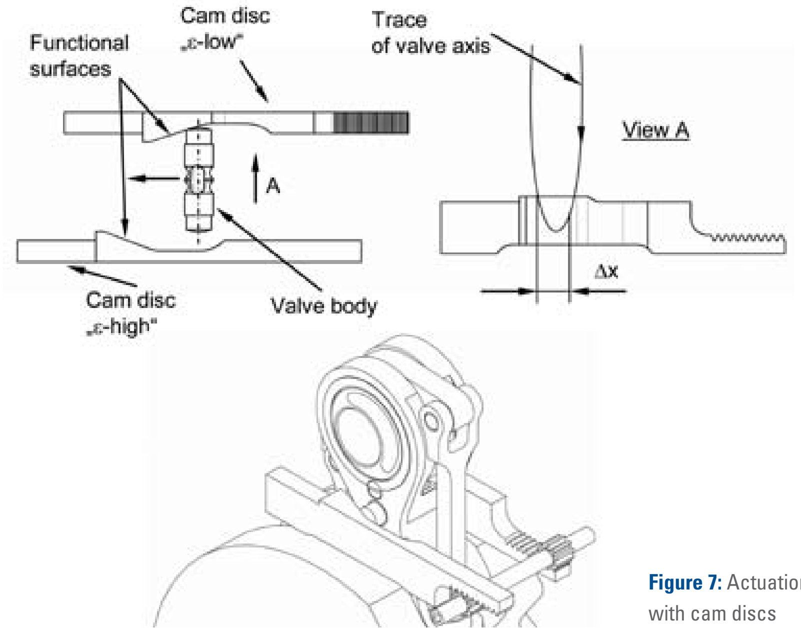

Figure 7: Actuation with cam discs

tus is realized through inversely oriented travel of the cam discs.

In the shown embodiment the mechanical switch is located just underneath the conrod's small eye. The cam discs are located between the envelope of the counter weights of the crankshaft and the piston pin boss. This arrangement has the advantage that the velocity of the valve body is relatively small when getting in contact with the cam discs. On the other hand it requires that the sufficient clearance is available between counter weight envelope and piston pin boss in BDC position. In general there are plenty of other solutions to actuate the mechanical switch from outside the moving conrod. From the big variety of solutions the cam disc actuation is considered as the most robust one.

3.2 Functional Testing under Motored Operating Conditions

In a first step the functionality of the variable-length conrod was investigated in dynamometer tests under motored conditions. During this test phase, switch-over operations were performed at various engine speeds. The change of the CR can be followed during testing through sequence of the measured PFP values, as shown in **Figure 8**, exemplarily for a switch event from high to low CR at unthrottled motored operating condition.

It is expected that the transition times are shorter under fired operating conditions and at adequate high loads, as a higher gas pressure benefits the adjustment process toward the lower compression ratio. Furthermore to demonstrate the basic functionality the hydraulic resistances were not yet trimmed towards maximum switching speed.

After the basic functionality of the mechanism was confirmed over the entire engine speed range and for different manifold air pressures, the reproducibility of the measured transition times as well as the system's durability had to be investigated. For this purpose, approximately 70,000 switch events were performed at varying engine speeds, recording the transition times at fixed intervals. As shown in **Figure 9**, only slight transition time variations were detected. Subsequently, the components were disassembled for inspection. The parts did not show any significant signs of wear [10].

3.3 Refined Design of the VCR Conrod for Gasoline Engines

After the general functioning of the VCR conrod was demonstrated under motored operating conditions, the design was further refined. Major development targets are:

- Reduction of the oscillating mass
- reduction of switching times
- layout of the structure to withstand a PFP of 140 bar.

These partially conflicting targets were fulfilled by using advanced CAE methods and by substituting steel by aluminium for the eccentric. **Figure 10** shows the latest design.

An important design feature is the asymmetric embodiment of the support chambers, to support the eccentric moment in each direction in a tailored way. During switching from high to low CR "only" the small chamber volume needs to be filled ,what allows switching times in this direction of less than 1 s.

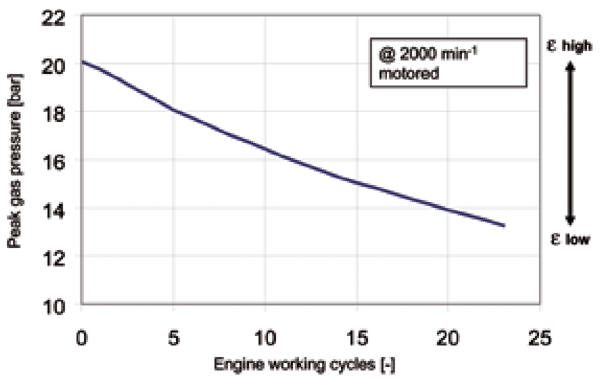

Figure 8: Switching event at motored operation

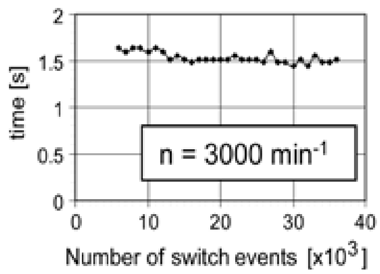

Figure 9: Reproducibility of transition behaviour

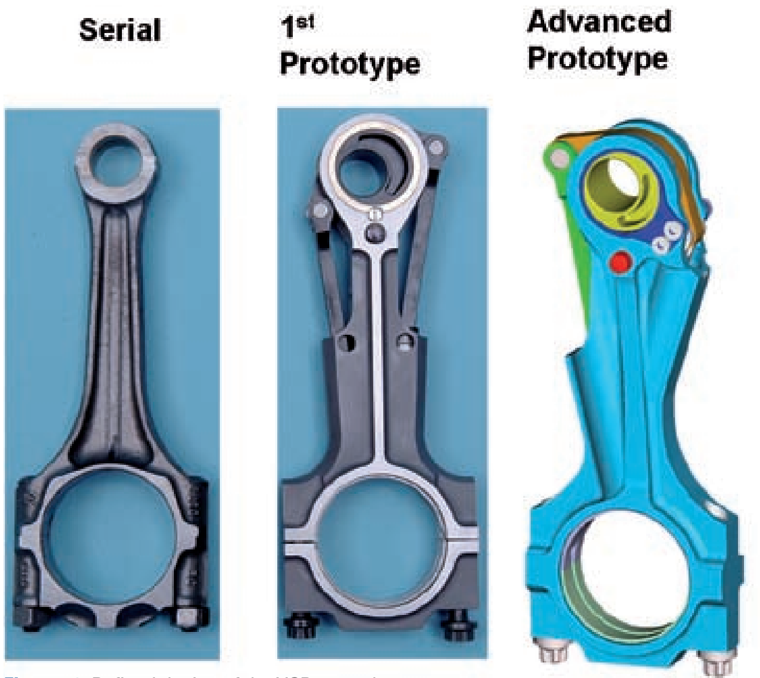

Figure 10: Refined design of the VCR conrod

While the total amount of oscillating mass at the first prototype was 45 % more than in case of the serial cranktrain the increase of oscillating mass at the refined design is reduced to 30 % compared to the serial cranktrain.

In order to quantify the impact of the increased oscillating mass on the engine's friction behavior, friction measurements were conducted on a cranktrain whose oscillating mass was increased by 50 %, **Figure 11**: at the 2000 rpm / 2 bar operating point, the overall engine friction is increased by less than 3 %, resulting in a fuel consumption increase of under 1 %. Thus, the additional oscillating mass only slightly impairs the efficiency benefits of the variable compression.

3.4 Design of a VCR Conrod for Heavy Duty Diesel Engines

In the EU founded project „GREEN" a VCR conrod was designed for a heavy duty diesel engine application. The structure protects for a PFP of 180 bar and allows the compression ratio stages 14 and 17. A very challenging task was to package the support mechanism within the given space in the piston. The realized design of this system is shown in the **Title Figure**.

The basic principle of the actuation mechanism was retained; the 3/2-way valve, however, was integrated into the conrod bearing cap and the actuating cam discs were positioned below the crankshaft, due to package constraints. The piston and piston pin of the production engine were retained almost unmodified. The increase in the cylinder unit's oscillating mass amounted to 19 %.

3.5 Functional Testing under Fired Operating Conditions

Test runs under fired conditions were conducted on a six-cylinder in-line engine for use in a diesel utility vehicle, examining the engine's CR transition behavior over the entire engine speed and load range. The measured transition times from CR-14 to CR-17 and vice versa were in the range of 1 to 2 s.

Figure 12 shows the peak pressure curve over the number of working cycles for a selected high-load operating point. As in the motored test runs, the transition between the two CR stages under fired operating conditions turned out to be monotonic and steady.

In order to arrive at a deeper understanding of the mechanism's systemic behavior, the rotating angle of the eccentric was measured as a function of crank angle. The measurements were conducted by means of travel sensors attached to the conrod. **Figure 13** shows the arrangement of the travel sensors in the conrod as well as the linkage system to guide the sensor cables.

Figure 14 shows a curve representing the length variation of the conrod, which can be calculated from the measured rotating angle of the eccentric, for one cycle within a high-to-low CR transition

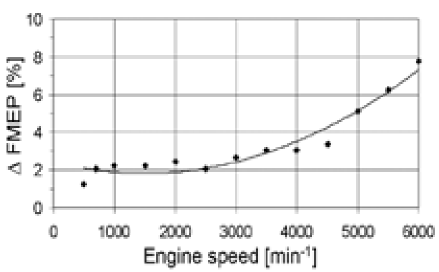

Figure 11: Influence of an increase of oscillating mass by 50 % on the total engine friction

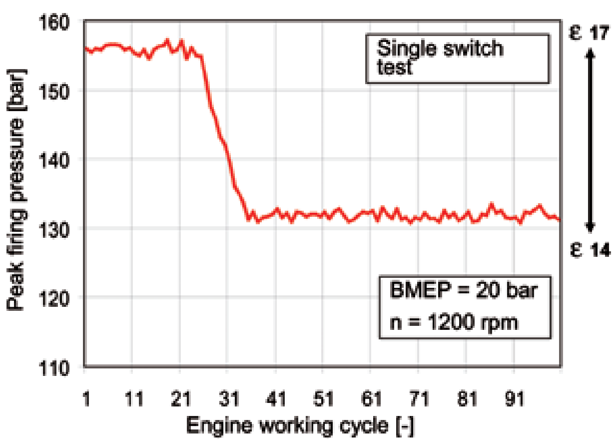

Figure 12: Development of peak firing pressure during a transition at high load

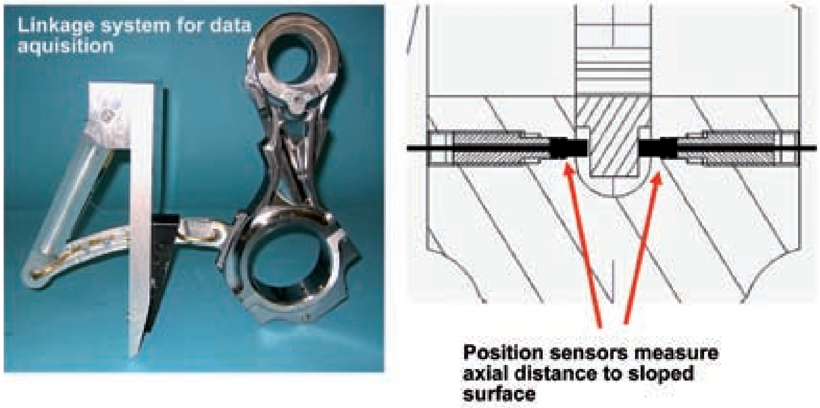

Figure 13: Integration of the position sensors and linkage system

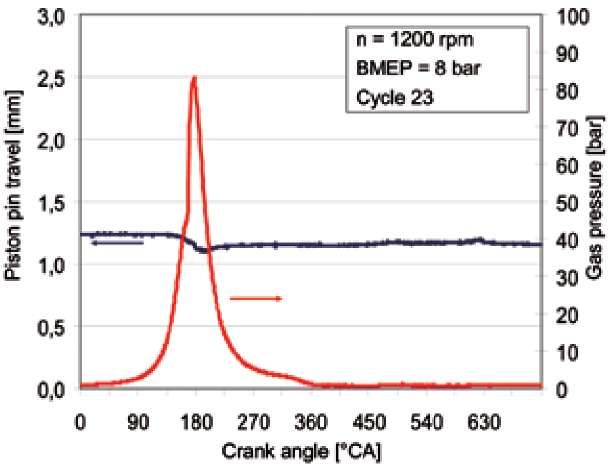

Figure 14: Change of conrod length during a transition during the high pressure phase

phase. The curve illustrates the marked variation in conrod length close to the ignition TDC; elsewhere in the crank angle range, the conrod length remains constant. The other recorded transition processes show comparable length adjustment characteristics.

4 Conclusion

Variable compression ratio as a key to improved engine efficiency will be increasingly in the focus of interest: For the SI engine, the trend towards higher degrees of downsizing raises the appeal of systems which are capable of adapting the compression ratio to load conditions throughout the entire engine map. Also in combination with future combustion processes such as CAI or in tandem with alternative fuels, VCR is capable of opening up further optimization potentials.

At two-stage VCR systems FEV develops a variable length conrod with eccentric piston pin suspension which uses gas and mass forces for actuation. The function of this VCR system was demonstrated both in motored and fired engine operation. The applied principle of the exploitation of gas and mass forces for the actuation was proved to be robust and reliable.

The results presented in the present paper can be seen as promising steps towards the implementation of a variable compression ratio into serial production, which are relevant in view of the pressing concern for a reduction of carbon dioxide emissions, especially within the downsizing trend.

Acknowledgements

Some of the results presented in this paper are taken from work on a project funded by the European Union („GREEN Heavy Duty Engine" as part of the Framework 6 program).

References

[1] Pischinger, S.; Yapici, K.I.; Habermann, K.; Baumgarten, H.: Der Weg zum konsequenten Downsizing – Motor mit kontinuierlich variablem Verdichtungsverhältnis in einem Demonstrationsfahrzeug. In: MTZ 64 (2003) 5
[2] Bollig, C.; Habermann, K.; Schwaderlapp, M., Yapici, K. I.:Variable Verdichtung – Ein Weg zur effizienten Hochaufladung. In:MTZ 62 (2001) 12, S. 984 ff.
[3] Bergsten, L; Drangel, H.: Der neue Saab SVC Motor – Ein Zusammenspiel zur Verbrauchsreduzierung von variabler Verdichtung, Hochaufladung und Downsizing. 9. Aachener Koll. Fahrzeug- und Motorentechnik, 4-6.10.2000, Aachen
[4] Houben, M.; Bick, W.; Thiel, R.; Stöck, H.-P.; Wittek, K.: Umsetzung innovativer Konzepte in die Serie. In: MTZ 68 (2007) 10
[8] Rabhi, V.; Dionnet, F.; Beroff, J.: Die MCE-5 Technologie: eine neue technische Möglichkeit des variablen Verdichtungsverhältnis bei SI Motoren. 13. Aachener Kolloquium Fahrzeug- und Motorentechnik, 2004
[9] Bergsten, L.; Drangel, H.: Der neue Saab SVC Motor – Ein Zusammenspiel zur Verbrauchsreduzierung von variabler Verdichtung, Hochaufladung und Downsizing. 9. Aachener Kolloquium Fahrzeug- und Motorentechnik, 2000
[10] Wittek, K.: Variables Verdichtungsverhältnis beim Verbrennungsmotor durch Ausnutzung der im Triebwerk wirksamen Kräfte. Dissertation RWTH Aachen, 2006
[11] Kreuter, P.: Der aufgeladene Ottomotor mit variabler Verdichtung: Wirkung und Potentiale, 26. Internationales Wiener Motorensymposium, 2005
[12] Schwaderlapp, M.; Pischinger, S.; Yapici, K.I.; Habermann, K.; Bollig, C.: Variable Verdichtung – eine konstruktive Lösung für Downsizing-Konzepte. 10. Aachener Kolloquium Fahrzeug- und Motorentechnik, 2001
[13] Yapici, K.I.: Variables Verdichtungsverhältnis beim Verbrennungsmotor durch exzentrische Kurbelwellenverlagerung. Dissertation RWTH Aachen, 2001

Heavy Duty Composite Piston for Euro 6 and Beyond

Composite pistons have been the state of the art in large bore engines – such as large marine engines – since the 1960s. The thermal and mechanical load of these engines is typically higher than the load of truck engines. Additionally composite pistons are being used for large bore engines because of their durability and reliability. Based on the experience with composite pistons for large bore engines, Mahle was able to transfer this reliable bolting technology to steel pistons for commercial vehicles, the „MonoXcomp“ piston.

1 Introduction

The one-piece-steel „Monotherm“ piston is in widespread use in commercial vehicles today, and meets every requirement for the emissions standards Euro 5 and US2010. Looking beyond the year 2010, most likely the temperature load on the piston will increase further. For this reason, Mahle started developing the next generation of pistons back in 2005. The objectives in the list of requirements of this development were cylinder pressures of 26 MPa and a drop in the maximum bowl rim temperature of at least 50 K. At the same time, the excellent blow-by values and oil consumption (less than 0.1 g/kWh) of the „Monotherm“ piston, successfully used in series production for years, had to be maintained.

The high requirements for reliability and service life for large bore engines are met today by so-called composite pistons, which are made up of a steel crown and a piston skirt that can be made of the materials steel, aluminium, or cast iron. The multi-piece concept allows to design the piston for optimised cooling efficiency, which makes the piston suitable for higher thermal loads. Both piston parts are connected with one or more stretch bolts. Mahle engineers can look back on about 45 years of experience with this mature joining technology for large bore engine pistons. It became obvious that this proven joining technology could also be applied to pistons for commercial vehicle engines.

2 Basics of Bolt Connections

A basic requirement for a reliable bolt connection of dynamic load carrying components is elastic pre-stress within a large elongation length. This leads to the fact that external influences which lead to different states of deformation – for example caused by temperature distributions, inertia forces and/or gas forces – can only cause a fairly little effect on the stress situation in the bolt and hence on the pre-load situation of the entire bolt connection. Additionally, it is made impossible for the pre-load to become zero, which definitely prevents the bolt from coming loose. Numerous examples of stretch bolts can be found in and around the engine. At this point only a few should be mentioned: Cylinder head bolts (primarily loaded with thermal and mechanical loads), connecting rod bolts (primarily loaded with inertia loads), bolts in the valve train area, in the crank shaft housing area, etc.

A simple mathematical exercise is used to illustrate the concept of a stretch bolt, **Figure 1**. There is a linear relationship between the tensile stresses in the stretch area of the bolt and the length of this area. The cross-section in both cases is equal. Starting at a pre-stress situation point M, a theoretical elongation of ±10 μm is being applied. The length of the stretch area of B is five times the length of A. As a result the stress amplitude of B is only one fifth of A. The lowest load situation for A is at a very low level. This work principle is an essential requirement for a reliable layout of a bolt con-

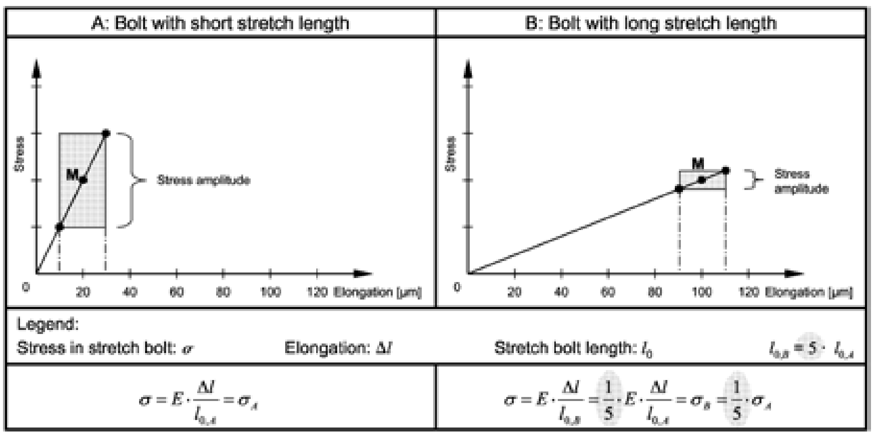

Figure 1: Comparison of elongation length

The Author

Dipl.-Ing.
Rainer Scharp
is head of design steel pistons Europe Product line piston systems at Mahle GmbH in Stuttgart (Germany).

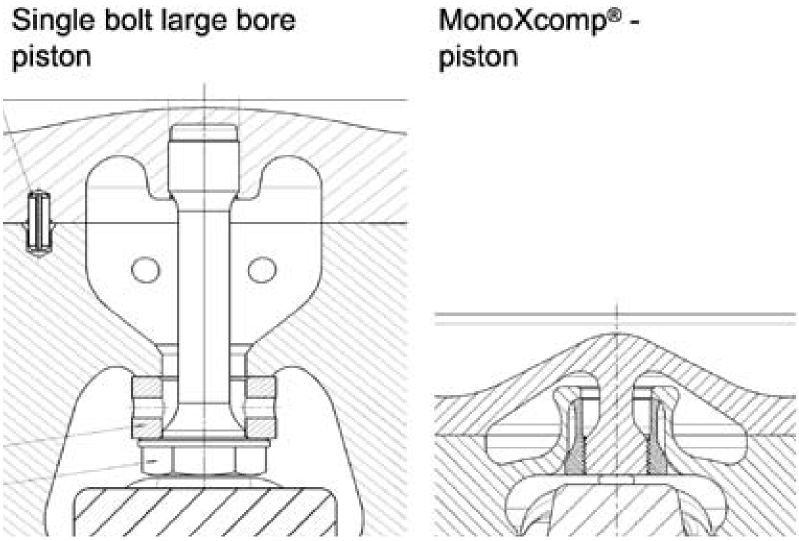

Figure 2: Comparison of available packaging space

nection for dynamic load carrying components. It had to be considered for the development of a new piston concept.

3 Optimisation of the Bolt Connection

The challenge with the „MonoXcomp" piston was to use the limited packaging space optimally, **Figure 2**. In comparison to large bore pistons, the compression height of commercial vehicle pistons is significantly less, so that stretch bolts will not fit. Consequently the piston concept evenly distributes the required elastic elongation length among all the components, so that the total elastic elongation of typical stretch bolts is achieved. The achieved spring characteristic has a flat slope, with the effect that the alternating stresses remain low. Most large bore pistons require additional components (e.g. for a better load distribution, especially when the load is being transferred into an aluminium piston skirt). The new concept minimises the number of components, and thus minimises the number of interfaces and potential risks. The piston is made up of only three elements, **Figure 3**:

- The piston crown, on which a threaded stretch bolt is integrally formed
- the thrust sleeve, which features the nut thread and an elastically deformable part, and on which a suitable contact zone is integrally formed to carry the load to the piston skirt
- the piston skirt with the counterpart to the contact zone. It has an integrally formed stretch collar and can deform in its interior like a disc spring.

The specifically set elasticity within the bolt joint of the piston ensures that the minimum required bolt force is always present. This guarantees that the piston crown will not lift off, even at high speeds such as, for example, 3,000 rpm. The abutment surfaces are thus always closed.

4 Layout of the Bolt Joint

The layout of the bolt joint and the stress and residual gap situation of the abutment surfaces between piston crown and skirt, **Figure 4**, is being done via finite-element calculations. There is the possibility to apply different profiles (dish shaped, roof shaped, etc.) to the abutment surfaces and/or an axial offset between the abutment surfaces in order to come to an optimal solution. Before the first piston is running in the engine, one test piston is being equipped with strain gauges in the area of the bolt stud, **Figure 5**, in order to determine the actually applied elongation, respectively the calculated pre-load is being verified. At the same time the torsion load during assembly is being considered. Based on these investigations the required tightening angle of the thrust sleeve is being determined.

In general the highest bolt force occurs when the piston is in the state of deformation caused by the maximum temperature load and no external forces are present. The state of deformation caused by the maximum cylinder pressure leads

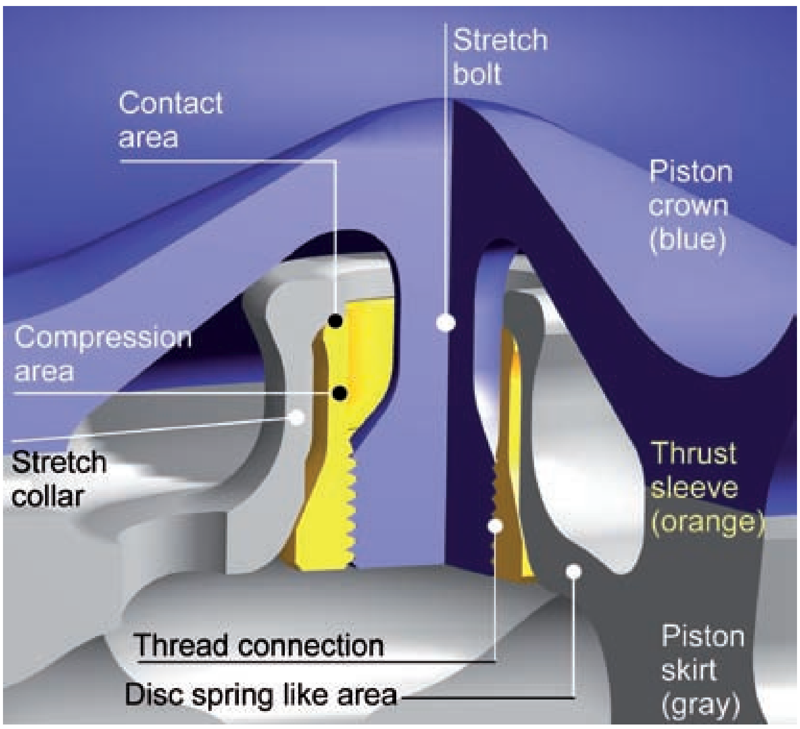

Figure 3: Components of the piston

to a reduction of the bolt force to the minimum level overall. This load cycle is relevant for the determination of the safety in the bolt connection and the thread safety according to VDI2230 itself. Inertia forces, which occur during high over-speed conditions, lead, because of the deformation happening, to a decrease of the load in the bolt connection. Explanation: The sum of the reaction forces on the inner and outer abutment surface is equal to the force in the bolt stud ($F_{outer\ abutment} + F_{inner\ abutment} = F_{bolt\ stud}$). The deformations caused by the inertia forces lead to a decrease of the reaction forces of the abutment surfaces. As a result, the bolt force decreases. At the same time the whole inertia force ($F_{inertia} = m \cdot a$) of the crown relative to the center of gravity causes an increase in bolt force. The sum of the reductions of reaction forces caused by deformations is larger than the forces caused by the inertia force. Hence, the total tensional load within the bolt stud is reduced. This holds true until the reaction forces on the abutment surfaces become zero, which leads to an interruption of the load path in the bolt connection. This is a situation which has to be ruled out by design in the first place.

The assembly process is taken from the state-of-the-art process used for stretch bolts. Apart from the fact that it is not necessary to tighten beyond the yield point. An initial low torque value ensures that the nut makes contact to the counterpart on the piston skirt. In order to reduce the influence of the friction variations on the pre-load, approximately 80 % of the total tightening angle is being applied angle-controlled. The assembly machine monitors the actual end torque. The whole tightening sequence is done twice. In-between both steps the nut is being loosened. Additionally the first sequence reaches higher tightening angles than the final one. This ensures a very high repeatability and reliability within the tightening process of the bolt joint.

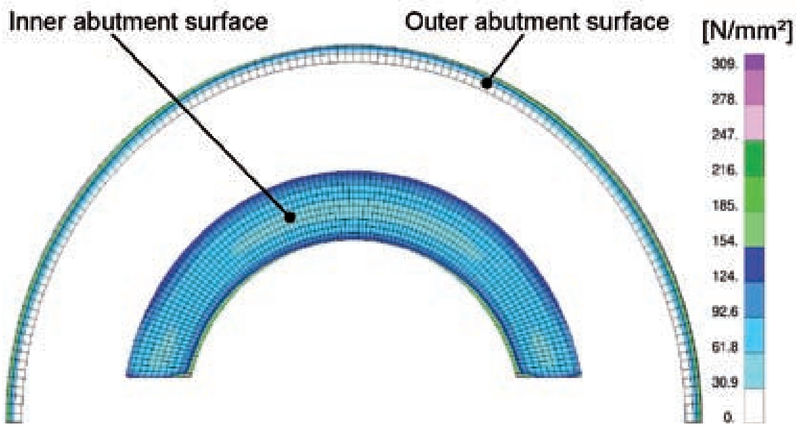

Figure 4: Surface pressure distribution of the abutment surfaces; load case: temperature+bolt force+gas force

5 Optimisation of the Piston Temperature

The multi-piece concept enables us to realise a much larger outer cooling gallery. This is especially important for the cooling of the thermally highly loaded bowl rim. There is a second cooling channel in the interior, which effectively reduces the piston crown temperature. Additionally it is used to cool the bolt stud and the other connection relevant areas, in order to keep the temperature values in the area of high mean stress below 250 °C to prevent relaxation within the bolt connection. Both cooling galleries are connected via overflow channels. The layout of the fluid transfer cross-sections (inlet, outlets, overflow channels) is being verified on the shaker bench test. This bench test visualises the cooling oil movement via high-speed cameras and measures the fluid mass passing through the various channels. Depending on the results, the layout of the fluid transfer channels will be modified, respectively optimised. More and more numerical simulation systems are being used to analyse the fluid dynamics.

The closed, and therefore very rigid, structure reduces the deformation of the piston, so that thinner wall thicknesses are possible. This results in an additional improvement in piston cooling, which allows higher heat input. The closed

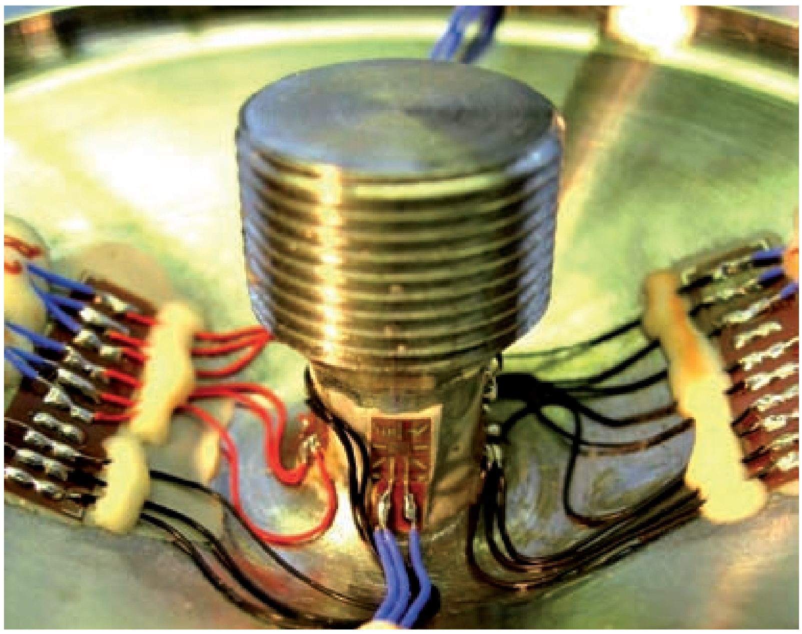

Figure 5: Piston crown with strain gauges

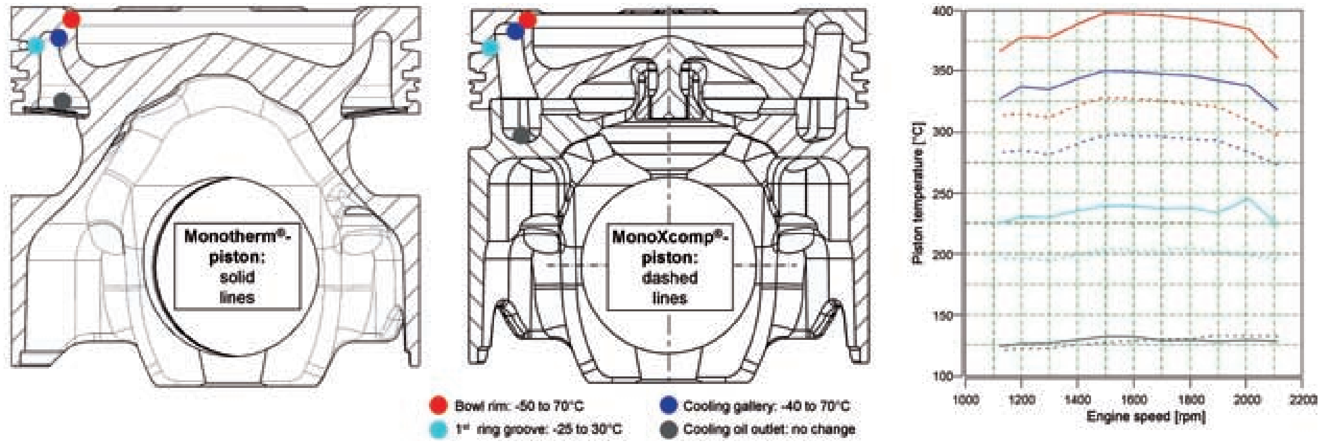

Figure 6: Temperature reduction

structure allows higher peak cylinder pressures than the required 26 MPa.

6 Further Features of the Composite Piston

The potentially different materials for the piston crown, piston skirt, and thrust sleeve make it possible to utilise each material potential optimally. For the piston crown in particular, the use of especially high temperature resistant and oxidation resistant material offers additional potential for load increase. Such material combinations are almost impossible to realise with a welded piston concept. In contrast to many welded concepts, the separate final machining of the individual components also makes it possible to minimise wall thickness tolerances, especially between the cooling galleries and the combustion chamber, and thus to reduce the piston temperature and piston mass variations. Only machining tolerances apply. A welded design, for example, requires additional tolerances for the premachining and for the welding process itself. The new piston concept allows also to assemble cleaned parts, so that the dictated, very stringent cleanliness requirements can be met.

7 Limits of the Piston Concept

Despite the fact that it is possible to use the „MonoXcomp" piston for very low compression heights, the excellent values known from the „Monotherm" piston today (less than 50 % of the piston diameter) cannot by achieved. A realistic limit can be seen at approximately 60 %. In some cases values down to 56 % could be realised. The new piston concept is suitable for most of the engines in the commercial vehicle market.

8 Summary and Outlook

Using finite element methods, Mahle has determined an optimum connection geometry and predicted a potential reduction in temperature compared to standard pistons. Pulsator tests confirmed the design of the bolt joint. The cooling oil motion was optimised on a shaker test bench. Temperature measurements with thermocouples, **Figure 6**, showed that the bowl rim temperatures of „MonoXcomp" pistons can be 50 to 70 K lower than on conventional steel pistons – under the same conditions. Similar temperature reductions were achieved on the cooling gallery side, due to better cooling.

After the „MonoXcomp" piston successfully passed internal engine tests, the project could be transferred from the advanced engineering group to the series production development group. For some customer projects, the series production development has already begun. ■


Events
Archiv
Karriere
Wissen
Topmeldung
Aktualität
1500 m
www.ATZonline.de
Optionen
NAVIGON

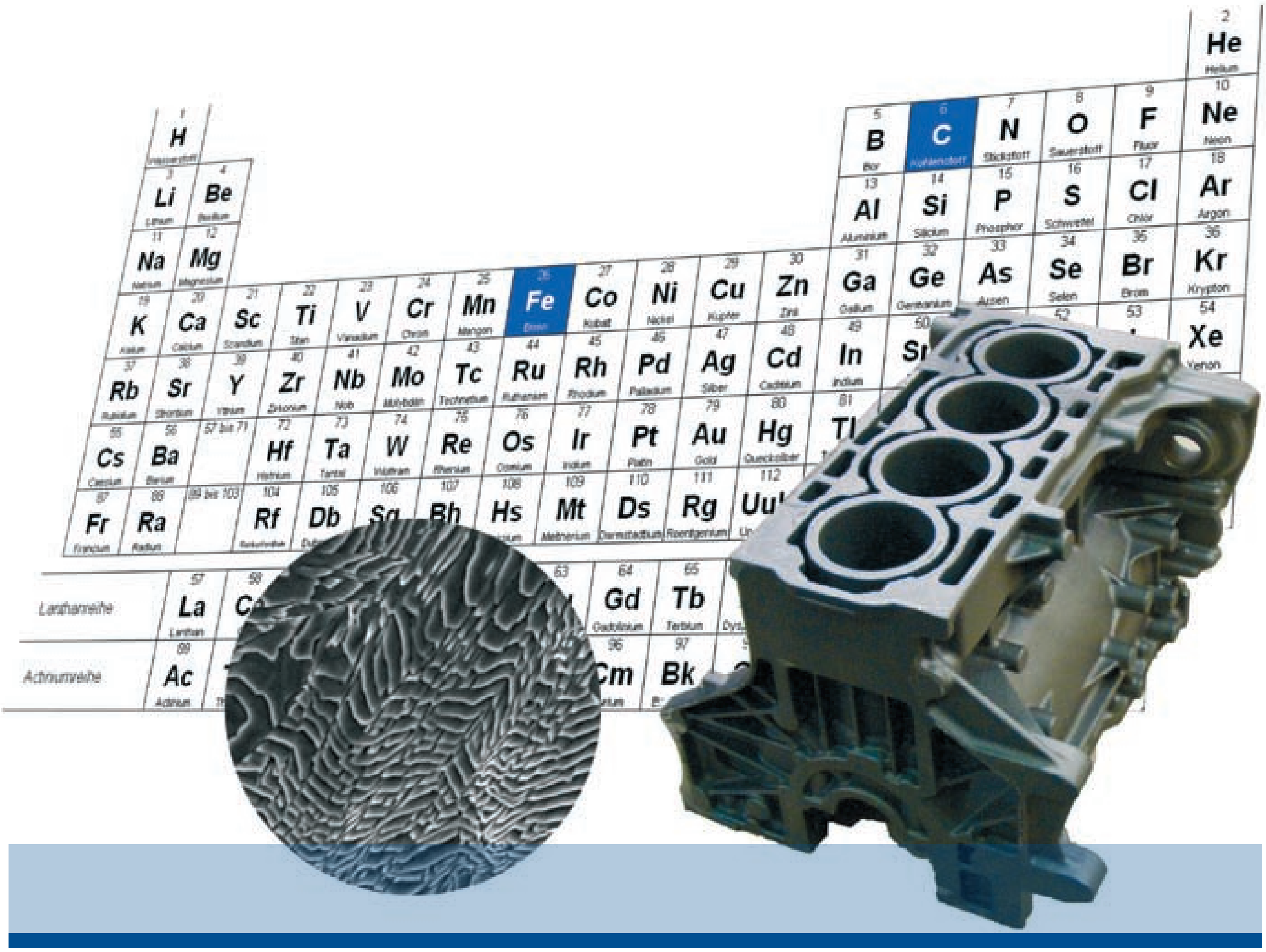

Modern Cast Iron Materials for Lightweight and Efficient Downsized Engines

Large sized engines are being replaced by smaller sized engines with the same performance. An example of this kind of downsizing are the VW 1.4 l TSI/TFSI engines. They are made out of grey cast iron (GI). Efficient engines are being built with high combustion pressure, where the advantage of a material such as GI with a high strength is used. With respect to downsizing, principally any solutions found through material or process technologies are particularly required, due to the increase in pressure on the parts. This article by Halberg Guss describes innovative alloy techniques and new possibilities for the metallurgic measuring techniques during the production process.

1 Material Strategy

The cylinder crankcase of combustion engines is produced in series by the original molding process of casting. Added to this is the weight reduction achieved by an increase of efficiency, known as downsizing. Consequently, the aims for foundry technology result from engine development. Many times, the downsizing of an engine is an intelligent combination of turbo charging, direct fuel injection and variable valve controlling. Typically, there is an increase in peak pressure, which in turn puts a continuously increasing demand on the material for higher strength. A big advantage of modern cast iron materials is their high strength, which is one of the main requirements. Other advantages are good tribological qualities of the cylinder runners, good oscillation damping as well as low thermal expansion which permits less bearing movement in the engine. An example of an engine constructed with these advantages, is the 1.4 l four-cylinder TSI/TFSI gasoline engine with an open deck construction from Volkswagen. The rigidity with open deck constructions is generally lower than with a closed deck building method. When grey cast iron (GI) is used, its high E-module is able to balance out the differences in rigidity. A further example is the diesel engine segment with the new engine generation Daimler OM651. The material of the Daimler engine OM 651 is grey cast iron (GI). Also with the lightweight construction, economic factors press into the foreground. Additional factors such as resources, content of the alloying elements and necessary strengths also have to be taken into consideration with downsizing. With every material strategy the cost effectiveness also has to be examined and taken into consideration. Just knowing the market price is not sufficient. With reference to the alloying elements, is there a large strength increase with a small amount or only with many additional elements? There is not an easy all-inclusive answer because they interact with each other. Another influencing factor is the construction, because the specific cooling conditions of the component geometry have an influence on the effect of the elements and consequently upon the strength. Therefore a cost-effective lightweight construction can be achieved through intensive cooperation and working closely together during the development phase. The foundry will supply all necessary knowledge concerning the interaction of the elements. At the moment for example, in the following the focus is on the elements vanadium (V) and magnesium (Mg).

2 Economic Alloy Design

The element vanadium with GI, demonstrates especially well the basic approach of an economic alloy design. What is the influence of vanadium on the tensile strength? In a test programme the content of V was varied on purpose, whereby the remaining chemical composition and cooling conditions were held constant. The ultimate tensile strength (R_m) was measured at two specific places on a cylinder crankcase as a test carrier.

As the content of V was raised, the tensile strength increased up to a maximum. After this point, when the content of V was raised even further, the ultimate tensile strength dropped back again, **Figure 1**.

What does this mean for the cost-effectiveness? After having reached the maximum, more costs would exist for further additions of vanadium, but the efficiency of the material sinks with regard to stress. Any further additions after the maximum are economically unfavourable. Therefore, it is interesting to see how the maximum is created. New

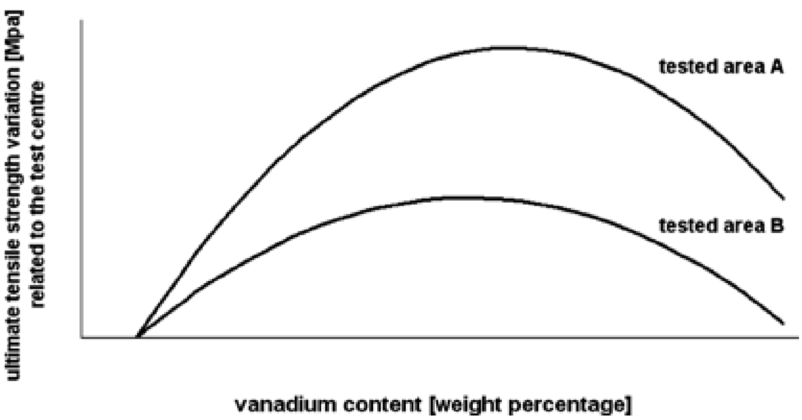

Figure 1: Test carrier

The Author

Dirk Radebach
is head of metallurgy at the Halberg Guss Management GmbH in Saarbrücken (Germany).

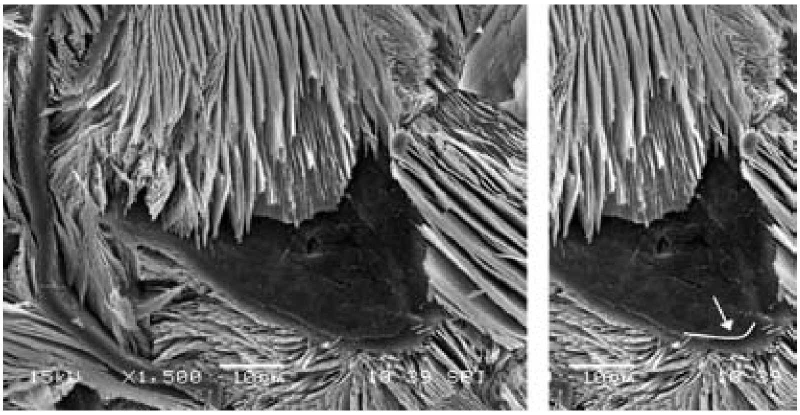

Figure 2: Rounded graphite edge

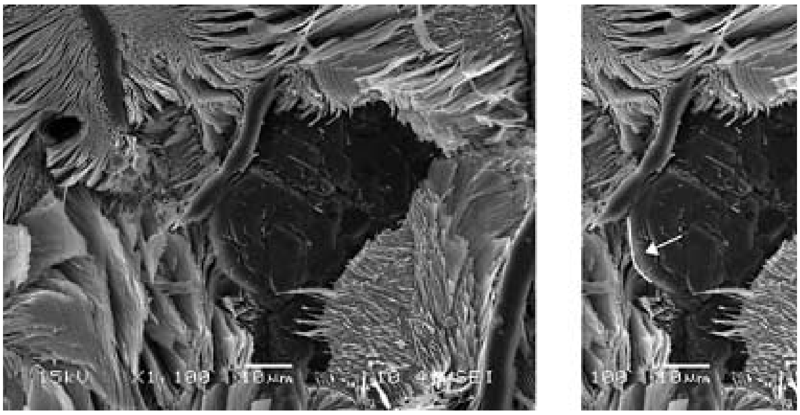

Figure 3: Rounded graphite edge

possibilities arise from the investigation of the relation between the construction characteristics with the formulation of suitable metallurgy models.

3 Relation Between the Microstructure and the Properties

GI for cylinder crankcase is a multi phase material. The main phases are graphite, pearlite and particle. Vanadium changes the morphology and shaping of the phases. The graphite edge is rounded by V, which you can see in the deep etchings, **Figure 2** and **Figure 3**. The effect on the strength is derived from the model of understanding, **Figure 4**. The model body shown in each case is the flake graphite of an eutectic cell: on the left – with rounded edges; on the right – angular edges. The internal notch effect of both bodies is different. In 2D-view this is not evident because both bodies show the same 2D-cut. The 3D-figure shows a better conclusion with respect to the structure construction and its mechanical characteristics. Therefore, the deep etching is an important development tool. The 3D computer reconstruction by nanotomography is even better as can be seen in tests made by Halberg Guss, for example, in the BMBF project [1].

Does V also influence the pearlite? Comparative structure is the usual lamellar pearlite. With the addition of V, the pearlite formation becomes finer. It is remarkable that this changes the morphology of the pearlite in parts. In **Figure 5** a colony can be seen, where parts of the inside particle slowly turn from a compacted form into a lamellar form as it moves outwards. Compacted structures mostly lead to a higher strength than lamellar. In literature, the creation of pearlite starts from the edge of austenit grains [2]. The interface of the grain should work as a metallurgical seed. Could vanadium or vanadium connections on the inside of the austenite grains, be the seed for the pearlite? Seeds would lead to an increased density in the colonies of pearlite. In this way, the observed refining of pearlite would be explained by using V as an alloy.

From a certain content of V onwards, a comparative amount of carbide is formed in the structure, **Figure 6**. Looking at the deep etching in 3D, **Figure 7**, the morphology can be clearly recognized. The non-uniform, sharp edged formation leads to a big internal notch effect and has a diminishing effect on the strength. The elements iron (Fe), carbon (C) and chrome (Cr) were detected in the scanning electron microscope. There is an iron-(V, Cr)-mixed-carbide. In order to

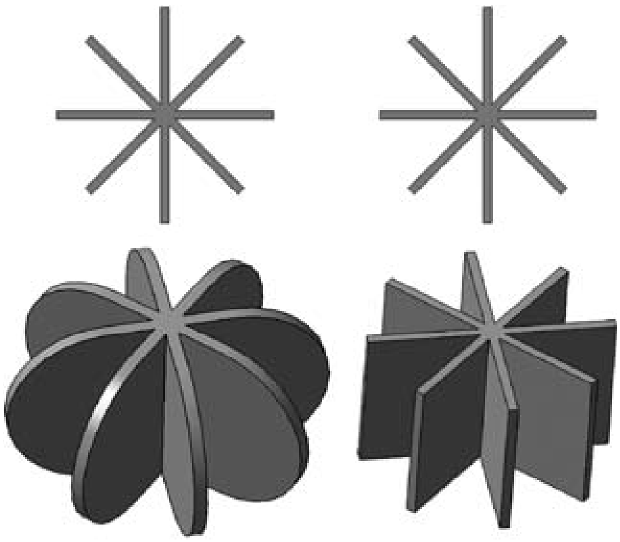

Figure 4: Model of understanding

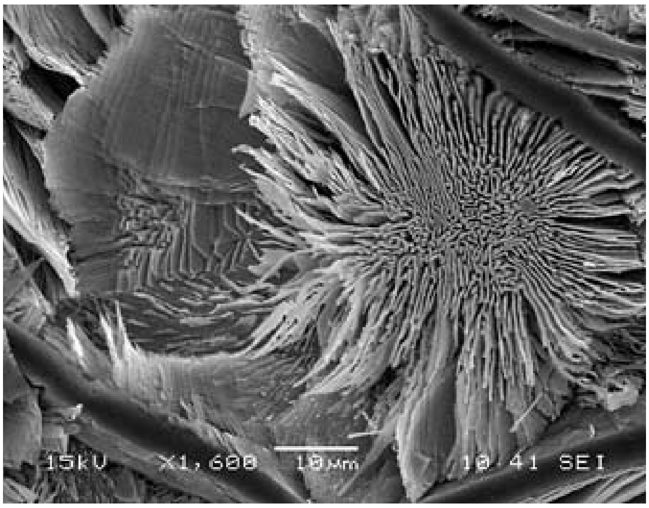

Figure 5: Morphology of Pearlite

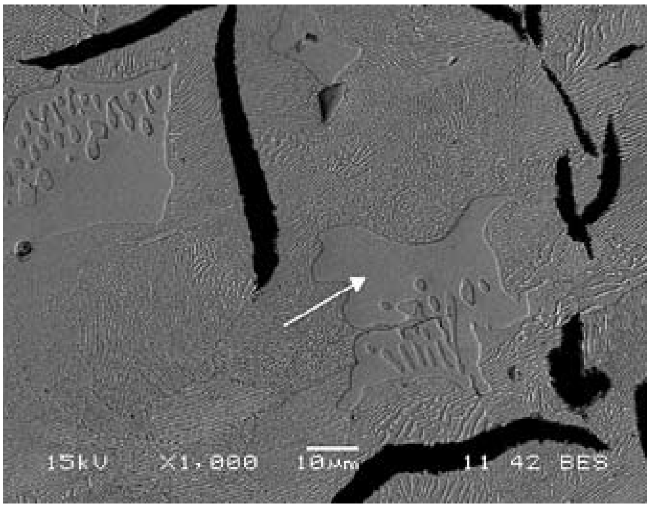

Figure 6: Vanadium-carbide

make it easier to read, it will be named in the following text as vanadium-carbide. Due to this vanadium-carbide, part of the strength-rising effect of the rounded graphite ends and the refining of pearlite of V is cancelled out, so that the strength reaches a maximum as a function of the V-content and drops with any further increase of the V-content. A big V-content predominates over the strength-diminishing quality of the vanadium-carbide in the total effect. Due to the fact that Cr was measured in the vanadium-carbide, it is obvious that the Cr content influences the position of the maximum. The function, Figure 1, showing the course between the ultimate tensile strength variation and the V-content, depends upon the position of the tested areas. The local cooling conditions, specific for this component are a clear factor of influence. Consequently, an individual application development makes sense, based upon the found legitimacies. This knowledge has been used with respect to the cylinder crankcase for Daimler engine OM651 for a lightweight design with high stability.

The knowledge concerning the formation conditions of vanadium-carbide, has turned out to be a quintessential point of vanadium-alloying. Alloying with vanadium can only be controlled by a foundry, if the technology is fully understood. Otherwise, the material efficiency is low and bad experiences of machining problems with vanadium-carbide are pre-programmed.

4 Lightweight Construction – Searching for Limits

Is there an increase in efficiency through an even higher ignition pressure with respect to downsizing? How much material can be reduced in areas of stress, without falling outside of the required dimensions. Lightweight construction is the search for limits. In the lightweight construction system of the computer simulation (FEM), the construction engineer can use the component behaviour with respect to known characteristics. One aim is the continued improvement in simulation precision. A good starting point would be to use material groups of individual mathematical material models for the calculation. For example, the function (1) for grey cast iron (GI) shows a mathematical model for the description of a measured tension-expansion-curve, **Figure 8**, of a standardized tensile strength test.

$$\sigma(\varepsilon) = \frac{\Psi}{\sqrt{1+\left(\frac{\Psi}{10 \cdot E \cdot \varepsilon}\right)^2}} \qquad \text{Eq. (1)}$$

σ = tension [MPa]

ε = expansion [%]

Ψ = approximationscoefficent [-]

$E = \frac{d\sigma(\varepsilon)}{d\varepsilon}$ (0) E module in origin [GPa]

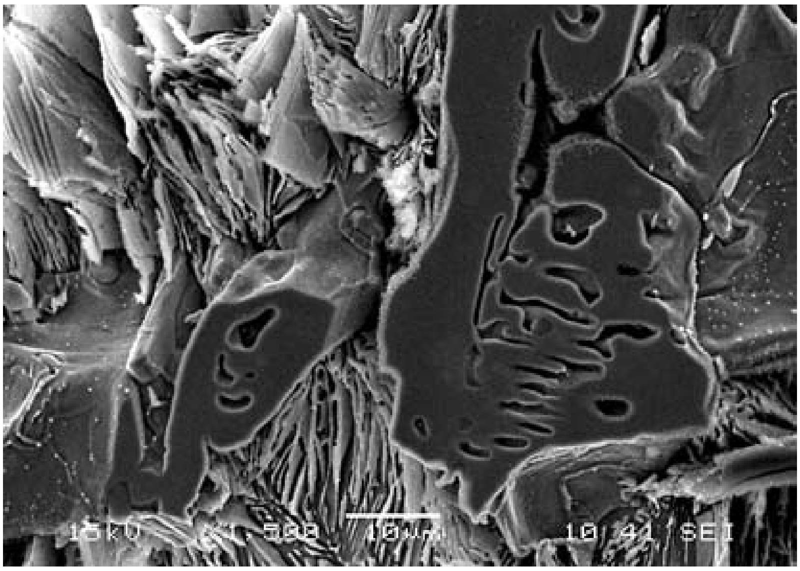

Figure 7: Deep etching Vanadium-carbide

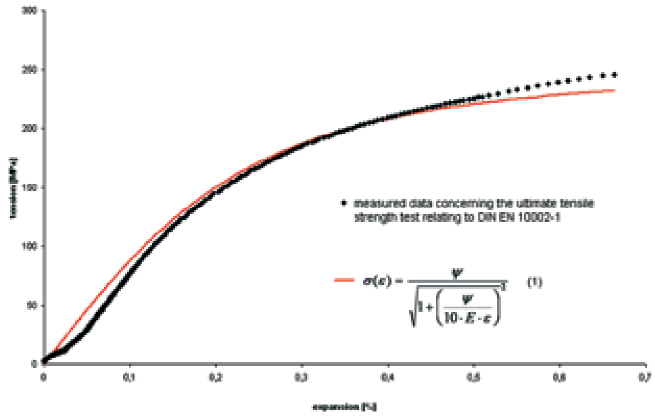

Figure 8: Approximation

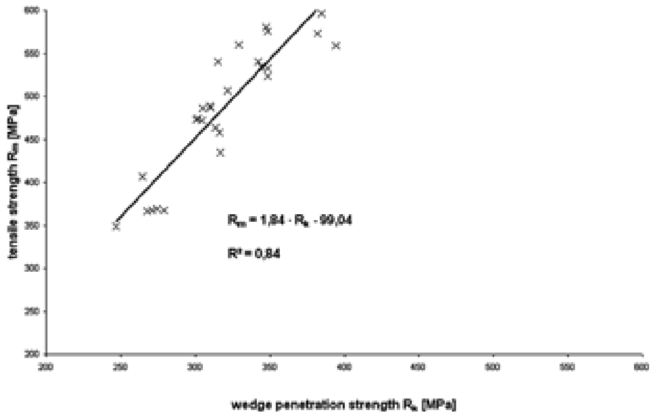

Figure 9: Wedge penetration strength (CGI 400 and CGI 450)

Another starting point would be to have a closer look at the local character of the material identity values. The work of Daimler AG [3] takes a closer look at thin walled components from grey cast iron (GI). The CGI test carriers were produced by Halberg Guss. Sometimes, test sticks are unable to be taken from thin areas. The limit of a classical material test is reached. Lightweight construction requires a conformist metallurgy measuring technique. To receive strength values also with reduced material volume, VW uses the wedge penetration test with grey cast iron. Here, the counterpart to the ultimate tensile strength R_m is the ultimate wedge penetration strength R_k. Can this test method be transferred to CGI 400 and CGI 450? With reference to this, a test was carried out by Halberg Guss to find a connection between the wedge pressure resistance and the tensile strength. An extract from this can be seen in **Figure 9**, test specimens were test plates.

CGI has the highest strength qualities under the standard materials for cylinder crankcases, for example, the 4.2 l TDI V8-engine from Audi. Lightweight construction means also to penetrate into limits. Accordingly, the demands on quality management become higher and higher. More knowledge gained by measurement means more security. Continuous improvement of process security is obtainable through new possibilities of the metallurgy measuring technology. The strength of CGI is achieved by alloying with magnesium (Mg). But the essential point with respect to material production is the knowledge concerning the interaction of Mg with other elements and putting this knowledge to a specific use. The most important thing for the CGI structure form is being able to master the sum (Mg + MgO + MgS + $MgSiO_2$ + remaining Mg connections). The possibility of producing gradient cast iron verifies its legitimacy [4]. The interaction of Mg with oxygen (O) becomes measurable by electro-chemical sensoring by Heraeus: An electro-chemical sensor for cast iron melts which calculates the oxygen activity with regards to a fix-point from the actual oxygen activity and the actual temperature, known as $a_{O,1420}$. The fix-point was defined at 1420 °C.

The degree of complexity is considerably reduced by the introduction of the fix-point methodology in practical use. With the new activity measure, melts with different temperatures are easier to compare. The content is not to be mistaken for the activity. Simply put, the activity is a measure for the effective concentration of an element. In a CGI component in its hard state, the analysis shows approximately 20 weight-ppm oxygen. The oxygen activity $a_{O,1420}$, of a CGI-melt which is ready to cast, is measured with this sensor at 0.2 ppm.

The application spectrum of the oxygen activity measurement in the CGI production is varied:

- uncovering procedure faults
- combining with already widespread metallurgy measuring technologies, such as resonance analysis, thermal analysis ("SinterCast" measuring system)
- realisation of own CGI procedures by integration of the oxygen activity measurement and a thermal analysis in the procedure-technical basic operations of melt production.

The use of cast iron has a long history, but despite this, there is no stagnation in development due to the consistent use of metallurgical measuring techniques.

References

[1] Mücklich, F.: Neue Möglichkeiten der objektiven Graphitklassifizierung in Gusseisen durch Nano-Tomographie und internetbasierte Online-Verfahren. Gießtechnik im Motorenbau. Anforderungen der Automobilindustrie. In: VDI-Berichte 1949. Düsseldorf: VDI-Verlag GmbH, 2007
[2] Riehle, M.; Simmchen E.: Grundlagen der Werkstofftechnik. 2. Auflage, Seite 268. Stuttgart: Deutscher Verlag für Grundstoffindustrie, 1997
[3] Scheib, H.: Untersuchung des Zusammenhangs zwischen Erstarrung, Abkühlung, Gefüge und mechanischen Eigenschaften von dünnwandigen GJV-Bauteilen. Magdeburg, Universität, Dissertation, 2007
[4] Radebach, D.: Gradientenwerkstoffe zur verbesserten Bearbeitbarkeit und Tribologie von Komponenten im Motorenbau. In: MTZ 2007 Nr. 10

lightweight-design

Ideas that make you stand out

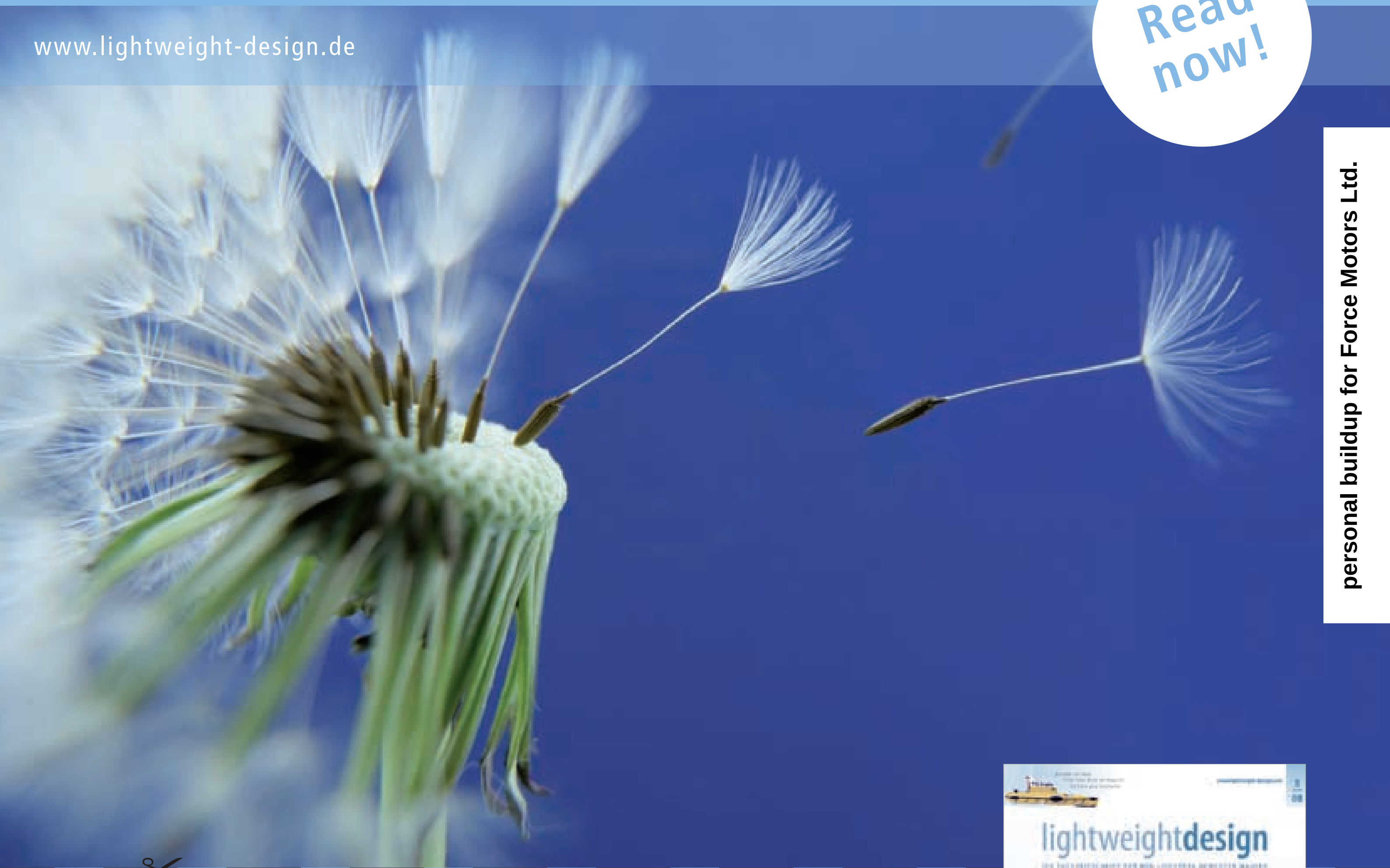

Subscription*

◯ Yes, please send me the trade magazine lightweightdesign immediately (6 issues + access to online archive) for at least 12 months for the subscription price of 96,– € plus postage.

Test subscription*

◯ Yes, please send me the next issue of the trade magazine lightweightdesign free of charge and without obligation. If I wish to continue receiving the magazine, I do not need to do anything. I will otherwise send you a short notice within 14 days upon receipt of the magazine. To meet the deadline, timely mailing shall suffice. In case you do not hear from me, send me the trade magazine lightweightdesign (6 issues + access to online archive) for the subscription price of 96,– € for 1 year.

***You may unsubscribe at anytime prior to your receipt of the next available magazine issue. Any overpayment for undelivered magazines will be reimbursed.**

◯ Yes, I would like to receive the lightweightdesign newsletter free of charge by e-mail.

Vorname

Nachname

Firma

Branche / Abteilung

Straße / Nr.

PLZ / Ort

Land

Telefon / Fax

E-Mail

Datum / Unterschrift

Vieweg+Teubner Verlag Leserservice
Abraham-Lincolnstr. 46
65189 Wiesbaden
Fax 0611-7878-440
viewegteubner@abo-service.info

Please simply fill out and submit the form above by fax to 0049-611 7878-440 or post your order.

Right of withdrawal: I have the right to cancel this agreement in writing within 14 days after the purchase order date at Vieweg Verlag, Leserservice, Abraham-Lincoln-Str. 46, 65189 Wiesbaden. It is sufficient if the cancellation is sent off before the end of the cancellation time limit. Vieweg Verlag, GF: Dr. R. Birkelbach, A.F. Schirmacher, AG Wiesbaden HRB 9754.

311 08 012

Avoiding Cavitation in Engine Cooling Pumps

Cavitation occurs quite frequently in engine coolant pumps and can produce various problems, notably erosive wear on pump components, aeration of the coolant, excessive noise and vibration. This commonly results in failure of the pump's seal, followed closely by bearing failure, leading to reduced engine cooling and ultimately failure of the pump itself. This article from Haldex Concentric sets out some basic design considerations that will significantly reduce the likelihood of cavitation occurring as well as the associated failure modes.

1 Introduction

Seal failure in coolant pumps is of particular concern for OEMs, since it is a major cause of engine-related warranty claims. This has tended to focus attention on the seal‘s design, but in many cases seal failure is symptomatic of other inherent problems within the cooling system, which have not been avoided at the design stage.

In such cases, even the pump may be only part of the problem and, by taking a system perspective, designers can achieve significant improvements in performance as well as reliability. This article sets out some simple basic design considerations that will significantly reduce the likelihood of cavitation occurring as well as the associated failure modes.

2 The Phenomenon of Cavitation

Cavitation is the term used to describe the phenomenon of fluid vaporising, followed by the implosion of the vapour bubble within the coolant circuit. Vaporisation of the fluid occurs if the fluid reaches its vapour pressure point, normally as a result of a combination of pressure and temperature conditions.

The graph shown in **Figure 1** illustrates a typical vapour pressure characteristic for long-life engine coolants. As can be seen, the concentration of coolant relative to the water content has a major influence on the temperature and pressure at which vaporisation occurs.

With engine coolants typically operating within the 90 °C to 110 °C range and coolant concentration levels usually being 50 %, it can be seen that the pressure to cause vaporisation typically occurs between 50 kPa and just over 100 kPa absolute pressure, with 100 kPa being atmospheric pressure. The graph highlights the need for vehicle coolant systems to operate at elevated pressures during hot running conditions.

Normally the worst-case scenario will be when the engine is running hot, with the coolant running through the radiator at full flow rate. If there is relatively low pressure at the radiator outlet, combined with high coolant temperature, the fluid is in danger of vaporising. The coolant temperature at the pump inlet is lower than that at the engine outlet because of the temperature gradient across the radiator. Ideally, radiators are sized to accommodate a sufficient temperature gradient from the engine outlet, when there is minimum airflow, based on a high load condition of the engine, typical of a hot ambient trailer tow test.

3 Additional Localised Pressure Consideration

Within the coolant pump, it is normal for a local pressure reduction to occur at the entry to the pump impeller. This local

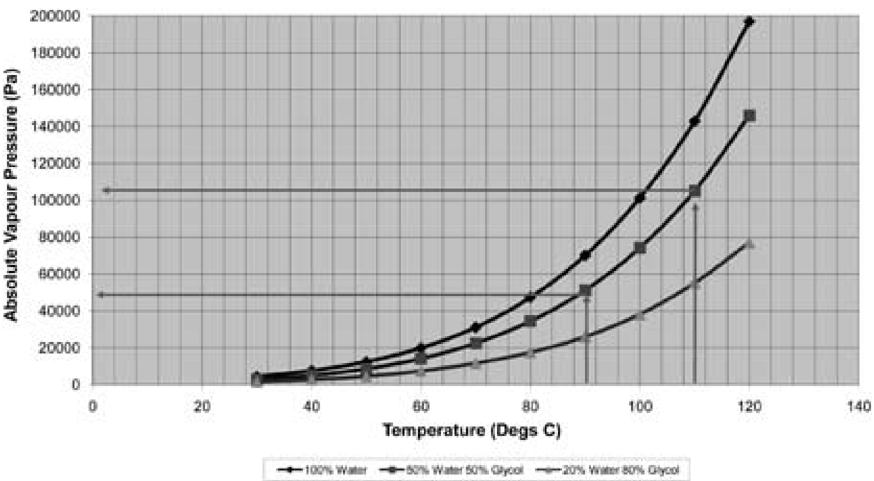

Figure 1: Typical vapour pressure characteristics for long-life coolant

The Author

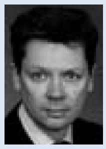

David J. Williams
is Technical Director
at Haldex Concentric
in Birmingham
(United Kingdom).

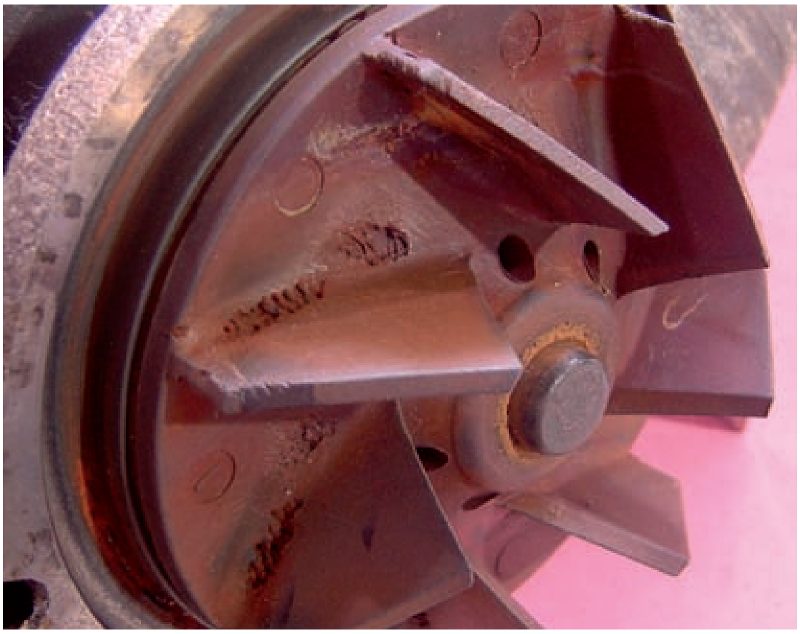

Figure 2: Extreme damage patterns from cavitation within centrifugal pumps

pressure reduction is caused by the sudden acceleration in the velocity of the fluid as it enters the rotating impeller. If this local pressure reduction, along with the increased temperature of the coolant, enables the fluid to reach the vapour pressure point, then fluid vaporisation will occur, normally within the passageways between the blades of the pump impeller. As the fluid pressure increases across the diameter of the impeller, the vapour bubble is likely to implode causing localised damage to the impeller and to a lesser extent to the pump housing, Figure 2.

4 Net Positive Suction Head Evaluation

By comparing the conditions required to prevent the fluid reaching its vapour pressure point at the pump inlet and contrasting these with conditions that are actually available within the cooling system, it is possible to determine if a margin of safety is available or not. This can be determined from the following equation for the net positive suction head (NPSH):

$$NPSH = Ps\ Abs - Pv + V1^2 / 2g,$$

where Ps Abs is the absolute pressure head of the fluid at the point normally considered the pump inlet (m), Pv is the vapour pressure head of the fluid at the temperature and concentration considered (m), V1 is the fluid velocity at pump inlet (m/s) and pressure head = P / ρ g (m), where p is pressure in Pa.

It is normal to determine the NPSH for a given speed and flow rate prior to vaporisation and term this NPSHr (Net positive suction head required). Most pump manufacturers are able to provide NPSHr curves which indicate the reduction in total pressure head at individual flow conditions at a constant speed, based upon tested data, Figure 3.

From the NPSHr against total head plot, an NPSHr against flow plot can be produced for individual operating speeds of the pump.

Given the NPSHr data supplied by the pump manufacturer, it is possible to cal-

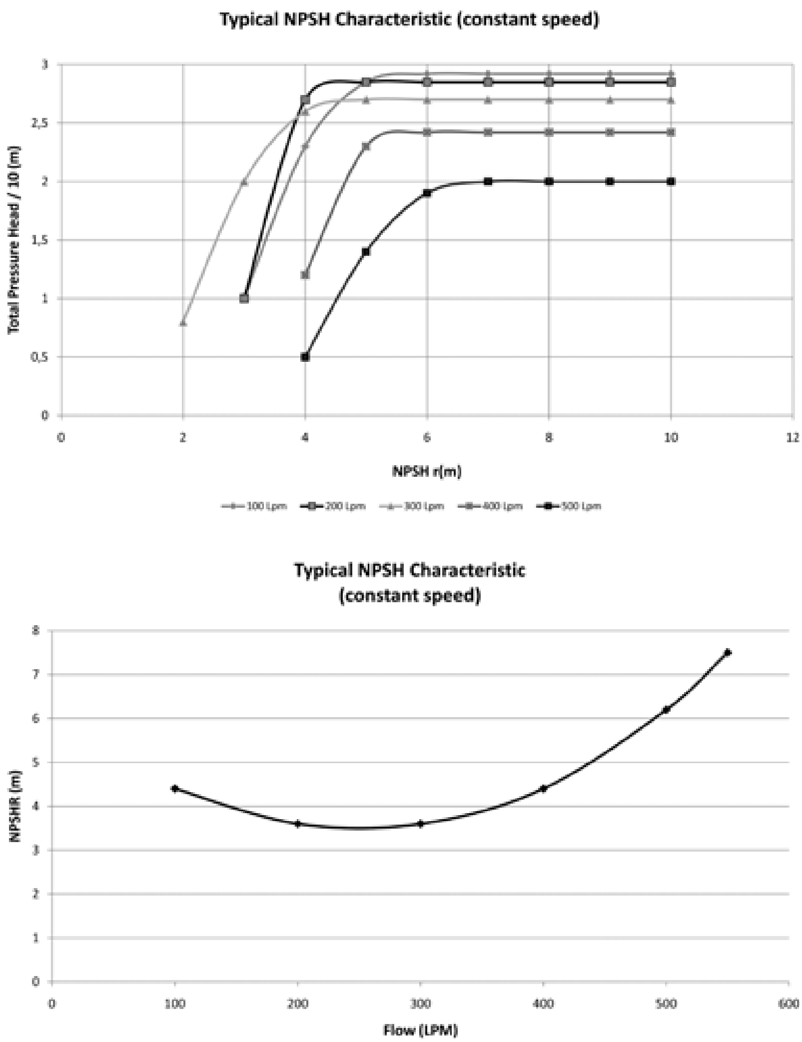

Figure 3: Typical NPSHr curves

culate the NPSHa (Net positive suction head available) from the cooling system. This involves considering the lowest pressure at the pump inlet connection and highest estimated coolant temperature possible at the pump inlet, then calculating the NPSHa. If the NPSHa is greater than the NPSHr, then cavitation should not occur. However in the author's experience many engine coolant systems have a lower NPSHa than the NPSHr at the coolant pump.

5 Optimisation of NPSH

Haldex Concentric has developed its own in-house design software that can accurately predict NPSHr at the specification stage within a pump project. By considering NPSHa relative to NPSHr up-front, this software identifies the potential for cavitation and any related problems early in the engine design cycle.

5.1 Improvements to NPSHa

Heat rejected into the coolant is a function of engine load; therefore an extreme form of protection could be to de-rate engine power as coolant temperature begins to rise to problematic levels. Clearly this would be regarded as undesirable by the OE manufacturers, since it limits the power capability of the engine. Such an approach would also require an additional control strategy linked to a fluid temperature measurement, adding cost to the coolant system.

Increasing the pump inlet pressure can be achieved by means of the pressure relief setting on the header tank cap, but caution is required since this has implications for the pressure rating of all components within the cooling system. It is not always practical to ensure a minimum header tank pressure, particularly as it is possible to run the engine without the cap, thereby reducing the coolant system pressure to atmospheric levels. One possible solution would be to provide for a proportion of the outlet flow from the coolant pump to recirculate back into the pump inlet so enabling a ‚supercharge effect' which boosts pressure at the pump inlet. If this is achieved with significant additional inlet flow rate but without impeller geometry changes, then the gain can be offset by increases in eye velocity. However, in practice,the resulting reduction in static pressure will dilute the effect of the incoming boost pressure.

As can be seen from Figure 1, increasing the concentration of the engine coolant will cause an increase in NPSHa; however this requires the coolant concentration to be maintained at these levels throughout the engine life, which will be difficult to control due to coolant changes at scheduled service intervals and occasional top-ups.

5.2 Improvements to NPSHr

The coolant pump designer and the coolant system designer can minimise the losses that lead to reductions in pressure, which is particularly important at the pump inlet. Simple considerations at an early point in the design process can make a good contribution, such as avoiding sharp bends near the pump inlet, as they tend to cause unwanted fluid rotation at the impeller entry. In addition, any bends in the system will reduce the static pressure through friction losses. This loss will be related to the inlet velocity, as shown in **Figure 4**.

Rapid accelerations or decelerations in the pump entry must be avoided, in particular sudden expansions or contractions, as these can lead to significant losses, again related to velocity, as illustrated in **Figure 5**. The coolant pump impeller, if designed correctly, will be optimised, particularly at the vane leading edge to minimise any shock losses as the fluid impacts the impeller vane. This is achieved by matching the incoming velocity vector with the correct impeller vane angle.

Because centrifugal pump impellers normally have fixed vanes, the inlet blade angle is optimised for a particular inlet velocity vector, normally at the design specification point, which will typically be peak operating efficiency. It is therefore preferable to operate the pump as close to its design point as possible, since this is normally the point of minimum NPSHr. Operation away from the design operating point also leads to recirculation flows within the impeller entry and exit as shown in **Figure 6**.

In non-automotive applications, it is not unusual to utilise an additional inducer impeller to provide a boost pressure for the main pump impeller. Normally the inducer would provide an extension to the main impeller, protruding into the pump inlet.

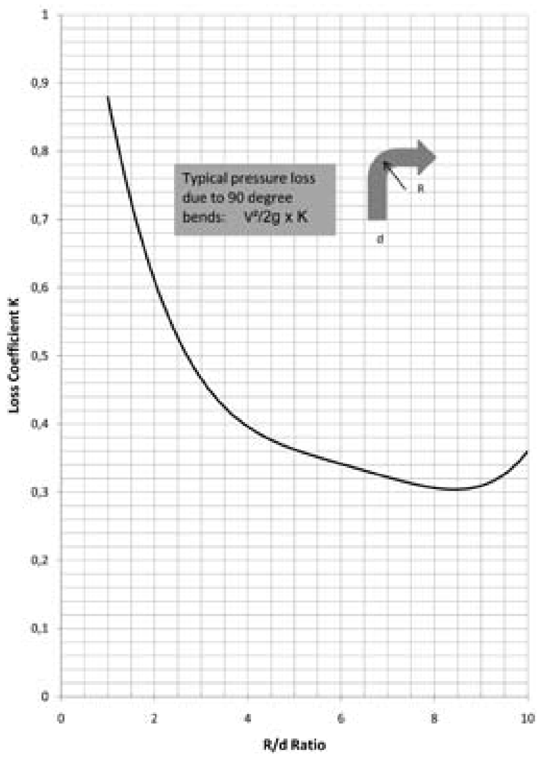

Figure 4: Typical 90° bend loss coefficients

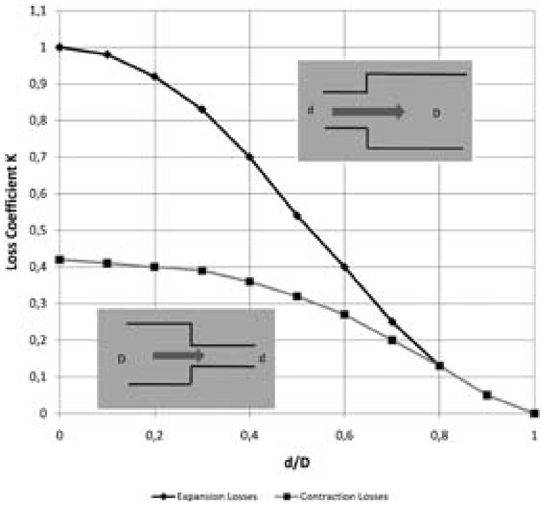

Figure 5: Typical expansion and contraction loss coefficients

Pump NPSHr in general will follow scaling laws for centrifugal pumps, which means NPSHr will vary in a squared relationship to changes in pump speed. This is because higher rotational speeds will lead to increased fluid accelerations as the fluid contacts leading edges of the impeller, resulting in larger localised reductions in static pressure. For these reasons, the pump designer would normally favour low rotational speeds to avoid cavitation. However, this needs to be balanced with the physical packaging constraints of the engine and the need to maximise pump efficiency, which can often be improved with increasing speed.

5.3 Predicting NPSHr

As is common in centrifugal pump design practise, empirical data is very important to correlating mathematical relationships. Haldex Concentric has been manufacturing coolant pumps for over 50 years and so significant data has been accumulated to enable accurate modelling of the factors that most influence the localised static pressure reductions at the pump inlet. The in-house developed software considers the velocity profile both in the pump inlet housing and at the impeller inlet which, together with empirical loss coefficients, enables accurate prediction of NPSHr for all but the most extreme geometries. As with all empirical relationships, once the geometry departs significantly from the base correlation data, the correlation between the two becomes less accurate.

Computational fluid dynamics (CFD) has advanced greatly in recent years, enabling much greater accuracy of even the most complicated flow regimes. Haldex Concentric is increasingly utilising both CFD and in-house software to refine predictions of NPSHr.

5.4 Margin of NPSH Consideration

To ensure that a suitable margin of NPSH is achieved on a new engine project, the coolant system designer should provide data concerning maximum coolant temperature, coolant specification details and the associated minimum coolant pressure adjacent to the pump inlet. In addition, the housing or pipework inlet geometry that may influence the pump inlet flow conditions needs to be defined. These conditions should be considered at both open and closed thermostatic valve conditions. Computational fluid dynamics (CFD) may be required to accurately calculate inlet pressure and velocity profile, dependant upon the complexity of the coolant system. With this information the pump designer can then confirm the NPSHa.

The pump designer‘s task is then to generate a design scheme to achieve the specification flowrate and pressures required at the specified engine speeds. NPSHr would be calculated on the basis of either an assumed drive ratio from engine speed or in some cases a defined drive ratio from the engine designer. With both NPSHa and NPSHr defined, the consideration of a suitable margin can be made. This consideration should be made at all operating speeds, with overspeed usually providing the most difficult condition.

It should be noted that a significant proportion of engines are likely to operate in negative NPSH margin at some point in their operating cycle. This needs to be considered relative to the anticipated time duration. Coolant pump seals will tolerate some degree of dry running; however the best form of defence against potential problems will always be avoidance of any dry running conditions wherever possible.

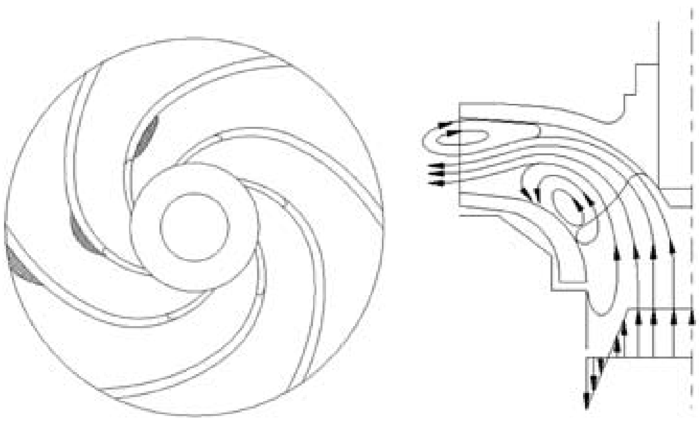

Figure 6: Possible consequences of operation at high or low flow conditions

6 Conclusions

Avoiding cavitation in engine coolant pumps is a system design issue that requires close co-operation between the pump designer and the coolant system designer. Once the system has been developed, any after-treatments that have to be adopted can be both expensive and of limited effectiveness. ■

ATZ live

29 AND 30 JANUARY 2009 | MUNICH | MTZ CONFERENCE - MOTOR

Alternative Propulsion Systems for Automobiles

International Conference

Event in cooperation with

- Hybrid Configurations
- Fuel cells
- Future IC Engines
- Alternative Fuels

ATZlive
Abraham-Lincoln-Straße 46
65189 Wiesbaden | Germany

Telephone +49(0)611. 7878-131
Telefax +49(0)611. 7878-452
atzlive@springer.com

PROGRAMME AND REGISTRATION
www.ATZlive.com

High Temperature Sealings for Exhaust Systems
to Achieve Global Environmental Initiatives

Federal-Mogul has developed a special portfolio of High Temperature Alloy (HTA) gaskets, and a corresponding High Temperature Coating (HTC). In the most basic sense, the HTA and HTC innovations work by providing material stability at extreme operating temperatures. They enable manufacturers of exhaust gas systems to meet the challenges for sealing performance up to 1000 °C with a highly durable product.

1 Background

Over the past decade, vehicle manufacturers have strived to reduce combustion emissions and significantly improve fuel economy. Nearly all governments have created, or otherwise adopted, increasingly stringent requirements limiting exhaust emissions of CO, NO_x, particulate matter, and unburned hydrocarbons, **Figure 1**. Additionally, escalating concerns of limited natural resources and growing levels of atmospheric CO_2 have prompted increasingly tough legislation to dramatically improve vehicle fuel economy.

Vehicle manufacturers have approached this challenge with an extensive portfolio of solutions, like exhaust gas recirculation, direct injection, variable valve timing, turbocharging, higher compression ratios and much more. Each solution addresses different aspects of the combustion process, but the overall objective remains the same – increase the engine efficiency and clean up the exhaust. In this technological evolution, combustion pressures and temperatures have increased considerably, while more components have been integrated into the exhaust stream, increasing temperatures are placing higher demands on the exhaust system. Turbocharging, in particular, has changed temperatures in the exhaust system from a manageable 400 °C to over 1000 °C.

While exhaust temperatures have soared, it has become equally critical to completely seal the exhaust. With allowable emissions approaching levels merely 1 % of 1990 requirements, imperfect exhaust sealing is no longer tolerated. Micro-leakage that would once be considered test noise now results in serious fines and expense for both manufacturers and consumers. Complicating this situation, exhaust joints tend to be very dynamic interfaces. Physical movement of the mating parts and excessive thermal gradients together ensure that a simple static gasket will not be sufficient.

The combination of these trends has created a sealing challenge that has far exceeded traditional sealing solutions. Materials that typically seal well generally cannot withstand extreme temperatures. To tackle the challenges of extreme temperature, stringent leak requirements, and dynamic joint motion, Federal-Mogul Corporation developed a portfolio of High Temperature Alloys (HTA). These alloys were designed to maintain superior sealing in very high temperature, highly dynamic environments.

Providing a metal gasket material was only half of the challenge for sealing highly dynamic joints. With surface imperfections in both the gasket and the mating flanges, a pliable coating was also necessary to provide the necessary exhaust gas micro-sealing. This coating required very low friction, to prevent galling and wear of these highly mobile joints. Typically, Molybdenum-based coatings had been used for micro-sealing. As temperatures exceed 600 °C, the Molybdenum coatings break down, causing joint wear and leaks. Federal-Mogul's High Temperature Coating (HTC) was designed to work with HTA to provide a complete, durable, long term exhaust sealing solution, **Figure 2**.

The Authors

Jim Zwick
is Global Director of Product Development – Gaskets and Heatshields for Sealing Systems at Federal-Mogul Corporation in Southfield, Michigan (USA).

Dr. Bhawani Tripathy
is Director of Advanced Technology and Materials Development for Sealing Systems at Federal-Mogul Corporation in Ann Arbor, Michigan (USA).

Trevor Groh
is Product Line Manager for Hot Gaskets and Heat Shields, responsible for Product Strategy and Marketing at Federal-Mogul Corporation in Southfield, Michigan (USA).

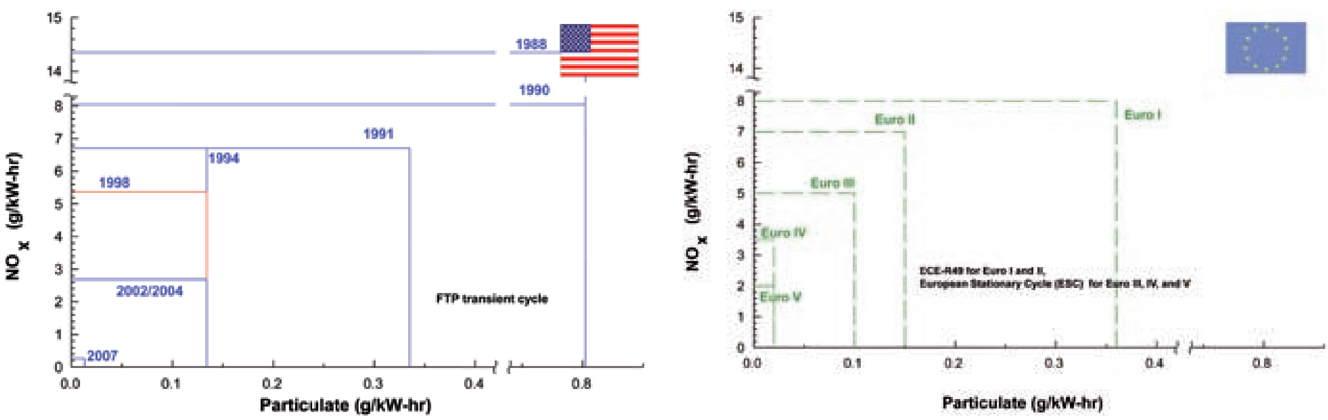

Figure 1: Emissions regulation trends

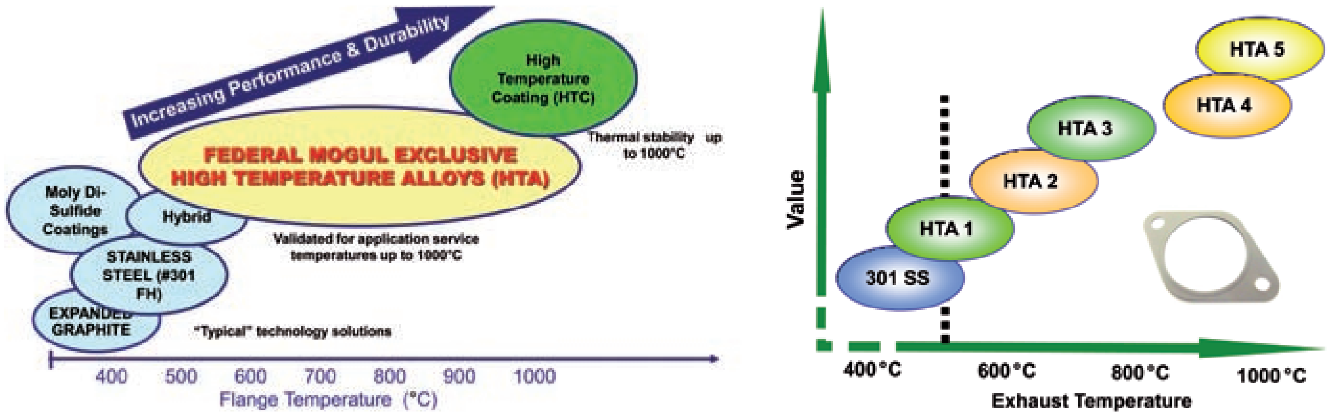

Figure 2: High temperature alloy exhaust sealing solution

2 The Need for High Temperature Alloy

As Federal-Mogul has worked with its customers to provide HTA solutions, it has been clear that certain segments need HTA much more urgently than others. Manufacturers of commercial vehicle engines, in particular, found that pushing turbocharged diesel engines beyond 220 bar cylinder pressure and the use of exhaust gas recirculation resulted in excessively hot exhaust temperatures. Similarly, automotive customers are discovering that modern variable geometry turbocharging is forcing exhaust temperatures to levels beyond 1000 °C. In both cases, Federal-Mogul has been able to provide HTA solutions that solve high temperature sealing problems and enable the exhaust system changes required to achieve the engine performance targets.

This trend of increasing exhaust temperatures will likely accelerate. The dominating global automotive strategies are downsizing and turbocharging, squeezing tremendous performance out of each engine. Boosted engines in the U.S., in particular, are expected to grow 65 % annually over the next half decade. Commercial vehicle manufacturers are also continuing this trend, with newer engines requiring increased combustion pressures and temperatures.

3 Material Innovation High Temperature Alloy

Today's high-performance automotive and truck exhaust gaskets have moved well beyond the traditional composite exhaust gasket technologies. As emission requirements have tightened, gasket design has evolved from fiber, to graphite, then finally into Single-Layer Steel (SLS) and Multi-Layer Steel (MLS).

SLS / MLS constructions, used for both cylinder head and exhaust gaskets, were a significant departure from historic flat gaskets. With SLS technology, a thin layer of hardened steel is stamped with bead-shaped embossments.

The bead shape in stainless steel effectively forms a spring. This spring is compressed during joint assembly and provides the gasket dynamics necessary to maintain a tight seal as the mating exhaust components bend and flex as a result of both thermal and mechanical stresses. The measured ability of the gasket bead to respond and conform to the joint dynamics is known as "recovered height," and is simply the amount of spring left in the material after compression, **Figure 3**. When a particular joint movement exceeds the recovered height potential of a single-layer gasket, additional embossed layers can be stacked together to form Multi-Layer Steel via springs in series theory.

As exhaust gasket temperatures climb above 425 °C, the Single-Layer Steel gasket system runs into difficulty. The higher temperature limits the ability of the 301 Stainless Steel to spring back, reducing its dynamic sealing performance. To some extent, this can be compensated by adding more gasket layers, increasing the overall spring working potential. However, the benefit of added layers is offset by added cost and additional leak path potential. As exhaust temperatures become extreme, stainless steel MLS gaskets may not be suitable at all, regardless

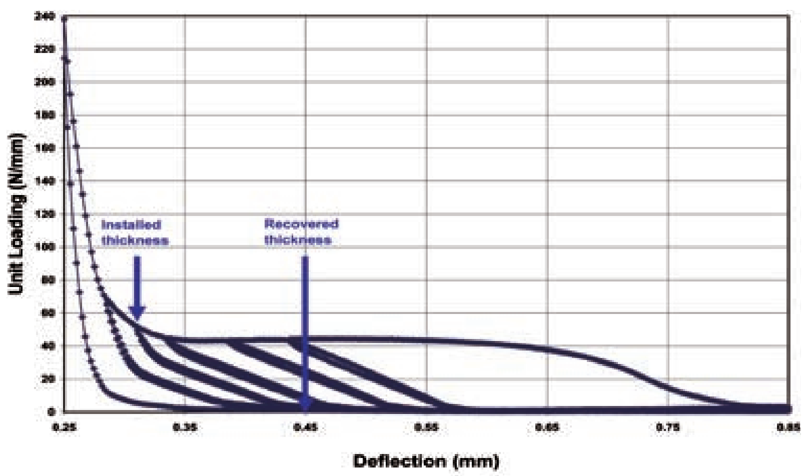

Figure 3: Load deflection/recovery characteristic

of the number of extra layers, due to the thermal degradation of the material.

To address the growing concern over increasing exhaust temperatures, Federal-Mogul developed a portfolio of High Temperature Alloy (HTA) materials. The HTA gaskets alloys were developed to fill the broad performance gap between low-end stainless steel and high-end specialty materials.

HTA gaskets provide several benefits for extreme temperature exhaust challenges. The ability of the alloys to maintain high strength under extreme heat ensures embossments maintain proper spring tension, delivering an effective dynamic seal under high pressure and temperature. Specifically, the portfolio of HTA products provides:

- 200 to 500 % improvement in recovered height, vs. 301 Stainless Steel
- superior sealing and creep resistance up to 1000 °C
- potential to reduce the number of active gasket layers, reducing complexity and potential leak paths.

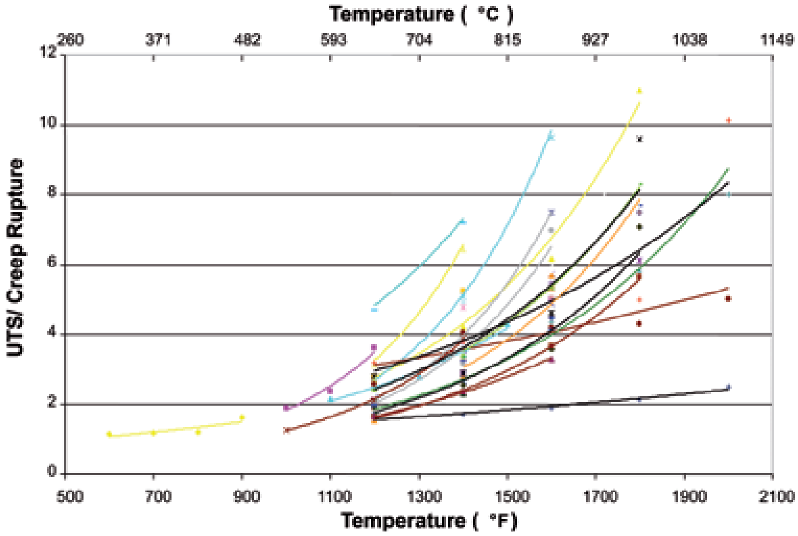

Figure 4: Alloy screening creep resistance

4 Material Development

The engineering of the High Temperature Alloys required an extensive screening process where numerous alloy chemistries were reviewed for creep resistance and thermal stability, **Figure 4**.

As candidate materials were identified, they were evaluated and directly compared with the typical exhaust sealing material – 301 (full-hard) stainless steel. The benchmark for performance was established to be the recovered height for 301 Stainless Steel at its known operating capability – 60 μm.

A laboratory screening test was developed where standard washers were clamped between two hardened pucks, acting as the bolted joint flanges. A load of 171 kg per centimeter of embossment length was applied to the assembly. After installing the test specimen, the fixture was placed in a preheated furnace at the appropriate test temperature for 17 hours, removed and allowed to cool. The residual embossment height on the test specimen was measured with a stylus-type profilometer. The recovered height performance of each alloy was plotted versus temperature, **Figure 5**. The metastable 300 series alloys, such as 301 and 316Ti provided good performance up to 427 °C, due to the presence of transformation-induced Martensite, but degraded rapidly as the temperature increased.

The rapid degradation of the 301 Stainless Steel was confirmed by a study of micro-hardness. As shown in **Figure 6**, the micro-hardness of 301 Stainless Steel changes significantly after exposure to temperatures above 427 °C, indicating a loss of mechanical properties. In the case of exhaust sealing performance, this limits the ability to provide dynamic recovery and maintain adequate contact for proper sealing.

Based on the results from this test, and similar evaluations, the high tem-

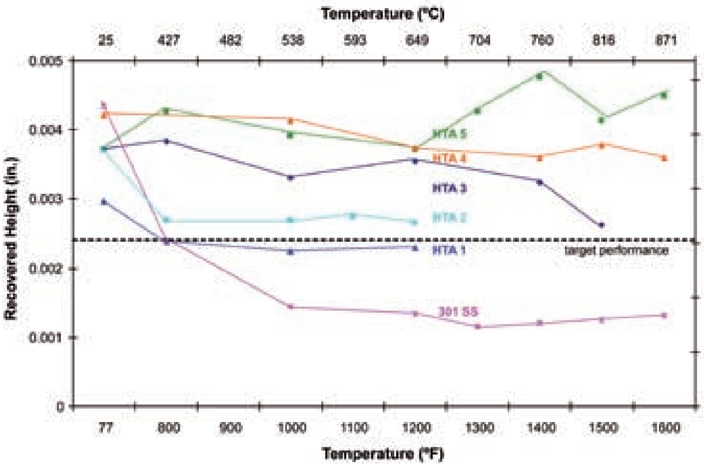

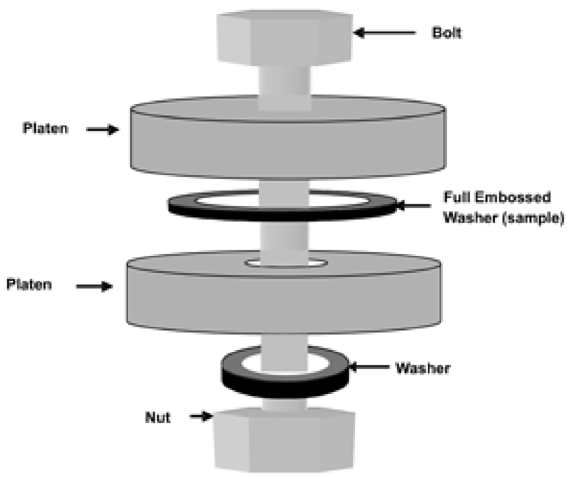

Figure 5: Lab clamp test – recovered heights

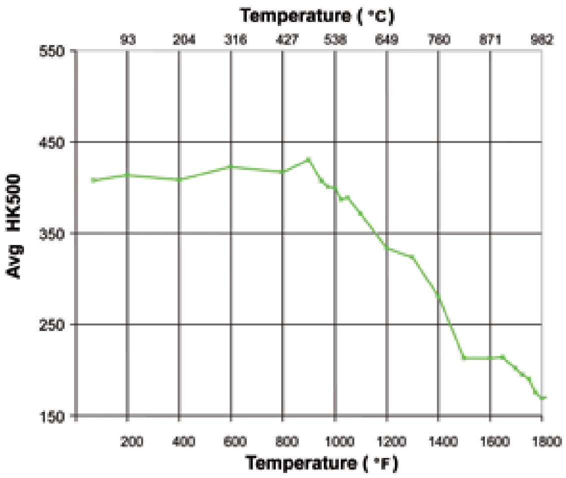

Figure 6: 301 SS hardness versus temperature

Table: High temperature alloy portfolio

Alloy #	Temperature Range
1	425 – 540 °C
2	540 – 650 °C
3	650 – 750 °C
4	750 – 850 °C
5	> 850 °C

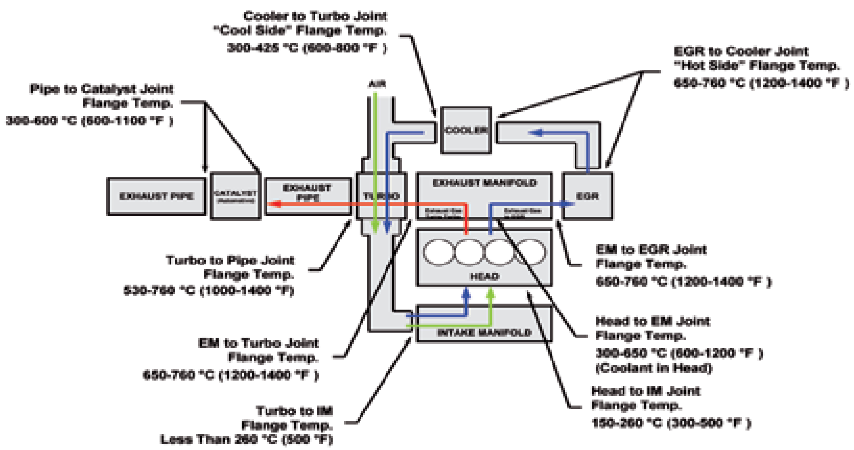

Figure 7: Illustration of exhaust system application environments

perature alloy portfolio was defined. Note the range of materials and suggested performance capability in the temperature ranges as illustrated in the **Table**.

A critical accomplishment in the HTA development was the definition of an entire portfolio of materials, permitting material selection based upon the specific application operating environment. The operating temperature at each joint drives the HTA grade selection, as temperatures vary considerably in the exhaust system, **Figure 7**. The turbocharger, downpipe, exhaust manifold and EGR (cold and hot side) all have different thermal stresses, and one universal solution is not always practical. Thus, the HTA portfolio enables the engineering of the right solution for each exhaust system application.

5 Material Innovation High Temperature Coating

Solving the challenge of high temperature material recovery was critical, but ultimately only addressed half of the sealing concern. The micro-sealing of an exhaust gasket is accomplished by a coating applied to the embossed gasket layers. In exhaust sealing applications this coating is often required to have dual functionality, sealing the surface asperities of the mating flanges and reducing the damaging effects of motion through reduced friction. At temperatures over 600 °C, traditional molybdenum-based coatings break down and lose functionality, leading to a loss of sealing function and galling of the mating flanges. **Figure 8** clearly illustrates this coating breakdown. Post test conditions of the gasket reveal evidence of cast iron material from the exhaust flange bonded to the gasket which

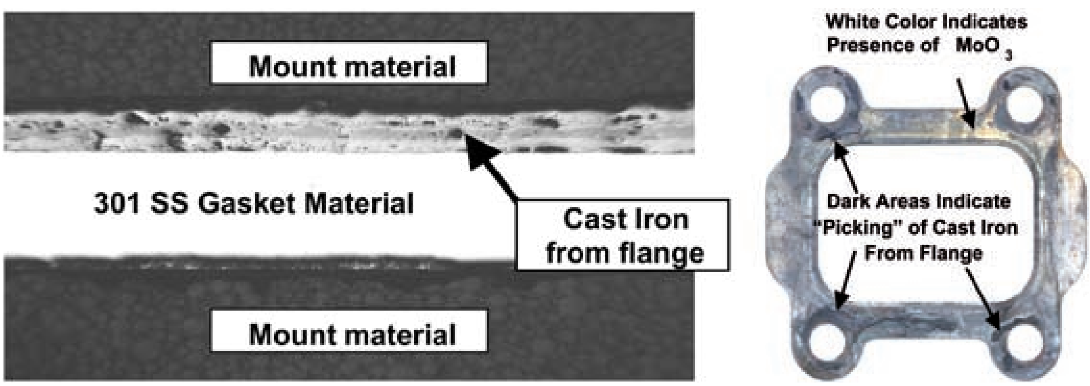

Figure 8: Typical failure mode – picking

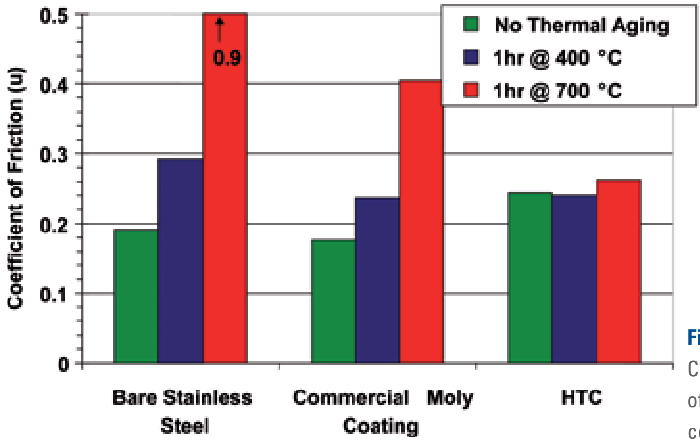

Figure 9: Coefficient of friction comparison

indicates micro-welding and material pull-out during operation. This is further indication of coating degradation and failure at elevated temperature.

To address the coating concern and complement the High Temperature Alloy portfolio, Federal-Mogul developed a unique High Temperature Coating (HTC). This coating is much more stable at extreme temperature than existing products. Additionally, the coating retains its film integrity at high temperatures, reducing the potential for galling of the flanges and allowing easy gasket removal.

The high temperature coating (HTC) is unlike any coating seen in applications before. It is free of molybdenum disulfide and it is not elastomer based. The coating contains a three binder system, which helps provide superior performance over a wide temperature range. The filler system was chosen to optimize sealing properties both at ambient and elevated temperatures while maintaining a consistent coefficient of friction over a range of operating temperatures.

Specifically, to provide the best possible coating for extreme temperature applications, the coating was designed to these specifications:

– thermally stable to at least 1000 °C
– effective seal both at ambient and at high temperatures
– excellent bond to the new HTA substrates
– resistant to warm water, for applications where condensation in the exhaust system could occur
– water-based and low hazard for the environment.

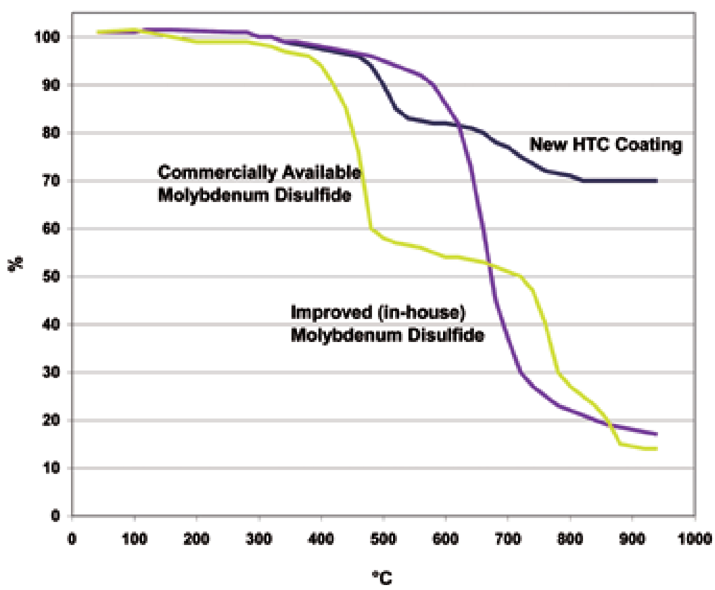

Figure 10: Thermogravimetric analysis of HTC

6 High Temperature Coating Material Development

The strategy to develop the coating free of Molybdenum disulfide was based on the fact that the MoS_2 will react in a high temperature, oxidizing environment to form Molybdenum trioxide (MoO_3). This MoO_3 molecule is a highly abrasive material and greatly increases the potential for bolted joint degradation and sealing failure.

Figure 9 illustrates the effect of this MoS_2 molecular transformation by a notable increase in the coefficient of friction as temperature increases. The HTC coefficient of friction, by contrast, is constant over the temperature range from ambient to 700 °C.

The thermal stability of the HTC coating was further analyzed using a thermogravimetric analysis (TGA) as shown in **Figure 10**. The HTC demonstrates thermal stability up to 1000 °C, while the conventional molybdenum based coatings were completely reduced to ash.

7 Conclusion

The dominating trends in the automotive and commercial vehicle industry are to improve the efficiency of the combustion process and to clean up the exhaust. This is undeniably necessary to meet stringent emission and fuel economy requirements. This efficiency trend is generating increasing exhaust temperatures, while the micro-leak can no longer be tolerated. Increasing the effectiveness of sealed joints in the exhaust system is paramount to meeting environmental and emissions regulations and to provide accurate engine management data. The exhaust system thermal and mechanical complexity continues to increase; this complexity is evolving the design of exhaust system sealing solutions to be a non-trivial task.

Lower applied loads, increased flange movement and distortions, plus temperatures in excess of 850 °C, make it difficult for traditional exhaust gaskets to provide an effective seal. Thus, advanced technical solutions, such as the HTA/HTC innovation, are required to develop highly robust solutions to this challenging technical problem. ■

Peer Review ATZ|MTZ

Peer Review Process for Research Articles in ATZ and MTZ

Steering Committee

Prof. Dr.-Ing. Stefan Gies	RWTH Aachen	Institut für Kraftfahrwesen Aachen
Prof. Dipl.-Des. Wolfgang Kraus	HAW Hamburg	Department Fahrzeugtechnik und Flugzeugbau
Prof. Dr.-Ing. Ferit Küçükay	Technische Universität Braunschweig	Institut für Fahrzeugtechnik
Prof. Dr.-Ing. Stefan Pischinger	RWTH Aachen	Lehrstuhl für Verbrennungskraftmaschinen
Prof. Dr.-Ing. Hans-Christian Reuss	Universität Stuttgart	Institut für Verbrennungsmotoren und Kraftfahrwesen
Prof. Dr.-Ing. Ulrich Spicher	Universität Karlsruhe	Institut für Kolbenmaschinen
Prof. Dr.-Ing. Hans Zellbeck	Technische Universität Dresden	Lehrstuhl für Verbrennungsmotoren

Advisory Board

Prof. Dr.-Ing. Klaus Augsburg	**Prof. Dr. rer. nat. habil. Ulrich Maas**
Prof. Dr.-Ing. Bernard Bäker	**Prof. Dr.-Ing. Martin Meywerk**
Dr.-Ing. Christoph Bollig	**Prof. Dr.-Ing. Werner Mischke**
Prof. Dr. sc. techn. Konstantinos Boulouchos	**Prof. Dr.-Ing. Klaus D. Müller-Glaser**
Prof. Dr.-Ing. Ralph Bruder	**Dr. techn. Reinhard Mundl**
Dr. Gerhard Bruner	**Dr.-Ing. Lothar Patberg**
Prof. Dr. rer. nat. habil. Olaf Deutschmann	**Prof. Dr.-Ing. Peter Pelz**
Dr. techn. Arno Eichberger	**Prof. Dr. techn. Ernst Pucher**
Prof. Dr. techn. Helmut Eichlseder	**Dr. Jochen Rauh**
Dr.-Ing. Gerald Eifler	**Prof. Dr.-Ing. Konrad Reif**
Prof. Dr.-Ing. Wolfgang Eifler	**Dr.-Ing. Swen Schaub**
Prof. Dr. rer. nat. Frank Gauterin	**Prof. Dr. sc. nat. Christoph Schierz**
Prof. Dr. techn. Bernhard Geringer	**Prof. Dr. rer. nat. Christof Schulz**
Prof. Dr.-Ing. Uwe Grebe	**Prof. Dr. rer. nat. Andy Schürr**
Prof. Dr.-Ing. Horst Harndorf	**Prof. Dr.-Ing. Ulrich Seiffert**
Prof. Dr. techn. Wolfgang Hirschberg	**Prof. Dr.-Ing. Hermann J. Stadtfeld**
Univ.-Doz. Dr. techn. Peter Hofmann	**Prof. Dr. techn. Hermann Steffan**
Prof. Dr.-Ing. Günter Hohenberg	**Dr.-Ing. Wolfgang Steiger**
Prof. Dr.-Ing. Bernd-Robert Höhn	**Prof. Dr.-Ing. Peter Steinberg**
Prof. Dr. rer. nat. Peter Holstein	**Prof. Dr.-Ing. Christoph Stiller**
Prof. Dr.-Ing. habil. Werner Hufenbach	**Dr.-Ing. Peter Stommel**
Prof. Dr.-Ing. Roland Kasper	**Prof. Dr.-Ing. Wolfgang Thiemann**
Prof. Dr.-Ing. Tran Quoc Khanh	**Prof. Dr.-Ing. Helmut Tschöke**
Dr. Philip Köhn	**Dr.-Ing. Pim van der Jagt**
Prof. Dr.-Ing. Ulrich Konigorski	**Prof. Dr.-Ing. Georg Wachtmeister**
Dr. Oliver Kröcher	**Prof. Dr.-Ing. Henning Wallentowitz**
Dr. Christian Krüger	**Prof. Dr.-Ing. Jochen Wiedemann**
Univ.-Ass. Dr. techn. Thomas Lauer	**Prof. Dr. techn. Andreas Wimmer**
Prof. Dr. rer. nat. Uli Lemmer	**Prof Dr. rer. nat. Hermann Winner**
Dr. Malte Lewerenz	**Prof. Dr. med. habil. Hartmut Witte**
Dr.-Ing. Markus Lienkamp	**Dr. rer. nat. Bodo Wolf**

Seal of Approval – this seal is awarded to articles in ATZ/MTZ that have successfully completed the peer review process

Scientific articles in ATZ Automobiltechnische Zeitschrift and MTZ Motortechnische Zeitschrift are subject to a proofing method, the so-called peer review process. Articles accepted by the editors are reviewed by experts from research and industry before publication. For the reader, the peer review process further enhances the quality of ATZ and MTZ as leading scientific journals in the field of vehicle and engine technology on a national and international level. For authors, it provides a scientifically recognised publication platform.

Therefore, since the second quarter of 2008, ATZ and MTZ have the status of refereed publications. The German association "WKM Wissenschaftliche Gesellschaft für Kraftfahrzeug- und Motorentechnik" supports the magazines in the introduction and execution of the peer review process. The WKM has also applied to the German Research Foundation (DFG) for the magazines to be included in the "Impact Factor" (IF) list.

In the ATZ/MTZ Peer Review Process, once the editorial staff has received an article, it is reviewed by two experts from the Advisory Board. If these experts do not reach a unanimous agreement, a member of the Steering Committee acts as an arbitrator. Following the experts' recommended corrections and subsequent editing by the author, the article is accepted. *rei*

MTZ Peer Review

The Seal of Approval for scientific articles in MTZ.

Reviewed by experts from research and industry.

Received ....

Reviewed ....

Accepted ....

24 – 25. MARCH 2009 | STUTTGART | 9TH STUTTGART INTERNATIONAL SYMPOSIUM

FKFS

personal buildup for Force Motors Ltd.

9th Stuttgart International Symposium

Automotive and Engine Technology

Event in cooperation with

ATZ live

___ Yes, I would like to know more! Please send me more detailed Information about the „9th Stuttgart International Symposium“ via e-mail.

First name ______ Family Name ______

Company/Institute ______

Department ______

Street/PO Box ______

Post code/town ______

Phone ______ Fax ______

e-mail ______

ATZlive
Abraham-Lincoln-Straße 46
65189 Wiesbaden | Germany
Phone +49(0)611. 7878-131
www.ATZlive.de

FAX +49(0)611. 7878-452

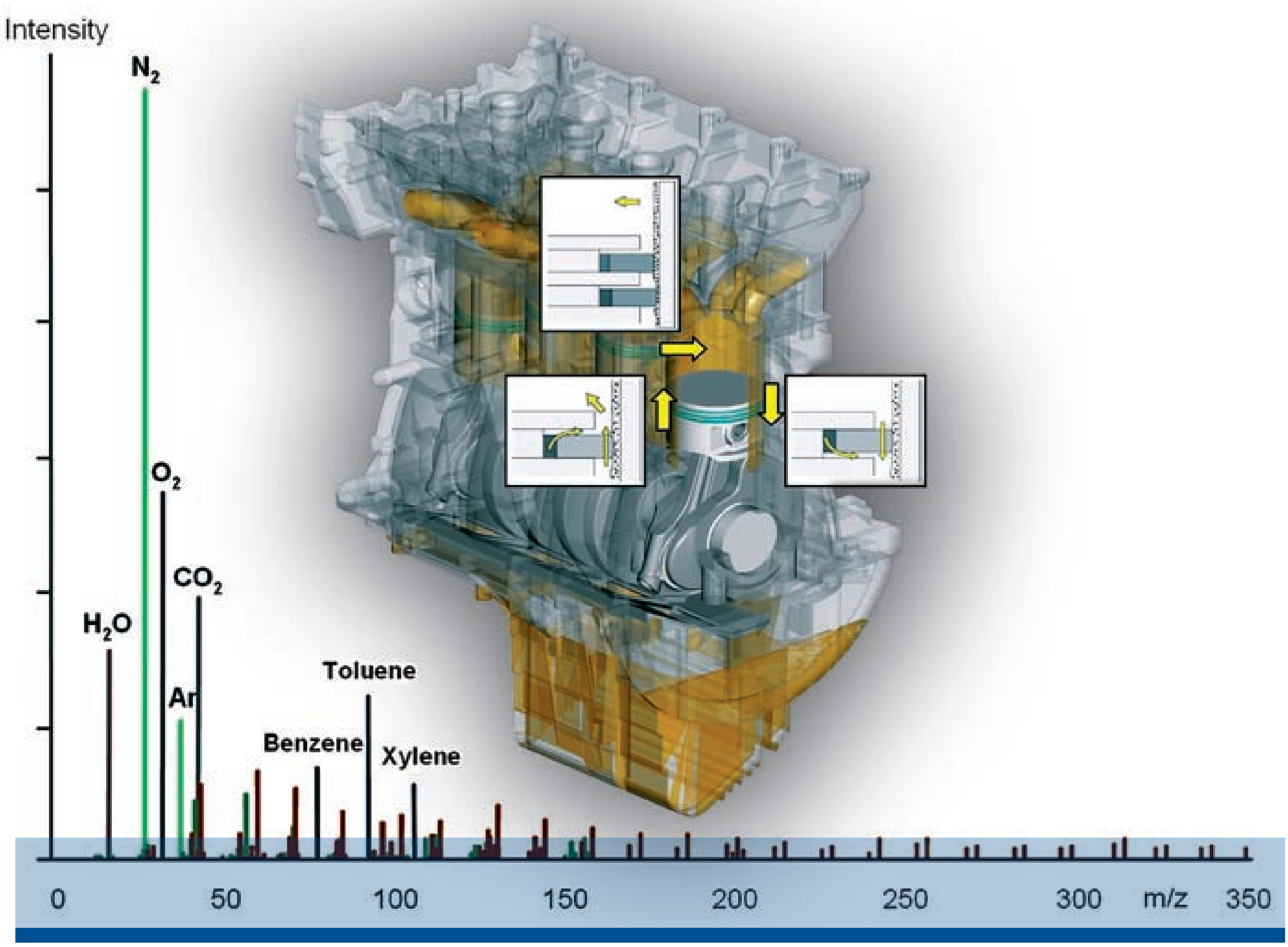

personal buildup for Force Motors Ltd.

Oil Emissions of a SI Engine

Process Development for Measurement and Simulation

The aim of the FVV research project "Oil Vaporization" I to III (FVV No. 902) was to measure the oil emissions using thermic and gas-dynamic processes of a combustion engine and subsequent validation of a simulation program. For the first time a cylinder-extraction and rapid emission measurement of the vaporized oil residues in the cylinder of a SI engine was carried out by Helmut Schmidt University (University of the Federal Armed Forces Hamburg), Technical University Hamburg-Harburg and University of Kassel (all Germany). The measurement results obtained made it possible to significantly develop the simulation of the piston ring/ cylinder oil emissions in this research project.

1 Introduction

Oil consumption of a combustion engine is generally understood as the time-related oil loss from the oil cycle and is mostly the result of lubricant oil entering the combustion chamber, which can be measured using a mass balance, **Figure 1**. The combustion chamber is regarded as an open system in which a mass exchange with the surrounding area takes place via the inlet (E) and outlet (A) and via the ring packet, **Table 1**. The mass flowing into the combustion chamber via the inlet reveals a proportion of lubricant oil, the origin of which could be the ventilation of the crankcase, the turbocharger or the valve spindle tracks. In the area of the piston ring packet components of the lubricant oil are emitted from the lubrication film on the cylinder wall into the combustion chamber. A further distinction is made between the Gas Flows blow-by (BB) and reverse blow-by (RBB). While the reverse blow-by flow transports the gas enriched with lubrication oil in the interim ring area into the combustion chamber, with the blow-by flow transport in the opposite direction takes place. In the combustion chamber the lubricant oil vapour concentration is further increased by the input of vaporized (V) oil from the cylinder wall and the centrifugation of oil above the first compression ring.

In the combustion chamber gas all the parts listed in the balance, except for the oil vapor particles transported with the blow-by into the crankcase can be measured. The measurements were carried out with a rapid mass spectrometry gas analysis system developed as a result of two FVV research projects [1, 2] at the Technical University Hamburg-Harburg. This system makes it possible to determine the sum of the hydrocarbons in the exhaust gas and indeed separately according to hydrocarbons, which stem from fuel and lubricant oil. The precise assignment of the concentrations measured to the individual work cycles of the engine allows the correlation to the simulation. The priorities of this work were in the extraction, the transfer to the mass spectrometer and the time-based assignment of the part taken from the cylinder charge.

The simulation technology of the project is based on the simulation programs KORI3D and PRO [3, 4 and 5] developed at University of Kassel. The piston ring dynamic simulation KORI3D provides the necessary basic conditions such as the oil quantities in the system (lubrication film height cylinder wall) and gas flows (blow-by und reverse blow-by) in the ring packet.

Next the program PRO uses these results to determine the oil consumption proportions in the cylinder. The thermal evaporation processes are calculated in the transfer of the lubrication film to the combustion chamber as well as the gas-dynamic proportions through blow-by.

The Authors

Prof. Dr.-Ing.
Gunter Knoll
is the director of the Institute for Machine Elements of the University of Kassel (Germany).

Prof. Dr.-Ing.
Wolfgang Thiemann
is the director of the Institute for Automotive and Power Train Engineering of the Helmut Schmidt University/University of the Federal Armed Forces Hamburg (Germany).

Dipl.-Ing.
Frank Schlerege
is the head of simulations at the Institute for Machine Elements of the University of Kassel (Germany).

Dipl.-Ing.
Philipp von Hollen
is scientific assistant at the Institute for Automotive and Power Train Engineering of the Helmut Schmidt University/University of the Federal Armed Forces Hamburg (Germany).

Prof. Dr.-Ing.
Gerhard Matz
is the director at the Institute of Measurement Technology of the Technical University Hamburg-Harburg (Germany).

Dr.-Ing.
Arnim Robota
is head of combustion engine testing at Federal Mogul Burscheid GmbH in Burscheid (Germany).

Dipl.-Ing.
Sven Krause
is scientific assistant at the Institute of Measurement Technology of the Technical University Hamburg-Harburg (Germany).

MTZ Peer Review
The Seal of Approval for scientific articles in MTZ.
Reviewed by experts from research and industry.

Received .... October 02, 2008
Reviewed .... October 28, 2008
Accepted .... November 16, 2008

2 Test Bed and Test Sample

For all oil emission measurements a $\lambda = 1$ controlled 2.0-litre four-cylinder SI engine from Volkswagen with a nominal power of 62 kW at 4300 rpm speed, which had been tested at the Helmut Schmidt University Hamburg (Drive Systems Technology Laboratory), was used. The gas enriched with lubricant oil from the crankcase was constantly discharged into the atmosphere via a separate track into a blow-by gas meter and the connection with the crankcase on the suction pipe side closed. The cylinder wall temperatures were measured at three levels parallel to the piston track on the pressure and counter-pressure side.

3 Oil Emission Technology

The main component of the equipment used to measure oil emissions is the mass spectrometer (MS), **Figure 2**, modified to measure lubricant oil (mass-to-charge ration m/z > 170) [1, 2].

3.1 Gas Transport

The measurement of the oil vapour proportion in the combustion chamber requires continuous gas transport from the combustion chamber to the gas analyser. A simple direct connection between the combustion chamber and the gas analyser, as for example has been achieved with a capillary, proved to be disadvantageous in two respects.

First, there is a pressure-proportional mass flow in the capillary from the transient pressure flow within the combustion chamber, which leads to operating pressure in the ions source that exceeds the permissible limit. Second, a rapidly falling pressure in the cylinder causes reverse flow in the capillary. The newly developed extraction system of this project has none of the disadvantages mentioned.

3.2 Construction

The system, **Figure 3**, consists of a probe head, a transfer track and a fore-vacuum area. The probe head terminates flush with combustion chamber wall and is provided with a bore hole that forms the first step in the gas extraction system. On the way to the mass spectrometer there is a series of transfer capillaries (TK), the internal diameter of which increases progressively.

The restriction capillary (RK), which leads to the ion source of the MS, protrudes into the exit area of the transfer capillary. The sampling area is located between the inlet valve and the spark plug of the first cylinder.

3.3 Transfer Time Correction

Depending on pressure and temperature within the combustion chamber the gas molecules require transfer times of different length to pass through the extraction system. These running time differences require a correction of the time axis. For this the known carbon dioxide concentration $CO_{2\ Sim}$ from the cycle process calculation in the combustion chamber is compared, as required by the combustion cycle from the indexing data, with MS measurement $CO_{2\ Mess}$.

A genetic algorithm generates a transfer time correction function S(φ). This is applied to the measurement $CO_{2\ Mess}$ and the difference from the known concentrations $CO_{2\ Sim}$ minimized in an iterative process. If this is minimal, the transfer time correction S(φ) is used to assign all

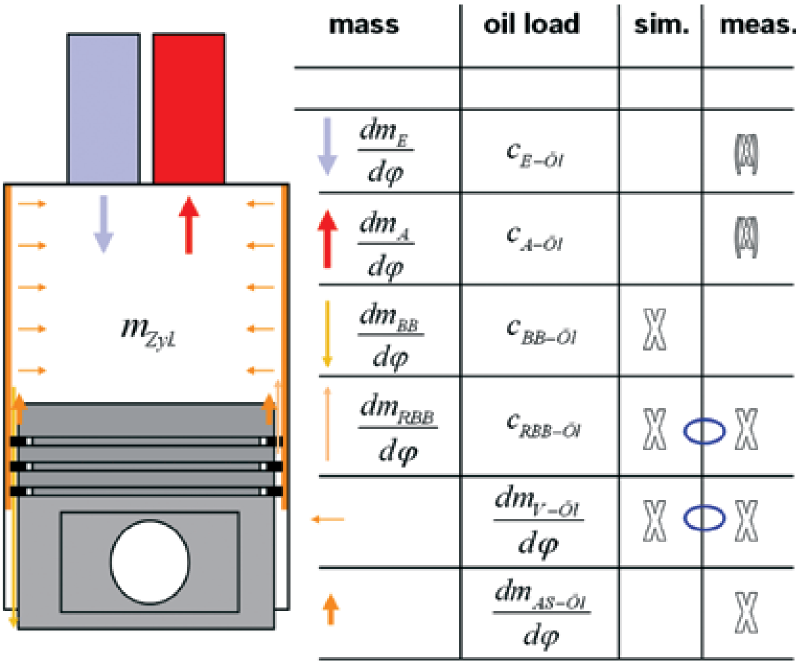

Figure 1: Balancing the cylinder oil emissions

Table 1: Nomenclature in Figure 1

Abbreviation	Meaning	Location
E	inlet	via intake valve(s)
A	exhaust	via exhaust valve(s)
BB	blow-by	gasstream into crankcase
RBB	reverse blow-by	gasstream out of the ring package
V	evaporated lubricant-oil	from cylinder liner
AS	centrifugated lubricant-oil	centrifugation of oil above first compression ring
C	concentration of mass	
$\frac{dm}{d\varphi}$	mass stream	as a function of degrees of crankangle
X	measureable, calculable	

further components measured in this operating point correctly to the time axis.

3.4 Preparation of Measuring Signal

For every operating point the measuring signals of the mass spectrometer for oil (m/z > 170) and carbon dioxide (m/z = 44) recorded and averaged crank angle-tag-triggered – in the time of 200 cycles. To assign the values recorded to the crankshaft position the measuring signal referenced on ITDC according to the method described earlier is displaced by the transfer time. The minimal increase time is $T_{10\text{-}90}$ = 2.5 ms.

The calibration of the measuring system is done with an appliance that produces an oil vapour-air mixture of known composition. A real process calculation provides the mass contained in the combustion chamber consisting of air, fuel and residual gas.

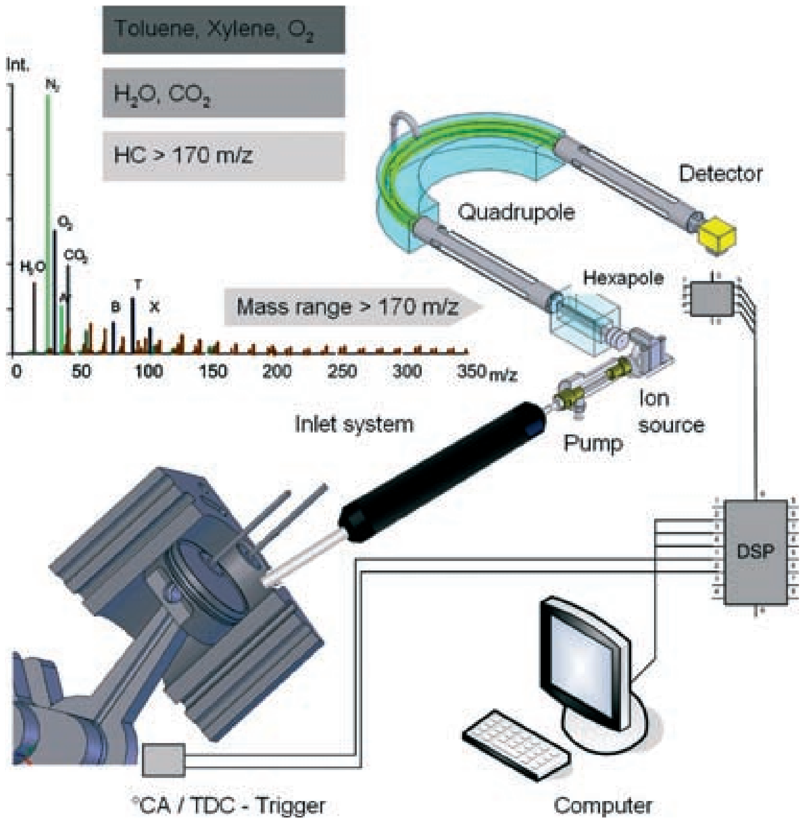

Figure 2: Measuring technique: combustion chamber gas sampling, transfer-line to the mass spectrometer, components for analytical determination; digital signal processor (DSP) for the data acquisition of the detector signal and crankshaft position (°CA/TDC); mass spectrum of the combustion chamber gas with filter adjustment to measure lubricant oil

4 Testing Program and Results of Oil Emission Measurement

To validate the program PRO the engine was fitted with selected components and measured in its operating area. Within the framework of the project comprehensive variations of roughness, ring fittings, temperatures and lubricants were carried out by means of simulation.

The results of these calculations served as the selection criterion for the test bed components used. The measurement was carried out with cylinder crankcase with low basic roughness and a piston ring packet with low oil wiping action, **Table 2** and **Figure 4**. The measurements of the oil emissions in the exhaust manifold (APK) and the cylinder measurement were carried out in the entire operation area of the engine. Load and revolutions were varied in 29 operating points that cover the entire grid of the test carrier.

4.1 Results of the Exhaust Manifold Measurement

The first measurement was that of the oil emissions in gas extraction from the exhaust gas manifold. In accordance with the trial plans set out operating parameters (operating points, coolant temperature) and important constructional elements of the engine (running surfaces topography, piston ring packet, lubricant oil with various viscosity and evaporation) were varied in two phases. The largest oil emission was investigated in all variants at the highest revolution and full load. A main effect analysis of the measured values produced the effects, listed in **Table 3**, on the performance-specific oil emissions.

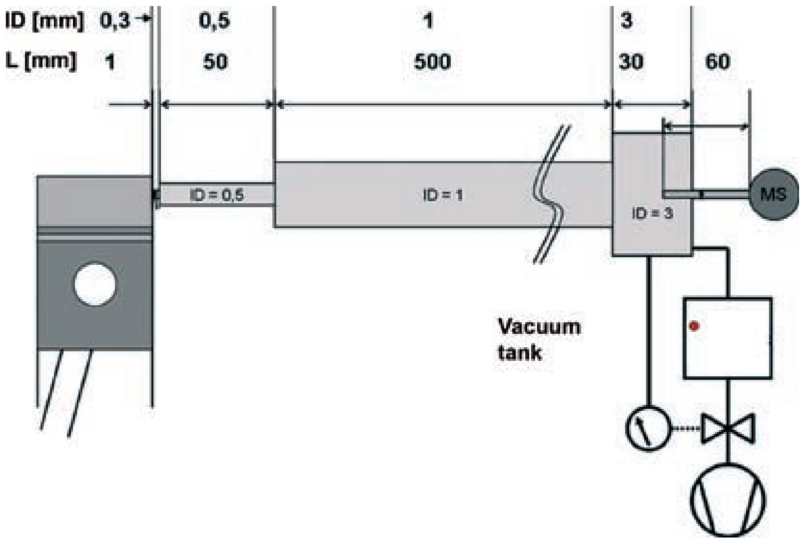

Figure 3: Cylinder inlet system

Table 2: Characteristic data of cylinder honing

Cylinder Crankcase	Value	Unit
Description	"Fine honing"	–
Core roughness depth R_k	0.6	µm
Reduced centre height R_{pk}	0.1	µm
Reduced groove depth R_{vk}	1.0 bis 1.5	µm
Honing angle	45	°

4.2 Results of the Cylinder Measurement

The gas composition of the cylinder was analysed with the gas extraction system described here. **Figure 5** shows oxygen, toluene, carbon dioxide and the oil concentration. The measured and time-corrected cycles of reaction educts and products can reasonably be assigned to the work cycles. **Figure 6** shows the effects of load and revolution on the oil evaporation in the combustion chamber. With all speed frequencies the load variation with increasing revolution momentum produces a significant increase of the oil amount evaporated into the cylinder per work cycle. With increasing revolution speed more oil, at constant load, is emitted per time unit into the combustion chamber and expelled at the fourth cycle.

1. Nut	dimensions [mm]	81,25/74,45 x 1,75
		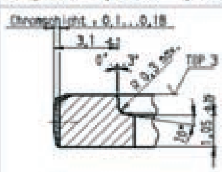
	material	KV1/ Cr
	clearance	0,2 ... 0,4 mm
	force Ft	8,4 ... 12,6 N
2. Nut	dimensions [mm]	81,25/74,35 x 2,0
		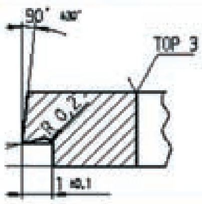
	material	Std./-
	clearance	0,2 ... 0,4 mm
	force Ft	8,6 ... 12,9 N
	angle	90'
3. Nut	dimensions [mm]	81,25/74,05 x 3,0
		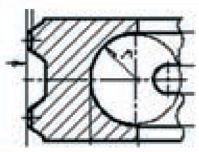
	material	Std./Cr
	clearance	0,25 ... 0,5 mm
	force Ft	33,5 ... 47,0 N
	surface pressure	1,988 N/mm²
PRO :	evaporation [g/kWh] :	**0.87**
	oil emissions [g/kWh] :	**1.39**

Figure 4: Data of the ring packet

5 Simulation of the Piston Ring Movement and Oil Consumption

The piston-ring dynamic simulation KORI3D was developed in the FVV projects "Piston Ring Friction" I/II for the design of the piston ring with regard to friction losses and seal effect and delivers both the oil amounts in the system (lubricant oil height cylinder wall) and the gas flows (blow-by und reverse blow-by). The movement behaviour of the rings with respect to the ring groove and cylinder wall dependent on internal and external forces is described.

The methodical procedure of the multi-bodied dynamic model formation and coupling with the EHD lubricant film reactions of the piston ring/piston groove/cylinder corresponds in principle to the procedure described in **Figure 7**. The basis of a transient calculation of the kinematics and kinetics of multi-bodied systems is the formulation of the Newtonian equation of motion. As a result the necessary basic conditions for the lubricant gap geometry and for the hydro-dynamic speeds can be calculated.

5.1 PRO Cylinder Oil Emission Calculation

At the heart of the program system PRO developed in a FVV research project is the tribological-thermic system of piston/piston ring/cylinder wall. PRO delivers, on the basis of residual oil film height, the cylinder oil emission of minimal gap width and blow-by and/or reverse blow-by gas mass flow from the KORI3D simulation. The free oil or residual film height released on the cylinder wall of the combustion chamber are thus based on optimized formulations of the reciprocal oil amounts that pass between the rings inside the ring movement and oil transportation. The models used in PRO record the lubricant oil inputs by evaporation from the freely-guided cylinder wall together with the oil evaporation parts transported with the gas mass flows (blow-by / reverse blow-by) in the area of the piston ring packet. During the combustion, expansion and expulsion process high combustion chamber gas temperatures and heat transfer rates result in the heating of the oil film. Both during the combustion process and in the exhaust stroke the result is evaporation of the lubricant oil film from the freely guided cylinder wall. The evaporated lubricant oil is emitted together with the other parts (reverse blow-by) into the combustion.

5.2 Calculation of the Lubricant Film

In PRO the temperature of the lubricant film will be calculated starting with the temperatures of the combustion chamber, the cylinder and the coolant. The oil consumption simulation therefore requires the solution of unsteady heat conduction equation in the area of heat exchange water/cylinder/oil film to investigate the oil film surface temperature and, building on that, material transition in diffusion and evaporation. The oil evaporation rates from the free cylinder wall in the combustion chamber depend on the material properties of the oil, the pressure and temperature on the oil film surface and the gas speeds.

A distinction is made between several mechanisms of oil consumption. If the pressure of the freely guided lubricant film surface element falls below the temperature-dependent vapour pressure, a certain amount of oil evaporates and evaporation enthalpy is release, which cools the oil film until a thermal equilibrium has set in. If the pressure is higher than the vapour pressure, the material transfer takes via diffusion place by means of material transfer laws. The gas mass flow takes part of the oil coating into the ring grooves and gaps on the ring. The ring-related gas temperature from KORI3D with the respective gas mass flow in the direction of the crankcase (blow-by) and of the combustion chamber (reverse blow-by) is included in a balance of the oil released in the gas.

Table 3: Exhaust manifold measurement, performance-specific oil emission

Factor	Unit	Stage 1	Stage 2	Main Effect
Oil viscosity	mm^2/s	10	14	-0.03
Noack number	%	15	7.5 (6)	0.09
Piston ring packet	–	Type A	Type B	0.24
Honing	–	rough	fine	0.22
Heat exchange water temperature	°C	80	100	0.06
Mean value oil emission	g/kWh			0.58

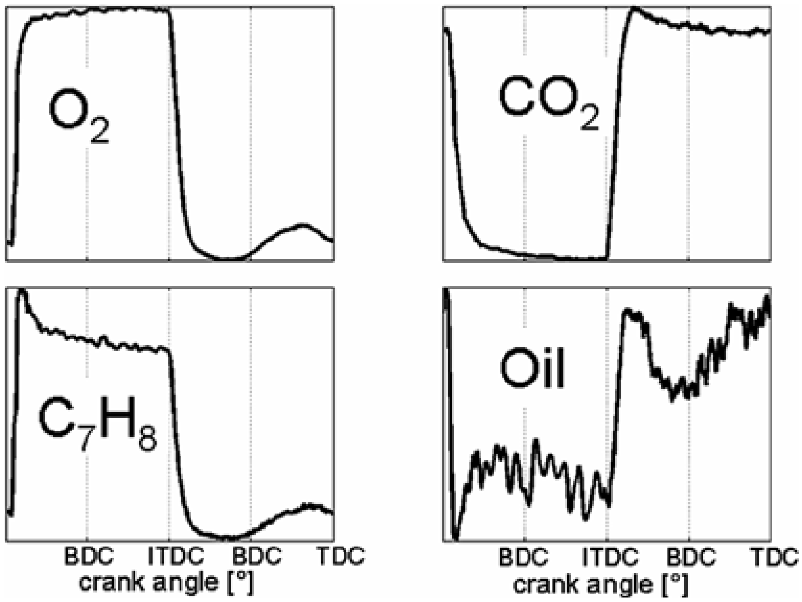

Figure 5: Running time-corrected measurement results of oxygen, carbon dioxide, toluene and oil at the operating point n = 2000 rpm; M = 145 Nm

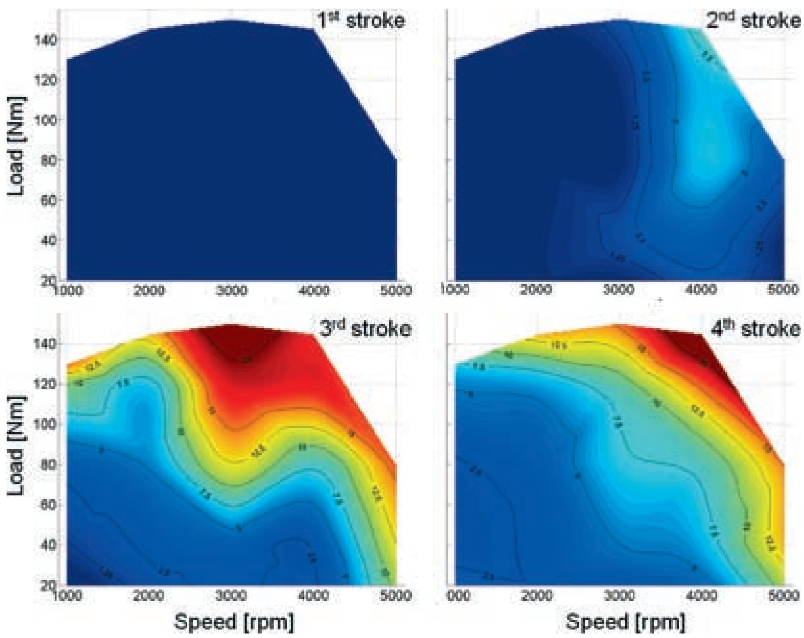

Figure 6: Effect of the strokes and operating points

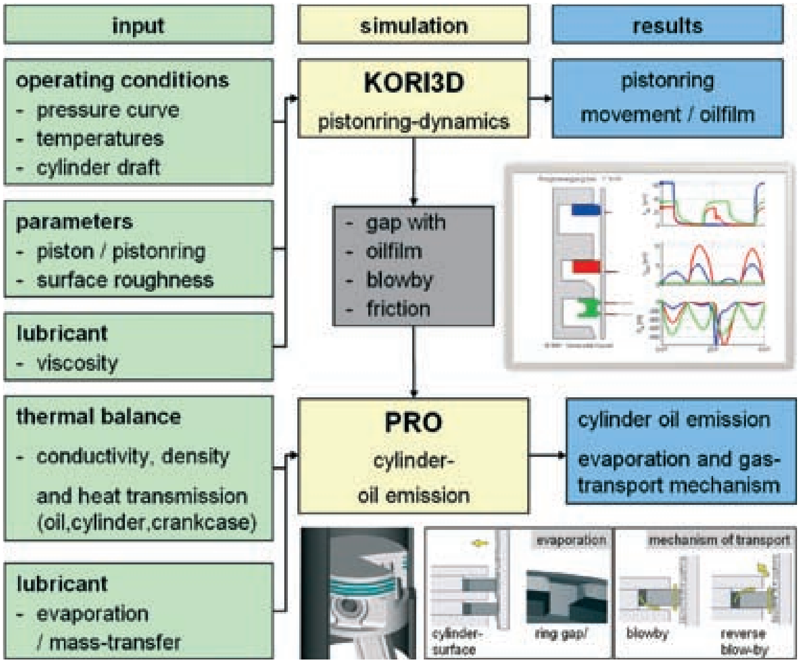

Figure 7: Simulation of the piston ring dynamic and cylinder oil emissions

6 Program Validation

The load case co-ordinated calculation results of the program system KORI3D formed the basis for the validation of the program system PRO. In addition to the plausibility control of the ring dynamic the measured blow-by values were adduced as a co-ordination variable. Based on the KORI3D simulation results the cylinder wall temperature was adjusted, depending on the operating point, to the measured temperatures in a second step. This happened through the adjustment of the heat transfer coefficients ($\alpha_{cylinder}$) of the heat exchange water until the estimated wall temperature agreed with the measured values, **Figure 8**. The green line represents the position of the cylinder wall temperature sensors, applied on the thrust side and anti thrust side. The red line is the march of temperature from the combustion chamber gas through the oil film and cylinder wall to the cooling medium. This temperature results from the unsteady thermal conduction calculation, with heat transfer coefficient ($\alpha = f(p, \vartheta, v, V)$) according to the equations of Woschni, Hohenberg and respecively Huber.

The validation of the stroke- and crank angle-dependent oil consumption calculations was carried out in the entire engine operating map.

The crank angle related characteristic data served to test and adjust the consumption mechanisms implemented in PRO. For this the quality of the runs and the consumption rates were adduced.

The results of the measurement and calculation are presented later in tabular form in the partial and full load area. **Figure 9** shows the comparison between the integral and stroke-related oil consumption from the simulation with the characteristic data of the GES. With the

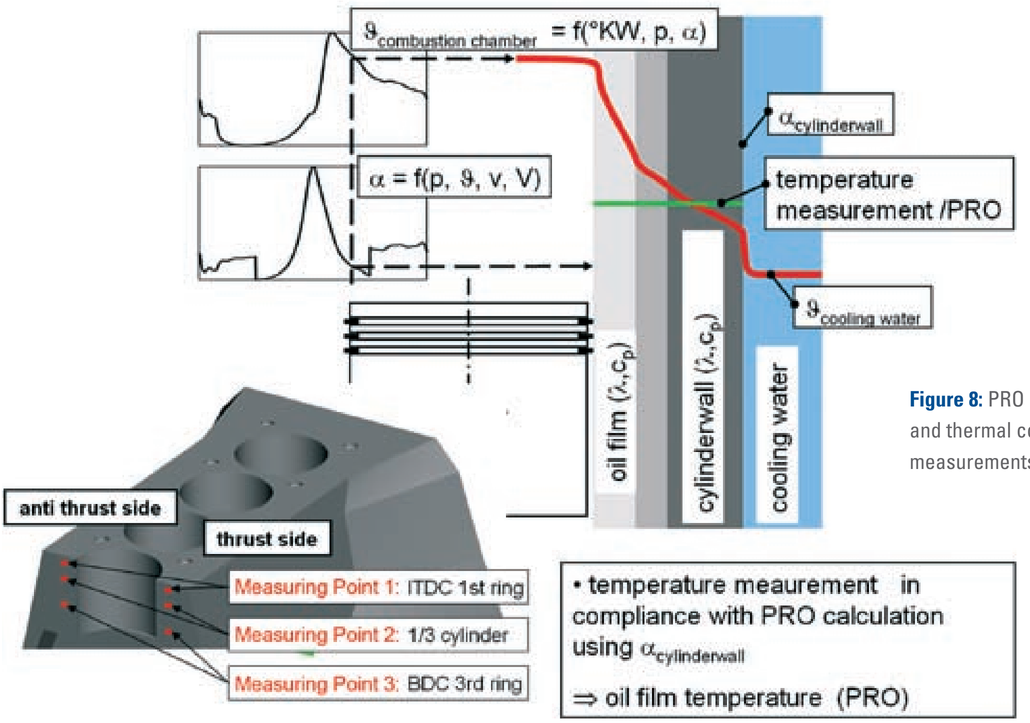

Figure 8: PRO model – unsteady heat conduction and thermal coordination with temperature measurements

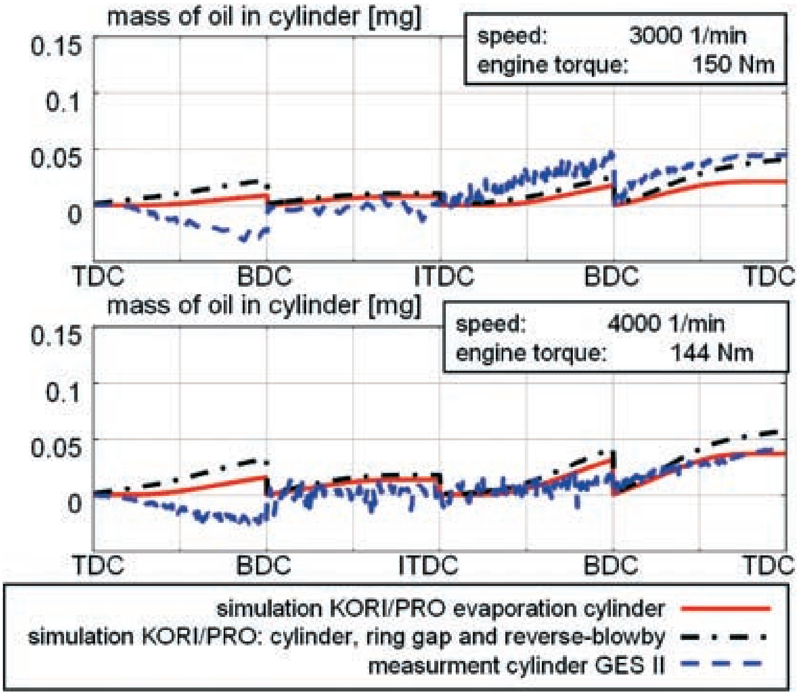

Figure 9: Time required by cylinder oil consumption, comparison between measurement and simulation (full load)

simulation values the oil consumption is represented both by evaporation of the lubricant film on the cylinder wall and as the sum of the evaporation on the cylinder wall, impact and reverse blow-by. It also shows the stroke depending mass of oil, emitted in the cylinder. The exhaust gas contains the final values at the end of the power stroke, ITDC (ignition top dead center) to BDC (bottom dead center) and the exhaust stroke, BDC to TDC (top dead center).

The inflowing fuel-air mix in the intake stroke (TDC-BDC) reduces the oil concentration that comes from the residual gas. For this reason no increase can be measured by the MS at the place of the sample taking in the intake stroke. As shown in Figure 9, a significant comparison between measurement and simulation is possible therefore only in the power and respectively the exhaust stroke. On the basis of the simulation results it can be seen clearly that in the work cycle the oil consumption is made up by evaporation and the reverse-flowing gas. The sole use of the thermal consumption proportion alone delivers to small amount at the end of the power and exhaust stroke that is too small in comparison with the measurement. The reverse blow-by also delivers important information about the load and speed-dependent consumption proportion of the strokes.

In connection with the validation of PRO operating points were calculated in the entire engine characteristics map. This took place for the test bed configuration used in oil evaporation II on the GES system development. In **Figure 10** the simulation results are compared with the characteristic data of GES II in the engine characteristics map for 90 °C heat exchange water. The comparison shows both a high level of agreement in the load dependency and a high quantitative agreement between simulation and measurement.

7 Summary

Knowledge of the temporal and physical interrelationship of cylinder oil emission makes it possible to reduce these oil consumption sources. The combination of measurements and simultaneous simulation of oil emission, by means of the analysis and program systems developed in several FVV projects (numbers 826/902/M0707), yields important information. The investigations were carried out by Helmut Schmidt University (University of the Federal Armed Forces Hamburg), Technical University

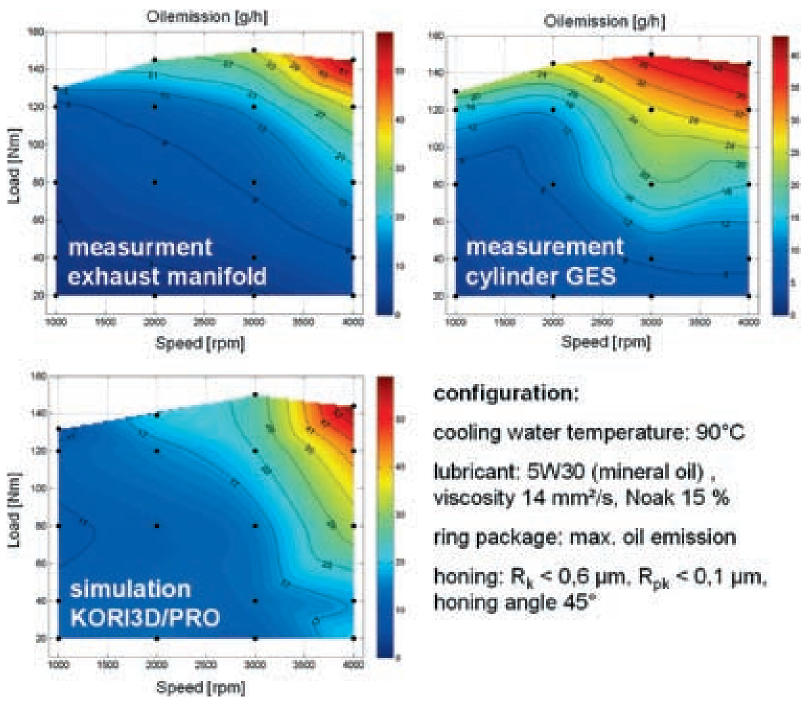

Figure 10: Cylinder oil consumption engine operating map (four cylinders), comparison between simulation and measurement (ϑKW = 90 °C)

Acknowledgements

This paper is the result of several academic research projects (FVV No. 826/902/M0707), set by the Research Association for Combustion Engine Vehicles (Forschungsvereinigung Verbrennungskraftmaschinen, abbreviated here to FVV, Frankfurt/Main, Germany) and carried out at the Institute for Vehicle and Drive System Technology (Institut für Fahrzeugtechnik und Antriebssystemtechnik) of the Helmut Schmidt University (University of the Armed Forces, Hamburg), Institute for Measurement Technology (Institut für Messtechnik) of the Technical University, Hamburg-Harburg and the Institute for Machine Elements (Institut für Maschinenelemente), University of Kassel. Financial support for the work was provided by the Federal Ministry of Economic and Technology (Bundesministerium für Wirtschaft und Technologie BMWi) via the Consortium of Industrial Research Associations (AiF), (AiF No. 13760 N/1) and the FVV itself. The Research Association of Combustion Engine Vehicles is grateful to the BMWi and the AiF for financial support. The project was monitored by a working group of the FVV under the direction of Dr.-Ing. Arnim Robota, Federal Mogul Burscheid. The authors wish to thank Dr. Robota and the working group for their generous support.

Hamburg-Harburg and University of Kassel (all Germany). By means of an agreed test and simulation program measurements on the exhaust chamber and cylinder measurements within the entire engine characteristics map were carried out. The absolutely necessary basic gas and thermodynamic conditions were recorded and implemented on the trial 2.0-litre SI engine.

With the gas extraction system developed more detailed information about the crank angle related oil concentrations in the cylinder is available. For the first time a cylinder extraction, rapid emission measurement of the vaporized oil components and timely assignment of the measured concentrations to the individual work strokes on the engine in the engine cylinder have been carried out. The important key to achieving the measurement proved to be the transfer time analysis and correction presented in combination with the signal calibration and preparation. In the combustion chamber gas all oil vapour parts (except for blow-by) can be measured. The biggest effects on the oil emissions of this engine are produced by the honing and piston ring packet. The effect of lubricant and cool water is smaller.

A basis for validating the PRO program system was the results calculated by KORI3D for the piston ring dynamic. In addition to the plausibility control of the ring dynamic measured blow-by values were also considered. In PRO the cylinder wall temperature was compared, depending on the operating point, with the temperatures measured by iterative adjustment of the heat transfer coefficients of the heat exchange water. The crank angle-related measurement readings then served to test and adjust the consumption mechanisms implemented in the PRO. For this, both the quality of the runs and the consumption rates were adduced.

A meaningful comparison between measurement and simulation is possible only in the power and exhaust stroke. By means of the simulation results it can be seen clearly that in the power stroke the oil consumption is made up by evaporation and the reverse-flowing gas. The use of the thermal consumption part alone delivers an oil emission that is too small in comparison with the measurement. The reverse blow-by also delivers important information about the consumption parts of the strokes that are load and speed dependent. In the entire engine characteristics map a good quantitative agreement between measurement and simulation is visible.

The rapid metrological recording of the cylinder oil emissions by means of the gas extraction and mass spectrometer analysis system now available makes it possible to allocate the operating point- and stroke-related oil consumption mechanisms to simulation technology. Because of the measurement results obtained it has been possible to decisively develop the simulation chain from KORI3D and PRO of the piston ring/cylinder oil emissions further.

References

[1] Kuhlmann, P.; Matz, G.; Gohl, M.; Ihme, H.: Massenspektrometrische Bestimmung des Ölverbrauches von Verbrennungsmotoren und dessen Einfluss auf die HC-Emissionen. FVV-Forschungsheft 691, FVV, Frankfurt/Main, 2000
[2] Kuhlmann, P.; Matz, G.; Gohl, M.; Ollesch, T.: Massenspektrometrische Bestimmung der Ölemission im Abgas von Otto- und Dieselmotoren. FVV-Forschungsheft 764, FVV, Frankfurt/Main, 2003
[3] Knoll, G.; Lechtape-Grüter, R.: Ölverbrauchssimulation. AIF-Nr. 10673, 1996-1999; FVV-Forschungsheft 707, FVV, Frankfurt/Main, 2001
[4] Peeken, H.; Knoll, G.; Lechtape-Grüter, R.: Kolbenringreibung I. FVV-Forschungsheft 502, FVV, Frankfurt/Main, 1992, und 513, 1993
[5] Knoll, G.; Lechtape-Grüter, R.: Kolbenringreibung II. FVV-Forschungsheft 570-1, FVV, Frankfurt/Main, 1994, und 570-2, 1995
[6] Knoll, G.; Matz, G.; Thiemann, W.; v. Hollen, P.; Krause, S.; Schlerege, F.: Ölverdampfung. FVV-Forschungsheft 873, AIF-Nr. 13760 N/1-3, FVV, Frankfurt/Main, März 2006